UNIVERSIDAD AUTONOMA DE MADRID

ESCUELA POLITÉCNICA SUPERIOR

"Digital Coherent Receiver for Optical Transmission"

-PROYECTO FIN DE CARRERA-

Lázaro Hermoso Beltrán

Noviembre 2009

Digital Coherent Receiver for Optical Transmission

AUTOR: Lázaro Hermoso Beltrán

TUTOR: Hadrien Louchet

PONENTE: Daniel Ramos Castro

Dpto. de Ingeniería Informática
Escuela Politécnica Superior
Universidad Autónoma de Madrid
Noviembre 2009

Palabras clave:

Detección Coherente, Oscilador Local, Sensibilidad, Ruido de Disparo, Multiplexación por Polarización

Resumen:

En este proyecto se estudian las bases de la detección óptica coherente y se implementa un receptor digital coherente para transmisión óptica capaz de demultiplexar señales previamente multiplexadas por polarización. El receptor digital coherente implementado está compuesto por tres módulos principales: un módulo recuperador de reloj capaz de obtener la señal de reloj a partir de la señal recibida. Un segundo módulo capaz de compensar la Dispersión Cromática y la Dispersión por Modo de Polarización haciendo uso de filtros adaptativos. Estos filtros están diseñados para que se puede elegir el modo en el que adaptan sus coeficientes mediante dos tipos de algoritmos adaptativos: LMS y CMA. El tercer módulo estima el ruido de fase y lo compensa.
Luego pasamos a comprobar el funcionamiento del receptor diseñado haciendo uso de la herramienta *VPItransmissionMaker*^{TM} .Se introduce el receptor en un sistema de transmisión y se estudia la habilidad del mismo para compensar distintas cantidades de CD, PMD y ruido de fase. Cambiando las propiedades del sistema se pone a prueba la robustez del receptor. Se comparan distintas configuraciones del receptor digital coherente como la utilización de los distintos algoritmos de adaptación de los coeficientes.

Keywords:

Coherent Detection, Local Oscillator, Sensitivity, Shot noise, Polarization Multiplexing.

Abstract:

The purpose of this project is to study the basis of optical coherent detection associated with digital signal processing and to design and implement such a receiver.
The investigated coherent can be used to detect arbitrary complex modulation formats as it is capable of splitting polarization multiplexed signals and provides the real and imaginary parts of the optical field. After coherent detection, the signal is digitize to perform DSP in order to digitally obtain the clock from the signal received and compensate for the linear impairments that previously affected the signal. For that purpose the digital coherent receiver implemented is composed by three modules: the first module is a clock recovery that can obtain the clock signal from the received signal. A second module that, using Digital Signal Processing (DSP), is able to compensate Chromatic Dispersion (CD) and Polarization Mode Dispersion (PMD) using adaptive filters. These filters are programmed to use two kinds of adaptive algorithms: LMS and CMA, which can be previously selected. The third module is in charge of the phase noise estimation to compensate for the rotation that causes this impairment in the constellation sent. Two different architectures for phase noise estimation are compared.
After designing the receiver in Matlab® we validate its functionality. For that we use the *VPItransmissionMaker*^{TM} tool in which we can simulate a realistic optical communication system, and, introducing our designed receiver model into the communication system the receiver’s capability to compensate CD, PMD and Phase Noise is studied. Furthermore, changing the optical communication system properties, we put the receiver’s robustness to test. We also change different configurations of the receiver and study how it influences the reception of the signal.

Agradecimientos

Me gustaría agradecer en primer lugar a toda mi familia por la educación, cariño y apoyo que siempre me han dado. En especial a mis padres a los que nunca les estaré lo suficientemente agradecido, a mi padre por su dirección, a mi madre por su devoción.

A VPIphotonics™ por darme la oportunidad de realizar mi Proyecto durante mi estancia en Berlín y a mi tutor Hadrien Louchet ya que sin su dedicación no habría sido posible la realización de este proyecto. También agradecer a la Escuela Politécnica Superior y sus profesores que con su trabajo han conseguido hacer de mi una persona competente.

A mis compañeros y amigos por hacer el día a día mucho más agradable. A Alejandro, por su ayuda, sobre todo en los primeros años. Gracias “socio”.

A Verónica por su amor.

Lázaro Hermoso Beltrán
Noviembre 2009

Acknowledgements

First I would like to thank my whole family for the education, love and support they have given me; especially my parents, to whom I will never be sufficiently grateful.

To VPIphotonics^{TM}, thank you for giving me the opportunity to make my project during my stay in Berlin and also my tutor Hadrien Louchet because without his dedication it would not have been possible to carry out this project. I would also like to thank the Escuela Politécnica Superior and their teachers whose work has converted me into a professional.

To my colleagues and friends for making everyday much more pleasant.

To Verónica for her love.

Lázaro Hermoso Beltrán
November 2009

TABLE OF CONTENTS

LIST OF FIGURES

LIST OF TABLES

GLOSSARY

Analog- to-Digital Converter, ADC:

An analog-to-digital converter is a device which converts continuous signals to discrete digital numbers.

Balanced detection:

A balanced detector, or balanced receiver, is a device that measures the difference in the intensity of two laser beams. It is a part of a receiver front-end architecture that provides better power efficiency for the receiver.

Band-Pass Filter, BPF:

A band-pass filter is a device that passes frequencies within a certain range and rejects (attenuates) frequencies outside that range.

Birefringence:

The decomposition of a ray light into two rays when it passes through certain types of material depending on the polarization of the light.

Bit Rate, Rb:

The number of bits transmitted per unit of time.

Constant Modulus Algorithm, CMA:

Algorithm used in adaptive filter for the coefficients adaptation.

Coherence Time:

The time over which a propagating wave (especially a laser) may be considered coherent. In other words, it is the time interval within which its phase is, on average, predictable.

Digital Signal Processing, DSP:

The group of techniques that treat a digital signal. These techniques are very useful because of their stability due to error detection and correction and their reduced vulnerability to noise. In the design of the digital coherent receiver DSP is used for compensation of chromatic dispersion, polarization mode dispersion and tracking the phase of the received signal.

Direct Detection Receiver, DD Receiver:

A receiver that works converting optical power directly to electrical domain. These kinds of detectors are not able to recover the information on the phase of the optical signal.

Dispersion:

The physical phenomenon in which the velocity of a wave (light) depends on its frequency. It can be material dispersion or waveguide dispersion. Chromatic dispersion is an example of material dispersion while modal dispersion and polarization mode dispersion are examples of waveguide dispersion. In optical communication, dispersion leads to signal degradation and thus to error detection in the receiver.

Dispersion Compensating Fiber, DCF:

It is a type of fiber that is able to compensate dispersion effects. Typical DCF has a negative dispersion and produces negative slope with nominal values that are typically ten times higher than those of the fiber to compensate for. Therefore, to adequately compensate for the dispersion in 90 km of G.652 fiber, approximately 9 km of DCF must be installed.

Erbium Doped Fibers Amplifiers, EDFA:

An optical amplifier. This means that it is a device that amplifies an optical signal without converting it into the electrical domain. It is able to amplify a group of wavelengths, so it is very useful when used together with WDM.

High-Pass Filter, HPF:

A high-pass filter is an LTI filter that passes high frequencies well but attenuates (i.e., reduces the amplitude of) frequencies lower than the cutoff frequency.

Intersymbol Interference, ISI:

The overlapping between symbols, in which one symbol interferes with subsequent symbols due to a distortion in the received signal that causes the spread of the symbols. In optical communication the distortion that causes this effect is dispersion.

Least-Mean-Square algorithm, LMS:

Is an algorithm specially used in adaptive filters. It is to find the filter coefficients that relate to producing the least mean squares of the error signal (difference between the desired and the actual signal).

Local Oscillator, LO:

Laser located in the receiver. Its lightwave is mixed with the incoming signal in the coherent optical receiver. The mixing lets to obtain the phase of the received signal

Mach-Zender modulator, MZ modulator:

External optical modulator able to modulate phase or and amplitude of an optical lightwave.

Monte Carlo Mehtod:

It is class of computational algorithms that rely on repeated random sampling to compute their results. Monte Carlo methods are often used when simulating physical and mathematical systems in a computer.

Multilevel Modulation:

A type of modulations that provides to the modulated signal N possible values, where N is an integer value greater than one. For example, QAM is a multilevel modulation with N=4. The

Optical Coherent Detection Receiver:

A receivers that mixes the incoming optical signal with a local optical source lightwave before converting the signal into electrical domain.

Optical Coupler:

A passive device for branching or coupling an optical signal. Generally, a coupler is centralized by joining the two fibers together so that the light can pass from the sender unit to the two receivers, or else it can be made by juxtaposing the two "receiver" fibers which will then be aligned and positioned so as to be facing the "sender" fiber. In our design the optical coupler is used to mix the incoming lightwave and the local oscillator lightwave.

Phase Diversity Receiver:

A coherent receiver front-end architecture that produces a signal that is independent of the phase difference between the received signal and local oscillator signal.

Phase Noise:

The Source of sensitivity degradation in coherent lightwave systems associated with transmitter laser and local oscillator. Phase noise comes from variations or fluctuations of the phase of the emitted optical signal by both lasers.

Polarization Multiplexing, POL-MUX:

The multiplexing method of sending two independent signals, one in each polarization of the light that is sent through the channel. It doubles the capacity of the fiber.

Power Penalty:

The extra optical power required to account for degradations due to reflections impairments and ISI.

Principal States of Polarization, PSP:

The orthogonal input states of polarization for which the corresponding output states of polarization are orthogonal and show no dependence on first order wavelengths.

Quantum Limit:

A physical low bound for the BER that an optical can achieve due to the quantum nature of light.

Quantum Noise:

The uncertainty of some physical quantity due to its quantum origin. In the case of number of particles the quantum noise is also called shot noise.

Responsivity of photodiode, R:

A parameter of the photodiode than represents the ability of the device to generate an electron-hole when light hit its surface.

Shot Noise:

A fundamental noise mechanism responsible for current fluctuations in all optical receivers even when the incident optical power P_{in} is constant. It is a manifestation of the fact than an electric current consists of a stream of electrons that are generated at random times.

Spectral Efficiency:

Also "spectrum efficiency". A concept that refers to the information bit rate that can be transmitted over a given bandwidth.

State of polarization, SOP:

Accordingly to light polarization , it is the shape traced out in a fixed plane by the electric vector such that a plane wave passes over it (also known as a Lissajous figure).

Thermal Noise:

A variable current generated by the photodiode due to the fact that, at a finite temperature, electrons move randomly in any conductor. Random thermal motion of electrons in a resistor manifests as a fluctuating current even in the absence of an applied voltage. Thermal noise sets a fundamental lower limit to what can be measured.

Wave Division Multiplexing, WDM:

The multiplexing method in which multiple optical carriers are multiplexed by using different wavelengths. Therefore an independents bit stream can be sent in the same fiber, one per wavelength.

Chapter 1

1 Introduction

In this thesis a digital coherent receiver is designed and tested by simulation. These type of receptors have several advantages over receptors based on direct detection which have been used historically in optical communications. One of the properties of a coherent receiver is that it provides the possibility of using *digital signal processing* (DSP) once the signal has been detected. Using DSP techniques, a digital coherent receiver is designed that is able to compensate two traditional impairments of optical communication: chromatic dispersion and polarization mode dispersion. It is also used to track the phase of the received signal.

The transmission system scheme where the designed receptor is included is therefore coherent. A scheme of the transmission system is depicted in Figure 1-1. The signal is phase modulated in the transmitter before sending it through the transmission line. Moreover the transmitter uses a multiplexation technique, *polarization multiplexing* (POL-MUX). This technique doubles the system capacity sending two signals, one per light polarization of the light that travels through the transmission line. Therefore the transmitter sends two phase-modulated signals one per light polarization, then the designed receiver is able to detect both signals.

The idea of using coherent systems for optical transmission is not new, it was strongly studied during ‘80s [1] [2] . However technology was not cheap enough and/or advanced for the commercial deployment of optical coherent systems. Furthermore, new technologies appeared, giving great potential to traditional optical systems based on direct detection receivers. Therefore the development of optical coherent receivers was restrained.

In optical communications there are two major kinds of detectors: direct detection (DD) and coherent detection (CohD). The direct detection detector is so named because the incoming signal is detected directly with the photodiode which is the element in charge of converting the optical power into a current. These detectors can only obtain the amplitude of the signal, losing its phase. On other hand, for coherent detection the incoming lightwave is added to another lightwave coming from a local oscillator (LO) before being detected by the photodiode. This mix is lineal and the signal detected by the coherent detector preserves both the amplitude and the phase of the signal. In chapter 2 this mix between the incoming signal and the local oscillator is more profoundly discussed.

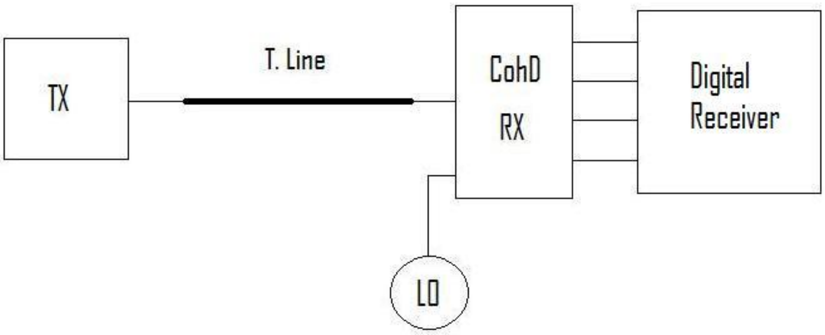

Figure 1-1. Transmission system scheme. TX - Transmitter. T. Line - Transmission line. In our case it is an optical fiber. CohD RX – Coherent detector receiver with a LO - Local oscillator. At the end is the Digital Receiver, in charge of the digital signal processing. The CohD together with the Digital Receiver is what is called Digital Coherent Receiver.

Coherent receivers have important advantages over direct detection receivers; however direct detection had been traditionally used in optical transmission systems. Direct detection is simpler than coherent detection, and the improvements that coherent detection brought in the ‘80s were not necessary since the bandwidth and capacity provided by optical systems based on direct detection were more than enough. It is now, with the increasing demand for bandwidth, that researchers are focusing their work on coherent receivers [3] .

In recent years, the increasing demand for bandwidth and the development of other technologies are again raising the interest of researchers in coherent detection. Coherent detection will provide more capacity to the optical transmission systems, providing the opportunity of using multilevel modulations. Moreover, coherent detection brings the possibility of using DSP into optical communications.

The next chapter offers a brief overview of optical communication history to discuss when coherent detectors were investigated and to explain why direct detection has overcome coherent detection despite the advantages of coherent detection. Later, in the following chapter *Motivations*, the main advantages of coherent detection are stated along with the new possibilities that coherent receivers offer nowadays; afterwards the objectives of this project are described. We finish the introduction with an overview of the project.

1.1 Historical perspective

Optical fiber has become the preferred technology for high capacity and long distance digital transmission because of its advantages: high bandwidth, low attenuation, interferences immunity and high security. The study of such systems began in 1970 and the history of its evolution is divided into generations. Each generation has included a great change that has greatly increased fiber capacity in optical fiber systems.

The first generation was utilized throughout the '70s. In this generation multimode fibers were used at low wavelengths, around 850 nm. This first generation suffered from three important limitations: high attenuation, chromatic dispersion and modal dispersion. The attenuation for 850nm was around 2dB/km, as is depicted in Figure 1-2, which was high in comparison with the attenuations that optical fiber offers at other wavelengths. Fiber *dispersion* put a limit on the velocity at which the information could be transmitted because it caused the spread of the pulses on time domain, leading to *intersymbol interference* (ISI). In this generation two kinds of dispersions are the most important: chromatic dispersion and modal dispersion. In this first generation, at the working wavelength the chromatic dispersion is high and it also suffers of modal dispersion caused by the use of multimode fibers. These systems operated at a *bit rate* (R) of 45Mb/s.

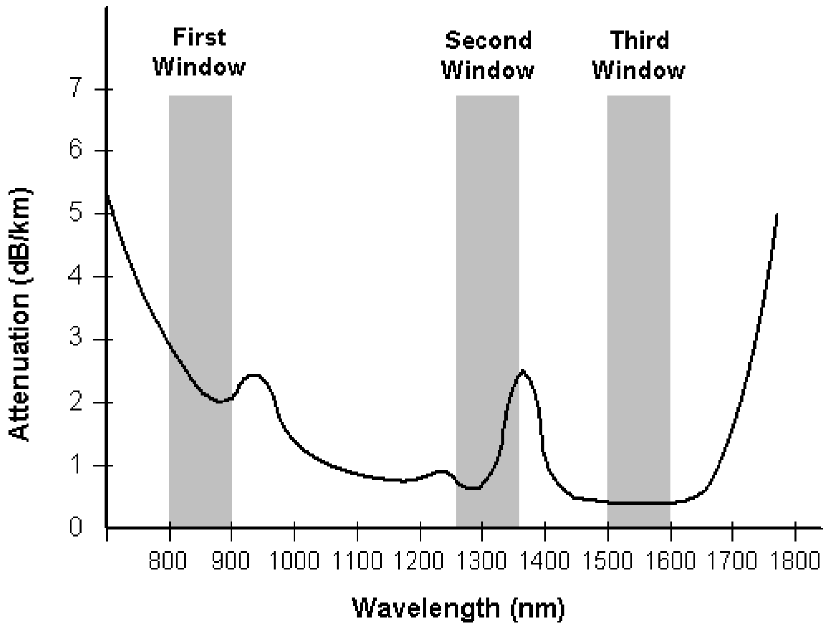

Figure 1-2. Attenuation vs. wavelength in a silicon fiber.

Second generation systems were introduced in the early '80s. They solved chromatic dispersion working in the second window at 1300 nm, the window in which chromatic dispersion acquires its lowest value. A second advantage of working at this wavelength is that the attenuation decreases to 0.5dB/km. Again this generation uses multimode fibers and still suffers from modal dispersion, but this limitation was overcome in the mid '80s with the advent of monomode fibers. In these fibers, the core radius is chosen to transmit one mode through the fiber, avoiding modal dispersion. Commercial systems based on multimode fibers achieved bitrates of 100Mb/s while systems based on monomode fibers achieved bit rates of 1.7Gb/s.

The attenuation minimum of an optical fiber, 0.2 dB/km is achieved between 1450nm and 1650nm. By exploiting this, low attenuation third generation systems appeared. They worked at 1550 nm and, because of their low attenuation, the distance between repeaters was increased. They were able to transmit at a bit rate of 10 Gb/s.

The fourth generation systems use optical amplification with *Erbium Doped Fiber Amplifiers* (EDFA) and *Wave Division Multiplexing* (WDM). Fiber capacity is therefore increased by number of WDM channels that are used. For example using 16 channels at 10 Gb/s we obtain a final velocity of 160 Gb/s.

In these four generations the reception scheme used is direct detection. Coherent detection appeared in 1980 and was studied intensely, the result being the following main properties [1] :

1. The shot-noise limited receiver sensitivity can be achieved with a sufficient local oscillator (LO) power.

2. The ability of phase detection can improve the receiver sensitivity

Both of these properties improve receptor sensitivity, leading to an increased distance between the repeaters. Moreover, the second advantage is that it introduces *multilevel modulation* in optical communication which increases the capacity of the systems. The second property also permits the use of digital signal processing techniques for impairments compensation that mainly affects to the phase of the signal as chromatic dispersion or polarization mode dispersion.

Despite these advantages, coherent detection was not used in practice because of the advent of EDFA and WDM in the early ‘90s. With EDFA, that are able to amplify optical signals in the optical domain, the distance between the repeaters was increased and the advantage 1 of coherent receivers became less significant. With WDM, fiber capacity was highly increased and the advantage of more capacity obtained using coherent receivers together with multilevel modulations was replaced by using WDM and direct detection. Thus, the two main advantages of the coherent detection scheme were offered by these two new technologies in a more efficient and economic way; therefore, the IM/DD modulation scheme has still been used in spite of the superiority of coherent reception.

1.2 Motivations and Objectives

The constant and increasing demand for bandwidth is the reason for the increased interest in coherent detection. WDM systems which first delayed the advent of coherent receptors now are augmenting the interest in such receptors. With the advent of WDM, *spectral efficiency* has become the main focus of researchers. In this context, the advantages of coherent receptors are conducive to achieving spectral efficiency limits, as multilevel modulations are very important to achieve these limits [4] . Moreover, coherent receivers nowadays offer more possibilities like the use of Digital Signal Processing(DSP) for Chromatic Dispersion(CD) and Polarization Mode Dispersion(PMD) compensation, or the ability to filter very narrow WDM channels in the electrical domain.

Maximal spectral efficiency could be achieved by combining coherent detection and WDM. The largest spectral efficiencies have been achieved using coherent detection [4] . In order to obtain the highest spectral efficiencies, multilevel modulations are required. These modulations formats can increase fiber capacity without increasing the bandwidth.

There are studies that attempt to introduce multilevel modulations formats into systems with direct detection [5] [6] , however these receivers become complex and more expensive. On the other hand, coherent receivers present a simpler architecture for these kinds of modulations.

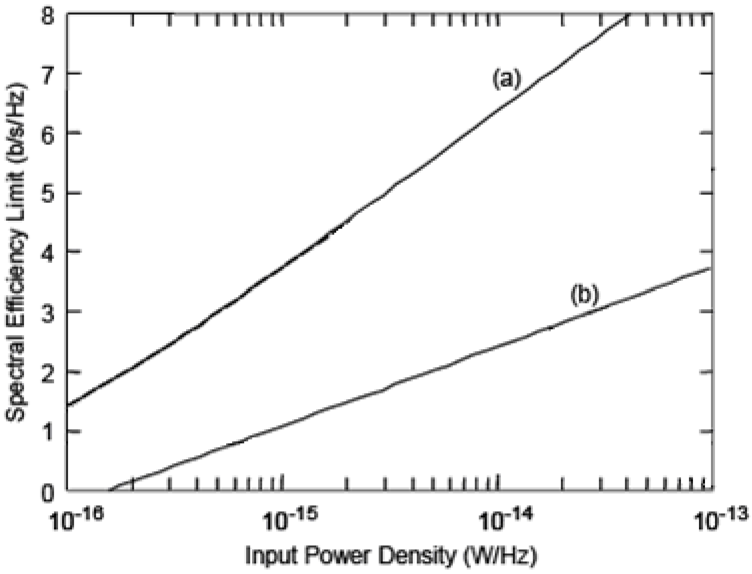

Figure 1-3. Spectral efficiency limit vs. input power density in amplified WDM systems: (a)Coherent detection, lineal (b)direct detection, lineal high SNR asymptote. Figure from [4]

Another way to increase spectral efficiency is with polarization multiplexing that can send information in both light polarizations, doubling capacity. Using coherent reception, it has been demonstrated that electrical polarization demultilpexing is feasible [7] [8] .

Another advantage of coherent receivers is their ability to filter narrow WDM channels with electrical filters.

Probably the biggest advantage of coherent detection is that it enables the utilization of DSP in optical communication systems. The improvements in high speed digital circuits and the fact that coherent receivers preserve the phase of the signal permit information processing after detection. Processing of the signal allows for phase and polarization tracking. It also provides the possibility of impairment compensation such as CD and PMD. Moreover DSP provides flexibility to the system because it is able to compensate for the frequency mismatch between the laser and the local oscillator.

It is apparent that there are many advantages that coherent reception can bring to optical communications. The present project has as its main objective, the design, implementation and testing of a digital coherent receiver. The receiver is implemented in Matlab, which allows the designed receiver to be tested afterward in VPI Transmission Maker.

The following objectives are targeted for the receiver design: a clock recovery circuit is implemented. Behind the clock recovery circuit there is to be an ADC and then the entire receiver has to be digital. It has to be capable of polarization demultiplexing and CD and PMD compensation with adaptive filters. The receiver also has to be able to estimate the phase of the signal and recover the signal from phase noise and phase shift due to the frequency mismatch between the transmitter laser and the local oscillator. It has to work with QPSK.

Once the receiver is implemented it is tested. The functionality of the receiver is tested in terms of how capable is the receiver for compensating CD and PMD, how many taps the DSP circuit needs for obtaining a certain BER or the power penalty to obtain a certain BER when a given number of taps for compensation is used.

1.3 Thesis Organization

The project begins with a presentation of the basis of optical coherent communication and some important concepts that are often used in coherent reception literature. First, a generic coherent receiver is described, differentiating between homodyne and heterodyne detection. In the next section, actual demodulation possibilities are described. Then sensitivity in coherent reception is presented and a comparison with DD is made. Also, some important concepts are introduced: shot noise and quantum limit. Thus, one of the great advantages of coherent reception is the possibility of the use of multilevel modulations, a section remarking on such modulations is included. There is also a description of polarization multiplexing, a multiplexing technology that coherent receivers can easily demultiplex using what is called a dual polarization downconverter. Later we introduce the main degradation effects on coherent reception to get a better understanding of how we compensate for some of them in our designed receiver and why our receiver cannot compensate the rest of them.

The third chapter explains the design of the digital coherent receiver implemented. First we describe the whole receiver, dividing it into 3 sections and then explaining each section individually. The first section explains how clock recovery works. In the second part, compensation in our receiver using DSP of CD and PMD is detailed. Finally, how the phase is estimated and compensated is explained. In this chapter it is described the modules that have been designed along the work done and the ones that are finally used in the receiver implemented.

The fourth chapter contains our receiver test results. First, the system where our receiver is tested is described. In the next section each module involved in the DSP of the receiver is tested individually obtaining their properties. The last part of this chapter is dedicated to the testing of the whole receiver.

The last chapter offers the conclusions obtained from the project and the ideas of the future of coherent receivers extracted from the project.

Chapter 2

2 Basic Concepts of Optical Coherent Systems

The main idea behind coherent detection is the mixing of the incoming signal with a local lightwave that allows the receiver to obtain the amplitude and phase of the incoming signal. This mixing also allows the receiver sensitivity to be improved by up to 20 dB compared with the sensitivity of IM/DD systems. How is this mixing done? Why is the sensitivity improved? How many types of coherent receivers exist?

In this chapter we respond to all these questions as well as explain important concepts related to coherent detection. We also explain and explain the basis of polarization multiplexing since it is used in our transmission system and review degradation effects that exist on optical communication since the digital coherent receiver we have designed is able to compensate for some of them. This chapter leads to a better understanding of coherent detection and the designed coherent receiver.

Before starting, a summary of the topics considered in this chapter is presented:

- In **section 2** the principle of coherent detection and cover concepts of coherent receivers as homodyne detection or heterodyne detection are described mathematically.

- In **section 2.2** different technologies behind coherent receiver architectures are shown.

- **Section 2.3** is to introduce the concept of sensitivity, one of the improvements offered by coherent receivers.

- In **section 2.4** an overview of different modulation formats supported by coherent receivers is presented.

- **Section 2.5** focuses on the basis of polarization multiplexing, a technique that is used in the transmission scheme into which the coherent receiver is introduced.

- **Section 2.6** provides a review of degradation effects in optical systems, some of which are compensated by our digital coherent receiver.

2.1 Generic Block Diagram for Coherent Reception

As previously stated, the main idea behind coherent detection is the mixing of the incoming signal with a local lightwave. The combination of the optical signal and the local optical oscillator is done with an optical coupler in front of the photodetectors. The local lightwave is generated continuously using a laser in the receiver. This laser is called the local oscillator (LO), which is a familiar term borrowed from microwave and radio systems. The main idea is to add a local oscillator signal to the incoming signal using an optical coupler. The resulting combined signal then arrives to the photodiode to be converted into an electrical signal.

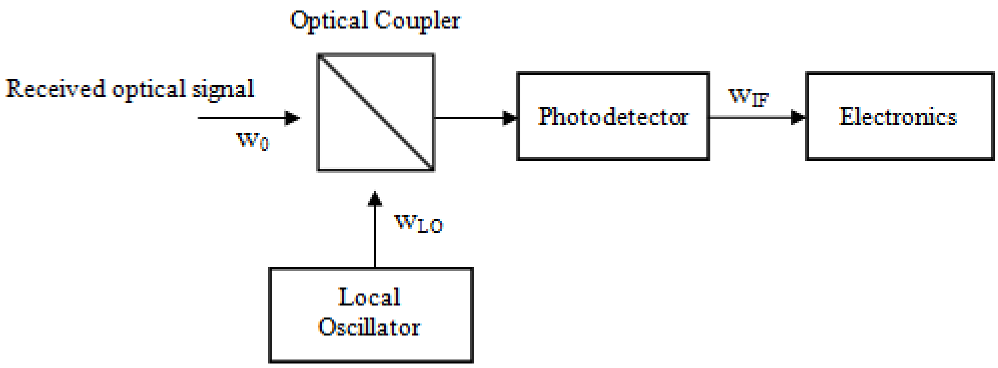

Figure 2-1. Schematic block diagram for a coherent receiver

To begin, we will consider a generic coherent receiver in which the signals are written using complex notation. Let's assume that both signals are equally polarized (polarization mismatch between the incoming signal and local oscillator is studied later in section 2.6.3)

The incoming optical signal is defined as:

$$E_S = A_S e^{-j(w_0 t + \phi_S)} \tag{2.1}$$

where w_0 is the carrier frequency, A_S is the incoming signal amplitude, and ϕ_S is the phase of the optical signal. The LO oscillator output field is expressed as:

$$E_{LO} = A_S e^{-j(w_{LO} t + \phi_{LO})} \tag{2.2}$$

where w_{LO} is the frequency of the local oscillator, A_{LO} its amplitude and ϕ_{LO} its phase.

The incoming optical signal and local oscillator signal are combined in 3dB couplers. There are different types and some different examples of receivers using different couplers will be discussed later. In order to simplify thing for now, we consider an ideal beam combiner whose output is the sum of its inputs

$$X_1 = E_S + E_{LO} \tag{2.3}$$

Let's call this signal a 'mixed lightwave' in order to indicate that the mixed signal is still a lightwave. Once the signal arrives to the photodetector it generates a current proportional to the power of the light that hits the surface of the photodetector. The expression of the photocurrent generated by the photodetector is

$$i(t) = RP_{X_1} = R|X_1|^2 \tag{2.4}$$

where R is the photodetector *responsivity*. Introducing (2.3) in (2.4) we obtain the photodetector output

$$i(t) = R(A_S{}^2 + A_{LO}{}^2) + 2RA_S A_{LO} \cos(w_{IF} t + \phi_S(t) - \phi_{LO}(t)) \tag{2.5}$$

where

$$w_{IF} = w_0 - w_{LO} \tag{2.6}$$

The w_{IF} frequency is known as the intermediate frequency. In expression (2.5) no noise introduced by the detector is included (important photodetector noise, like shot noise, is briefly studied in point 2.2). The information in (2.5) is carried by the second term while the first term is a constant.

Depending on whether w_{IF} is equal to zero or not there are two different coherent detection techniques: homodyne and heterodyne detection respectively.

2.1.1 Homodyne Detection

In this coherent detection technique, the local oscillator frequency w_{LO} is selected to match the carrier frequency w_0. Thus the intermediate frequency w_{IF} is zero, which means that the received signal is baseband detected. Applying that w_{IF}=0 to equation (2.5) is obtained the expression for homodyne detection:

$$i_{ho}(t) = R(A_S{}^2 + A_{LO}{}^2) + 2RA_S A_{LO} \cos(\phi_S(t) - \phi_{LO}(t)) \tag{2.7}$$

The first term is a constant that, following this model, cannot be precluded as the signal is baseband. We focus our attention on the expression carrying the information:

$$i_{ho\_f}(t) = 2RA_S A_{LO} \cos(\phi_S(t) - \phi_{LO}(t)) \tag{2.8}$$

From this expression can be noticed the coherent detection advantages mentioned above in the introduction. Can be seen that the phase of the signal is preserved, from which is inferred that multilevel modulations are feasible using coherent detection since we can not only introduce information in the amplitude of the wave but also into the phase and frequency of the signal. The other main advantage of coherent detection that was mentioned was the increased sensitivity such receivers have. Let us write equation (2.8) in terms of signal power,

$$i_{ho\_f}(t) = 2R\sqrt{P_S P_{LO}} \cos(\phi_S(t) - \phi_{LO}(t)) \tag{2.9}$$

We notice that if the local oscillator signal power P_{LO} is high, the power of the received signal is increased. However, shot noise is also increased, but the SNR is improved by a large factor, almost 20 dB better than in direct detection. This was one of the most important advantages of coherent receivers that were discovered in the '80s. The advent of EDFA's overcame this property; with such amplifiers, the SNR in reception was not a problem anymore. Another important advantage of homodyne detection is that it uses very low bandwidth since it downcoverts the incoming signal directly into baseband. Homodyne detectors use bandwidths around the bit rate of the signal.

The disadvantages of homodyne detection come from its phase preservation since it not only detects the incoming signal phase ϕ_S, but the local oscillator phase ϕ_{LO} as well. Ideally, both phases should stay constant except the phase modulation or phase information inside ϕ_S but in practice both phases fluctuate randomly over time. To clarify, if we have a phase modulated signal then $\phi_S(t) = \phi_M(t) + \phi_N(t)$ where $\phi_M(t)$ is the modulated phase information and is constant during a symbol period while $\phi_N(t)$ is the phase noise coming from fluctuations of the phase by the transmitter. If we introduce this in eq. (2.9) we obtain the following equation:

$$i_{ho\_f}(t) = 2R\sqrt{P_S P_{LO}} \cos(\phi_M(t) + \phi_{S-N}(t) - \phi_{LO}(t)) \tag{2.10}$$

Where ϕ_M is the modulated phase, ideally otro $\phi_{S-N}(t) - \phi_{LO}(t) = 0$, but normally the term is not zero and the phase information ϕ_M is blurred. This is called *phase noise* and is also present in heterodyne detection. Let us use $\phi_{S-N}(t) - \phi_{LO}(t)$ or ϕ_N indistinctly to refer to the phase difference between the signal and the local oscillator. Traditionally, to solve this issue in homodyne detection ϕ_{LO} is forced to be close to ϕ_{S-N} using an optical phase-locked loop (OPLL). These loops are complicated and expensive and can be avoided using heterodyne detection. Phase noise is treated deeply in section 2.6.4.

2.1.2 Heterodyne Detection

In heterodyne detection the local oscillator frequency w_{LO} is not matched with w_0 so the signal is detected around an intermediate frequency w_{IF} (2.6). The general equation for heterodyne detection is equal to (2.5), therefore from (2.5), since the first term of that equation is a DC term that can be filtered using a bandpass filter, if we write the expression again in terms of signal power, the following expression for the heterodyne information signal is obtained

$$i_{he\_f}(t) = 2R\sqrt{P_S P_{LO}}\cos(w_{IF}t + \phi_S(t) - \phi_{LO}(t)) \tag{2.11}$$

It is also feasible to send information in amplitude, phase and frequency using this signal. Moreover, we can still using use the local oscillator power to amplify the received signal, improving the SNR. However, the enhancement is 3 dB lower than in homodyne detection. This power penalty difference between homodyne and heterodyne detection does not exist in coherent microwave systems, so where does this power penalty in optics come from?. According to [10] : the demodulation of a modulated waveform requires the translation of the signal's spectrum from the carrier down to zero frequency; this translation is also applied to the surrounding noise doubling the noise density. In homodyne, the translation is done in one step from w_0 directly to zero. However, in heterodyne this translation is done in two steps: first from w_0 to w_{IF} and then from w_{IF} down to zero using an electrical oscillator/mixer (see 2.1.3). Since heterodyne has one more translation than homodyne, this additional translation doubles the noise density as compared to homodyne detection. Therefore the SNR in heterodyne is 3 dB worse than homodyne's. In microwave communication this is solved by prefiltering the signal before the mixing, avoiding the 3dB difference between both demodulation techniques. The problem is that in optical systems prefiltering does not work. Prefiltering works in microwaves systems since noise is generated before the mixer. The difference is that in optical systems noise in generated during the mixing, making prefiltering useless.

The advantage gained at the expense of the 3dB penalty is that no OPLL is needed, making the design simpler and cheaper. Another disadvantage of heterodyne receivers is that they require bandwidths of 5xRb, Rb being the bit rate of the signal. Thus for high bit rate systems homodyne detection is preferred with bandwidths of Rb.

2.1.3 Demodulation Schemes

According to [9] , in optical systems the term 'coherent' is used to describe every system that uses a local oscillator to demodulate the incoming signal. The classical meaning of coherent detection is the use of the carrier frequency and phase in the detection process. To avoid confusion, the classical meaning has its own term in optical systems: synchronous. In optical communication a synchronous receiver is a receiver that uses a technique to detect the carrier frequency and phase for downcoverting the signal into baseband. Therefore 'asynchronous' describes receivers that do not need to know the receiver carrier frequency or phase. Heterodyne coherent optical receivers can be either synchronous or asynchronous while homodyne coherent optical receivers are synchronous.

As we said homodyne detection requires a local oscillator that matches its frequency with the signal carrier frequency and whose phase is locked to the incoming signal. Thus homodyne detection is by nature synchronous. On the other hand, heterodyne detection could have a synchronous or asynchronous demodulation scheme.

Figure 2-2 shows a schematic synchronous heterodyne receiver. The current generated by the photodetector passes through a band-pass filter (BPF) centered at the intermediate frequency w_{IF}.

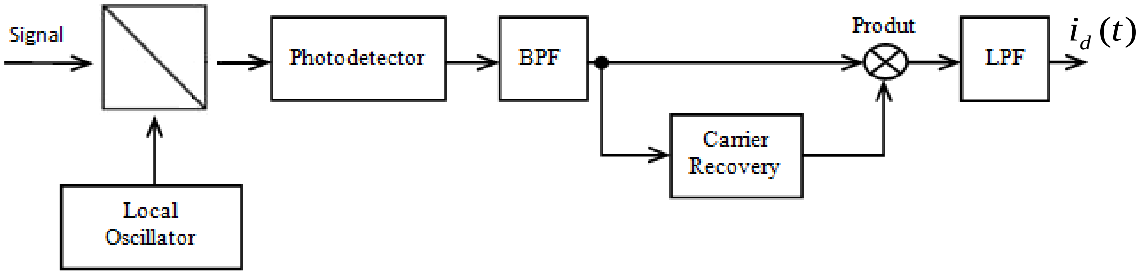

Figure 2-3. Block diagram for a synchronous heterodyne receiver

The filtered current has the same form as (2.11) if noise is not considered. As defined for synchronous schemes, a carrier recovery is used to downcovert the signal from the intermediate frequency into baseband. Since the signal is already in the electrical domain several schemes can be used for that purpose; for example, using just before the BPF and ADC, also digital solutions can be used to obtain the intermediate carrier frequency w_{IF} using a digital carrier recovery. The final signal obtained just after the low-pass filter is:

$$i_d(t) = R\sqrt{P_S P_{LO}}\cos(\phi_S(t) - \phi_{LO}(t)) \tag{2.12}$$

This is 3 dB worse than a homodyne case.

A much simpler heterodyne receiver is shown schematically in Figure 4. This type of receiver does not require the recovering of the intermediate frequency in order to convert the electrical signal into baseband, and thus is an asynchronous receiver. In order to downconvert the signal, an envelope detector is used. After the BPF, the filtered signal $i_f(t)$, with the same form as (2.11) if noise is not considered, passes through the envelope detector. Let us call the electrical signal at the output of the envelope detector i_{ed} (t):

$$i_{ed}(t) = |i_f(t)| = 2R\sqrt{P_S P_{LO}} \tag{2.13}$$

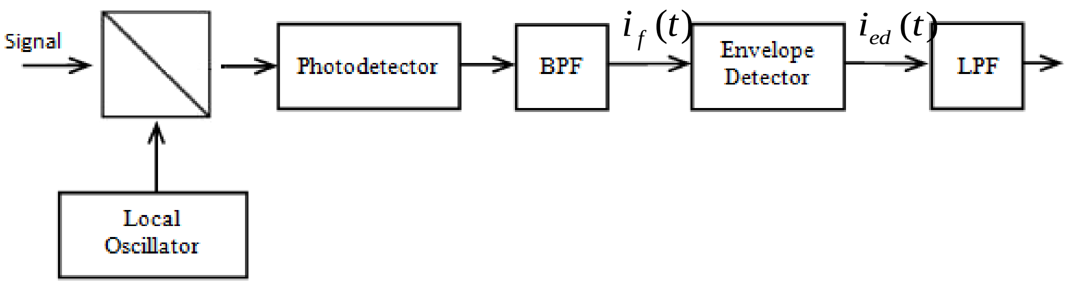

Figure 2-4. Block diagram of an asynchronous heterodyne receiver

These detectors cannot be used with PSK modulation format because the phase is ignored.

2.2 Front-end Architectures for Coherent Receiver

The coherent receiver described in 2.1 adds a LO lightwave to the received signal using an ideal beam combiner. This addition, in practice, is commonly implemented using a 3 dB coupler, a standard lossless network. There are many types of 3 dB couplers with four, six or more ports, these couplers are often named depending on the phase difference between their outputs. Let's consider the same inputs as in the ideal scheme: E_S and E_{LO}, described by equations (2.1) and (2.2) respectively. In order to characterize using a 3 dB coupler the coherent receiver previously described in 2.1 we need a 180º Hybrid. This is a device in which the outputs are equal to the sum and difference of its inputs, so we can perform the sum of the incoming signal and the local oscillator. The coupler matrix representation of a 180º optical hybrid is the following:

$$C = \frac{1}{\sqrt{2}} \begin{bmatrix} 1 & 1 \\ 1 & -1 \end{bmatrix} \tag{2.14}$$

If the inputs and outputs are represented by complex columns, vectors E=[E_S E_{LO}]´ and X=[X_1 X_2]´ respectively, then X = CE so the outputs of the 180º Hybrid are:

$$\begin{aligned} X_1 &= (E_S + E_{LO}) / \sqrt{2} \\ X_2 &= (E_S - E_{LO}) / \sqrt{2} \end{aligned} \tag{2.15}$$

As we can see, the output X_1 is equal to the sum of the inputs divided by the square root of two. Therefore, output X_1 performs the sum between the incoming signal and the local oscillator that we need for coherent detection but rated by $\sqrt{2}$. This is because of the behavior of the 180º hybrid; it divides the output power between its two outputs.

The most simple method to perform the mixing between the received optical signal and the local lightwave, therefore, is to use only output X_1 of a 180º hybrid to obtain the sum of the signal and the local oscillator and then use a photodiode to convert it from the optical to the electrical domain and perform the final mixing of both signals. An example of this architecture is shown in Figure 2-5 (a). Using this front-end architecture, the photocurrent i(t) produced by the photodiode is half the predicted one in equation (2.5) for the ideal coherent detection:

$$i(t) = \frac{R}{2}(A_S{}^2 + A_{LO}{}^2) + RA_S A_{LO} \cos(w_{IF} t + \phi_S(t) - \phi_{LO}(t)) \tag{2.16}$$

This is not surprising as it has been explained by the fact that half of the incoming input power is thrown away by the 180º optical hybrid because the second output is not used.

We can improve these results by using both outputs of the 180º optical hybrid, thereby no optical power is lost in the optical coupling process. For that purpose, balanced detector architecture can be used. This architecture is depicted below in Figure 2-5(b).

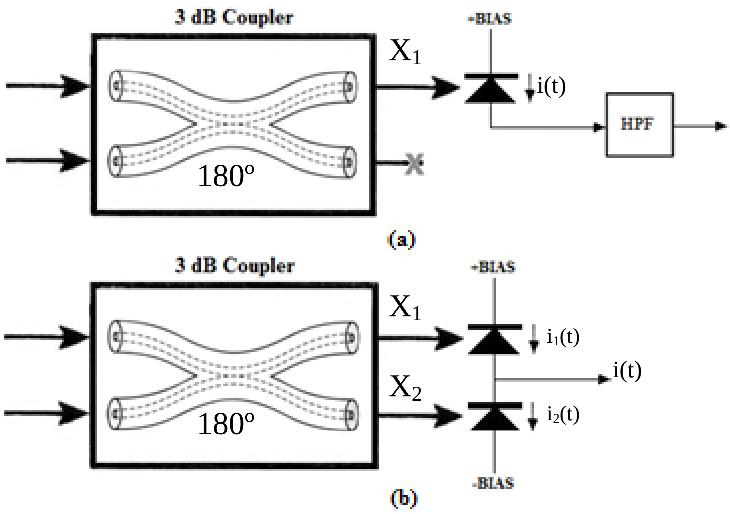

Figure 2-5. Front-end mixing architectures for optical coherent receivers. (a) A single detector using a 3dB coupler or 180º Hybrid (b) Balanced detector in which all the input power is used

In this case the final photocurrent generated at the end of the detection is provided by the following equation:

$$i(t) = i_1(t) - i_2(t) = R(|X_1|^2 - |X_2|^2) \tag{2.17}$$

Where $i_1(t)$ is the photocurrent generated by the photodiode at the first output of the optical coupler and $i_2(t)$ is the photocurrent generated by the photodiode that is hit by the lightwave coming from the second output of the optical coupler.

Introducing (2.15) into (2.17) reveals that the photocurrent generated using balanced detection is given by the expression below:

$$i(t) = 2RA_S A_{LO} \cos(w_{IF} t + \phi_{IF}(t)) \tag{2.18}$$

Last expression reveals that it has the same form as the photocurrent of the ideal scheme, equation (2.5), moreover, it does not have the constant term which is not of our interest and otherwise would be removed with a filter. Therefore, balance detection is even better than the ideal method showed in section 2.1 because in the photodetection process of a balance detector the filtering of the constant term is done without the necessity of a filter.

Balanced detection, therefore, makes more efficient use of the LO and received signal power than a single detector, and does not need a HPF to eliminate the DC term.

Another kind of front-end is named *phase diversity receiver* [11] [12] .It is showed this receiver using a 90º optical hybrid [13] .

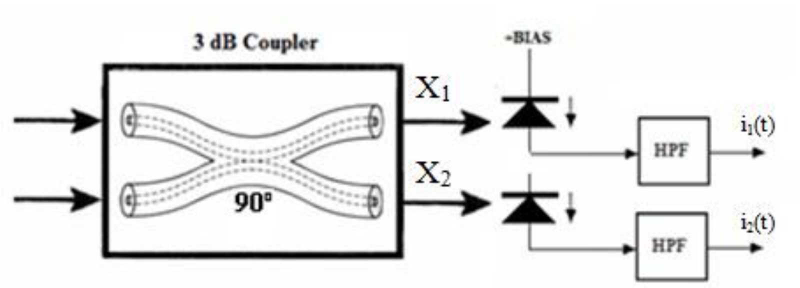

Figure 2-6. Phase diversity receiver front-end using a 90º optical hybrid

Considering the same signals that we have been using for the incoming lightwave and local oscillator and knowing that the 90º optical hybrid is defined by the following matrix

$$C = \frac{1}{\sqrt{2}}\begin{bmatrix} 1 & 1 \\ 1 & -1 \end{bmatrix} \tag{2.19}$$

then the outputs of the 90º Hybrid are

$$\begin{aligned} X_1 &= (E_S + E_{LO})/\sqrt{2} \\ X_2 &= (E_S + jE_{LO})/\sqrt{2} \end{aligned} \tag{2.20}$$

and finally, the currents filtered by the HPF are

$$\begin{aligned} i_1(t) &= RA_S A_{LO} \cos(w_{IF} t + \phi_{IF}) \\ i_2(t) &= RA_S A_{LO} \sin(w_{IF} t + \phi_{IF}) \end{aligned} \tag{2.21}$$

where ϕ_{IF} is the phase difference between the received signal and the local oscillator. These two currents are normally digitalized for processing them. Phase diversity receivers are often used to obtain a signal that is independent from the phase difference ϕ_{IF} by squaring each branch i_1(t), and i_2(t), before adding them together. As such, the resulting signal that only depends on the amplitude. This method can be useful for ASK, FSK and DPSK modulations formats.

Phase-diversity receivers can also be utilized with multilevel phase modulations as PSK since the currents obtained after the filtered currents i_1(t) and i_2(t) are the in-phase and quadrature components of the optical received signal as can be seen in eq. (2.21). The problem here is that, as we see in eq. (2.10), that the phase information would be blurred by phase noise from non-ideal behavior of the lasers. Another issue of the phase diversity receiver is the fact that, like the single detector, currents are half powered compared to the ideal case. That causes a loss of 3dB compared to the balanced detector. One solution to this issue is to use both technologies together: a balanced detector and phase diversity receivers.

Phase diversity receivers combined with balance detection is known as a phase diversity balanced detector. It can be implemented using a six port 90º optical hybrid in which the first two branches are for obtaining the in-phase component of the received signal using balanced detection and the second two branches for the quadrature component using balanced detection again.

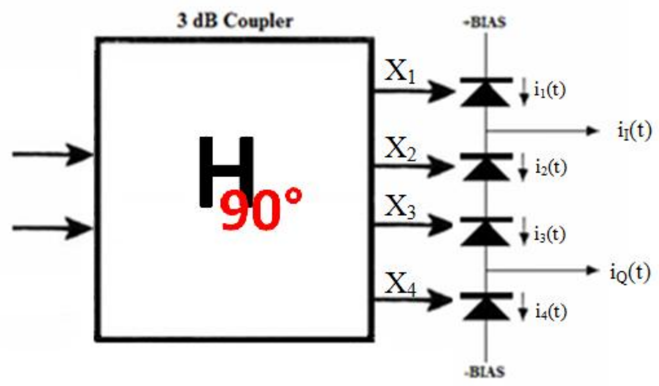

Figure 2-7. Phase diversity balanced detector

This optical coupler has the following matrix:

$$C = \frac{1}{\sqrt{2}}\begin{bmatrix} 1 & 1 \\ 1 & -1 \\ 1 & j \\ 1 & -j \end{bmatrix} \tag{2.22}$$

As can be inferred from the coupler matrix, the outputs of the coupler provide the first input intact while they shifts the local oscillator lightwave: 180º in the second branch, 90º in the third output and 270º in the third output.

Combining the operation for balanced detection and phase diversity receivers the currents obtained are:

$$\begin{aligned} i_1(t) &= RA_S A_{LO}\cos(w_{IF}t + \phi_{IF}) \\ i_2(t) &= -RA_S A_{LO}\cos(w_{IF}t + \phi_{IF}) \\ i_3(t) &= RA_S A_{LO}\sin(w_{IF}t + \phi_{IF}) \\ i_4(t) &= -RA_S A_{LO}\sin(w_{IF}t + \phi_{IF}) \end{aligned} \tag{2.23}$$

Finally, the two currents given by this method are the in-phase and quadrature component of Es:

$$
\begin{aligned}
i_I(t) &= 2RA_S A_{LO}\cos(w_{IF}t + \phi_{IF}) \\
i_Q(t) &= 2RA_S A_{LO}\sin(w_{IF}t + \phi_{IF})
\end{aligned}
\tag{2.24}
$$

With this architecture we obtain the advantages of phase-diversity receivers together with the power advantage of balance detection. This front-end architecture is the one proposed for the design of the digital coherent receiver.

2.3 Photodetector Sensitivity

One of the best advantages of optical coherent receivers is the improvement in sensitivity over direct detection receivers. In this section we will introduce the basis for the understanding of the concept of sensitivity and the concept of quantum limit is also defined, which is the physical limit of sensitivity in optical receivers due to quantum nature of light. Later in this chapter, sensitivity in direct detection receivers is defined for later comparison with coherent detection receivers. Before that, some noise basics are briefly introduced to provide a better understanding of this section.

Light is a form of electromagnetic radiation and it can be represented by its electric and magnetic fields. It is affirmed that light is also a group of particles called photons where each photon has an energy (in Jules) of

$$Photon_{Energy} = h\upsilon \tag{2.25}$$

where h is Planck's constant (6.626 x 10^{-34} J·s) and υ the cyclical frequency of the light.

The emitted optical wave can be described as a function of the power of the wave as

$$E_S = A_S e^{-j(w_0 t + \phi_S)} = \sqrt{P_S}\, e^{-j(w_0 t + \phi_S)} \tag{2.26}$$

where P_S is the average power in Joules emitted in one second. From (2.26) can be inferred that:

$$P_S = A_S{}^2 \tag{2.27}$$

Then, can be stated that the average number of photons emitted is

$$\lambda_p = \frac{P_S}{h\upsilon}(photons/\sec ond) \tag{2.28}$$

The exact time at which each photon is emitted from the light source cannot be predicted since the emission times of the photons are randomly distributed following a Poisson process [15] .

Let's consider an **ideal direct detection system**. It is an amplitude modulated transmission system over an ideal fiber with an ideal photon counter receiver. This photon counter receiver ideally counts the number of photons that arrive in a bit interval. In this system the transmitter sends a pulse of light when ONE is transmitted and no light when ZERO is transmitted, therefore, the probability of receiving any photon when zero is transmitted is zero. When one is transmitted, the probability of receiving N photons in T seconds is given by the Poisson distribution

$$P[Nphotons|ONE] = \frac{(\lambda_p T)^{Nphotons} e^{-\lambda_p T}}{N!} \tag{2.29}$$

where T is the bit duration. This means that exist a certain probability of receiving zero photons when a ONE has been sent, $P[0\,photons|ONE]$. This fact leads to a probability of bit error or bit error ratio (BER) and dictates that the ideal case has an important lower bound in the BER called *quantum limit:*

$$BER_Q = P[0\,photons|ONE] = \frac{1}{2}e^{-\lambda_p T} = \frac{1}{2}e^{-N} \tag{2.30}$$

where $N = \lambda_p T$ is used to simplify the expression and represents the expected number of photons per ONE bit. There is also a third common way to write the expression for the quantum limit, using the optical energy P_{DD} which is equal to the average number photons per bit $\overline{N}$:

$$P_{DD} = \overline{N} = \frac{1}{2}(\lambda_p T) + \frac{1}{2}(0) = \frac{1}{2}N \tag{2.31}$$

Therefore, eq. (2.30) can also be written as:

$$BER_Q = \frac{1}{2}e^{-2\overline{N}} = \frac{1}{2}e^{-2P_{DD}} \tag{2.32}$$

Now let's consider an **ideal homodyne coherent receiver**, where any kind of noise is neglected and it is assumed that $A_{LO} = A_S$. In this case we consider a photodiode and not an ideal photon counter as in the ideal direct detection scheme. Let's assume that the responsivity of the photodiode is one. Therefore, the BER is going to be obtained as a function of the power given by the photodiode.

As in coherent receivers, there is a previous step for mixing both the incoming and the local lightwave. Can be easily calculated from eq. (2.7) that the power of the current generated by the photodiode in homodyne coherent detection is A_S^2 and using eq. (2.27) the following equality is found:

$$P_{Coh} = 2{A_S}^2 = 2P_{DD} \tag{2.33}$$

This expression tells that the power provided by the photodiode in homodyne coherent detection is twice the size of the power in the ideal direct detection scheme. Using eq. (2.32) and eq. (2.33), the following expression is obtained:

$$BER_Q = \frac{1}{2}e^{-P_{Coh}} = \frac{1}{2}e^{-2P_{DD}} \tag{2.34}$$

Previous equation indicates that in order to obtain the same BER, the direct detection scheme needs twice the power needed for obtaining the same BER in the coherent detection scheme. From another point, the homodyne coherent scheme has a 3dB improvement over the quantum limit obtained in the ideal direct detection scheme. This result is often referred to as the “super quantum limit” and it comes from the assumption that the exact frequency, phase and magnitude of the transmitter laser is known.

If the ideal requirements are relaxed and the LO amplitude can be chosen randomly (though it must be higher than the transmitted signal amplitude), it implies that a more realistic result is obtained. To estimate the BER in this situation should be considered that, under *shot noise* limited systems, the output of the photodiode is well-approximated by a white gaussian noise process. Under this assumption, it can be proved that the resulting BER is approximately the quantum limit [15] . This is again possible by the availability of a large local oscillator optical power. In a similar way, could be proved that in an ideal heterodyne detector the BER is 3 dB worse than the quantum limit. Table 1 summarizes the asymptotic performance of the ideal receivers discussed above:

Table 1. Asymptotic performance of ideal receivers

BER of Ideal Performance Receivers	
Quantum limit	$BER = \frac{1}{2}e^{-2P}$
Super quantum limit	$BER = \frac{1}{2}e^{-4P}$
Ideal Homodyne Receiver	$BER = \frac{1}{2}e^{-2P}$
Ideal Heterodyne Receiver	$BER = \frac{1}{2}e^{-P}$

Quantum limit is often used as a benchmark when measuring the sensitivity of other digital receiver structures. It dictates the minimum signal power required by an OOK receiver to achieve a given BER. For example, in order to obtain a BER of $10e^{-9}$, N =20 photons per ONE bit are needed, or an average of $\overline{N}$ =10 photons/bit.

The quantum limit is in fact the ideal case for a direct detection receiver, unfortunately an ideal element for counting photons does not exist. Thus photodiodes are used, which inevitably introduces additional noise. The most commonly used type of photodiodes are p-i-n photodiodes and avalanche photodiodes(APD). Both operate under the same basic principles; the incident photons are absorbed by the photodiode surface, creating an electron-hole pair. The average number of incident photons that generate an electron-hole is denoted as *quantum efficiency*, whose symbol is η . It is close to one for p-i-n diodes and 0.5 for APDs. The difference between both kind of photodiodes is that the resulting current is larger in APD than in p-i-n by a gain factor G between 30 and 100 [15] . Therefore APDs are usually utilized on IM/DD systems because the incoming lightwave power is normally weak, however, this extra gain that APD photodiodes provide, also induces some statistical fluctuations that increase the noise. On the other hand, as we already know, coherent receivers increase the power of the received signal before the photodetector through its mixing with the local oscillator, making APDs unnecessary. Thus, in coherent receivers the light hitting the surface of the photodiode is strong enough, and therefore, the more quantum efficient and less noisy p-i-n diodes are used for such receivers

Let's compare a more realistic model for direct detection with the previous quantum limit obtained. For that purpose a more realistic model for p-i-n photodiodes is used in which the current generated has some noise parameters,

$$i(t) = RX_1 + n(t) + n_0(t) \tag{2.35}$$

where R is the photodiode responsivity, n(t) is shot noise and $n_0(t)$ describes other noise sources like dark current and *thermal noise*. Dark current is caused by the fact to the fact that photodiodes produce spontaneous electron-hole pairs regardless of the presence or absence of incident photons.

Using the realistic photodiode model for the IM/DD receiver with the following typical parameters [10] : quantum efficiency η=1, dark current I_{dk}=10nA , thermal current PSD N_{th}= 1pA^2/Hz, bit rate = 100 Mbps, and wavelength λ = 1500 nm; is obtained that the performance of the practical receiver is much worse than quantum limit and about 25 dB more power is needed for BER = 10^{-9} .A comparison between quantum limit and this real receiver can be seen in Figure 2-8 .However, there are ways to improve the sensitivity of IM/DD receivers, such as using APD instead of p-i-n, since practical IM/DD receivers still cannot achieve the performance level predicted by the quantum limit.

Quantum limit tells us that direct detection needs 10 photons/bit to operate at BER 10^{-9}, though this is never achieved by a real IM/DD receiver mainly because of thermal noise, dark current and other factors which degrade the sensitivity to the extent that $\overline{N}$ >1000 photons/bit is usually required. In the case of coherent receivers, $\overline{N}$ <100 can be accomplished simply because shot noise can be made dominant by increasing the local oscillator power. Normally, photodiode noise is dominated by thermal noise but, when the local oscillator power is high the signal arriving to photodiode is high, in which case dark current and thermal noise are negligible compared to the shot noise being the photodiode in the shot-noise limited case [9] . In next section coherent receiver sensitivities are presented for different modulation formats.

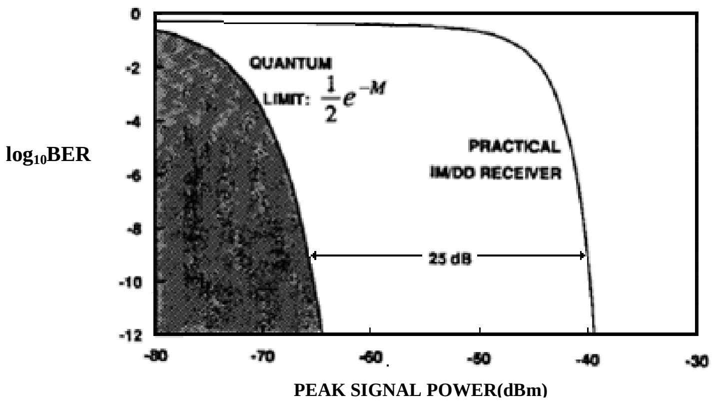

Figure 2-8. BER curves for an ideal photon counter receiver and a practical IM/DD p-i-n receiver with following characteristics: $\eta=1$, $I_{dk}=10nA$, thermal current PSD $N_{th}= 1pA^2/Hz$, bit rate=100 Mbps, and $\lambda=1500$ nm [10]

2.4 Modulation formats

Since coherent receivers maintain the phase of the received signal, they provide the possibility of sending information in the phase of the signal. Therefore coherent receivers can send information in the amplitude, phase and frequency of an optical carrier. In this section we will discuss the three possibilities for modulating the signals in optical communications: ASK, PSK and FSK.

ASK

ASK means Amplitude Shift Keying. It is a form of modulation that represents digital data as variations in the amplitude of a carrier wave. The amplitude modulated signal, taken the real part of eq. (2.1), can be written as follows:

$$E_S = A_S(t)e^{-j(w_0 t+\phi_S)} \tag{2.36}$$

where $A_S(t)$ indicates that the amplitude changes with time, carrying the information while the frequency and phase of the signal are kept constant. For example, in binary modulation, $A_S(t)$ can take one among two fixed values during a bit period T for sending information ONE or ZERO. In most practical situations, $A_S(t)$ takes the value 0 for sending ZERO. The ASK format in such an example is called on-off keying (OOK) and is identical to the commonly used modulation scheme for direct detection based systems IM/DD.

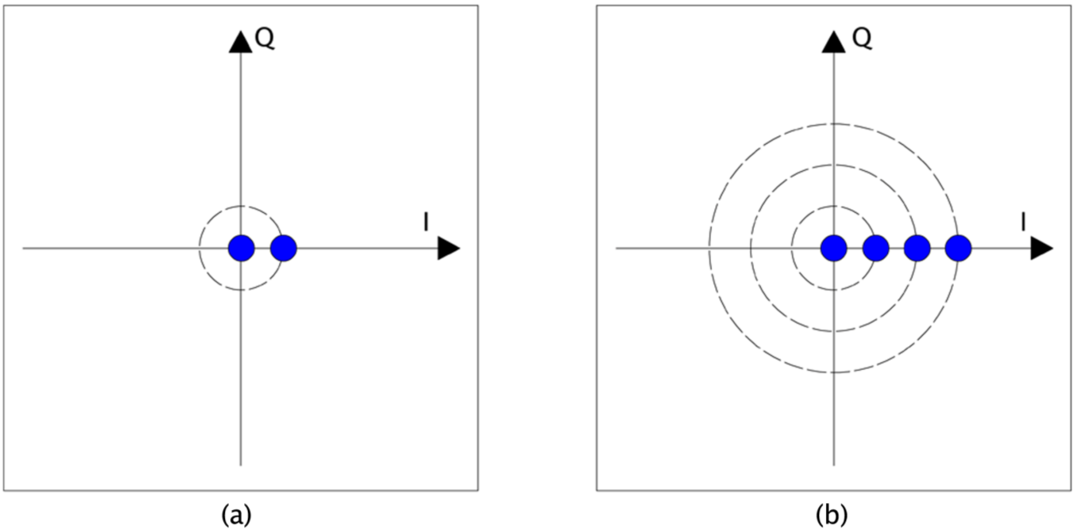

Figure 2-9. Constellations for ASK modulation (a) OOK (b) Four levels ASK

The implementation of ASK differs from IM/DD in that ASK requires external modulation. In IM/DD the light-transmitter is directly modulated but in ASK this cannot be done since direct modulation of a laser induces some phase changes. For IM/DD systems, phase changes are not important because photodetectors are not sensitive to them. On the other hand, coherent receivers depend strongly on the phase of the receiver signal since it is recovered using the local oscillator. Therefore the implementation of the ASK modulation format requires the phase ϕ_S to remain nearly constant.

PSK

Phase-shift keying (PSK) is a digital modulation scheme that conveys data by changing, or modulating, the phase of a reference signal (the carrier wave). In the case of PSK format the information is coded on the phase of the optical signal while the amplitude and frequency are kept constant

$$E_S = A_S e^{-j(w_0 t + \phi_S(t))} \tag{2.37}$$

For binary PSK, the phase takes two values: 0 and π for ONE and ZERO respectively, as can be seen on Figure 2-11(a). The sensitivity of such modulation is even better than the quantum limit. An interesting aspect of PSK modulation is that the optical intensity remains constant and therefore, the amplitude decision thresholds remain constant.

For PSK modulation format in the transmitter, an external modulator capable of changing the optical phase in response to an applied voltage is needed, the physical mechanism to achieve that is called electrorefraction [9] .

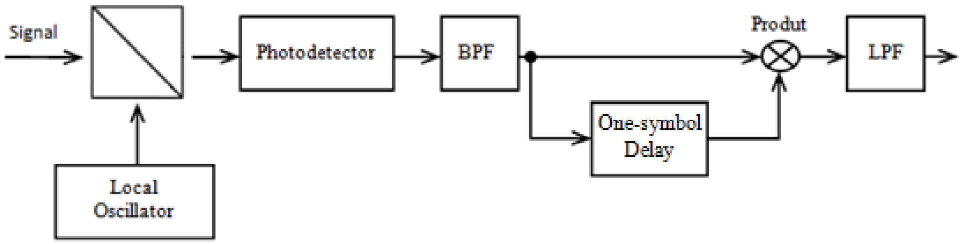

Figure 2-10. DPSK asynchronous heterodyne receiver

For the demodulation of PSK signals, coherent detection is needed since it has the information coded on the phase. With direct detection the phase is lost, so a coherent receiver using a local oscillator is needed to receive the phase of the signal. The demodulation of PSK format can be done with homodyne and heterodyne synchronous receivers but not with an asynchronous one, since this scheme ignores the phase of the signal as shown in 2.1.3.

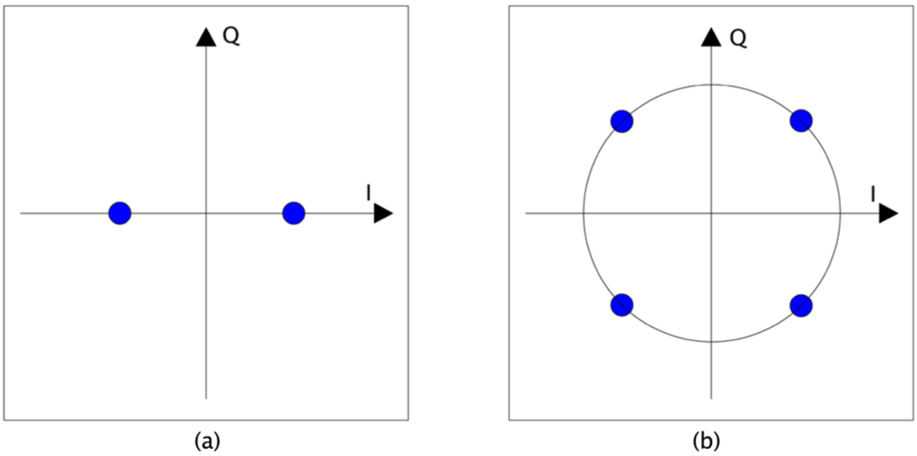

Figure 2-11. PSK constellations examples.(a) Binary PSK. (b) QPSK

The use of the PSK format requires that the phase of the optical carrier remains stable so that the phase information can be extracted at the receiver without ambiguity; this requirement puts a stringent condition on the tolerable linewidths of the lasers involved. This requirement can be relaxed if differential PSK(DPSK) is utilized. In differential modulation the information is encoded in the phase difference between consecutive symbols and the signal can be demodulated successfully as long as the carrier phase remains relatively stable over the duration of the two symbols involved. For the implementation of DPSK, a variation of the asynchronous heterodyne receiver is required. In this scheme, depicted in Figure 2-10, the idea is to multiply the received bit array with a replica of it that is delayed one symbol. The resulting signal then has a component of the form Φ_k-Φ_{k-1} where Φ_k is the phase of the symbol k. Since DPSK guards the information in the phase difference the bit pattern can be recovered.

Table 2. Sensitivity of synchronous receivers [9]

MODULATION FORMAT	N	$\overline{N}$
Direct Detection	20	10
ASK heterodyne	72	36
ASK homodyne	36	18
PSK heterodyne	18	18
PSK homodyne	9	9
FSK heterodyne	36	36

Table 3. Sensitivity of asynchronous receivers [9]

MODULATION FORMAT	N	$\overline{N}$
Direct Detection	20	10
ASK heterodyne	80	40
FSK heterodyne	40	40
DPSK heterodyne	20	20

FSK

In Frequency-shift keying **(**FSK) modulation, the information is coded on the optical carrier by shifting the carrier frequency. For example in a binary signal w0 takes two values, $w_0+\Delta w$ and $w_0-\Delta w$, depending on whether ONE or ZERO is transmitted.

$$E_S = A_S e^{-j((w_0 \pm \Delta w)t + \phi_S)} \tag{2.38}$$

The shift $\Delta f = \Delta w/2\pi$ is called frequency deviation. Depending on the frequency deviation FSK uses more or less bandwidth. The total bandwidth used by the FSK modulation format is $2\Delta f+2B$ where B is the bit rate. There are two cases that depend on the frequency modulation $\beta= \Delta f/B$; if $\beta>>1$ means that $\Delta f>>B$, this case is called wide deviation and the bandwidth required is high being approximately $2\Delta f$. The other case, called narrow-deviation, is when $\Delta f<<B$, in this case $\beta<<1$ and the bandwidth approaches 2B.

FSK demodulation schemes require some modifications of the schemes presented in chapter 2.1.3. FSK demodulation can be homodyne or heterodyne, synchronous and asynchronous. For synchronous detection two branches are needed in what is known as a correlator receiver. This receiver correlates the received signal with the two expected signals (one in each branch), two because we are considering binary modulation, and chooses the symbol corresponding to the branch with a larger correlation. If N-FSK modulations are used, then N branches are required.

If asynchronous detection is chosen, the scheme showed in Figure 2-4 with some modification is used, as depicted in Figure 2-12. Again two branches are needed (if binary FSK modulation is considered) one per each possible modulation frequency. In each branch a filter centered in the modulation frequency is used. This scheme can be used if the tone spacing is much larger than the bit rates, so that the spectra of ONE and ZERO do not overlap. Also one branch can be used like FSK receiver if the bandwidth is chosen to be wide enough to pass the entire bit stream. The signal is then processed by a frequency discriminator to identify ONE and ZERO bits. This last scheme works well only for narrow-deviation FSK for which tone spacing is less than or comparable to the bit rate.

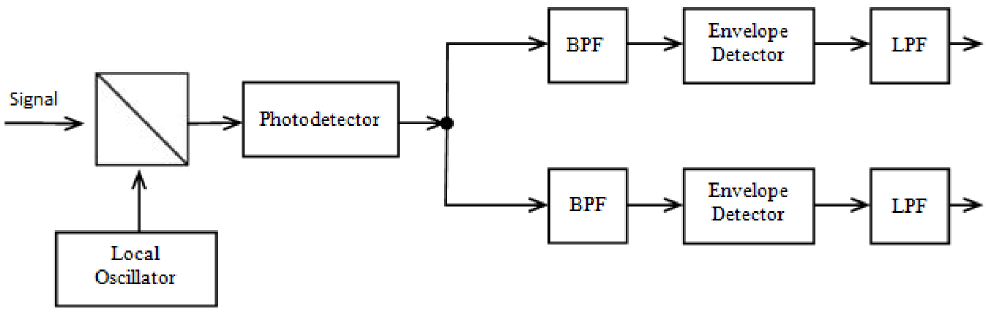

Figure 2-12. Dual-filter FSK

2.5 Polarization Multiplexing

Polarization multiplexing (POL-MUX), also known as polarization division multiplexing (PDM), is a multiplexing technique that uses polarization of light [17] . In this technique, two or more independently modulated data channels with the same wavelength, but orthogonal polarization states, are simultaneously transmitted in a single fiber. At the receiver end, the two polarization channels are separated and detected independently. Using this multiplexing technique the spectral efficiency is doubled, launching pairs of signals in orthogonal *states of polarizations* (SOP) and then receiving them by employing a polarization-resolved detector. Normally this technique is used for transmitting two signals using two different polarizations but there are studies using more than two polarizations and therefore improving the spectral efficiency even more [18] . In this section, the basis for understanding polarization multiplexing is explained.

First of all, one concept must be introduced: state of polarization (SOP). The state of polarization (SOP) describes the polarization of the light that travels through the fiber. When describing polarization, the electric field vector is used while the magnetic field vector is ignored, since it is perpendicular and proportional to the electric field. Therefore the polarization of the light is described by the electric field vector, and the figure drown in a fixed plane by the electric vector so that a plane wave passes over it; such is the description of the polarization state. The electric field of the lightwave can be split into two components: E_x and E_y and the figure formed by the resultant electric field depends on the amplitude and phase difference between the two electric field components. The SOP of a signal launched into a fiber will vary throughout the fiber. Some examples of SOP are depicted in Figure 2-13.

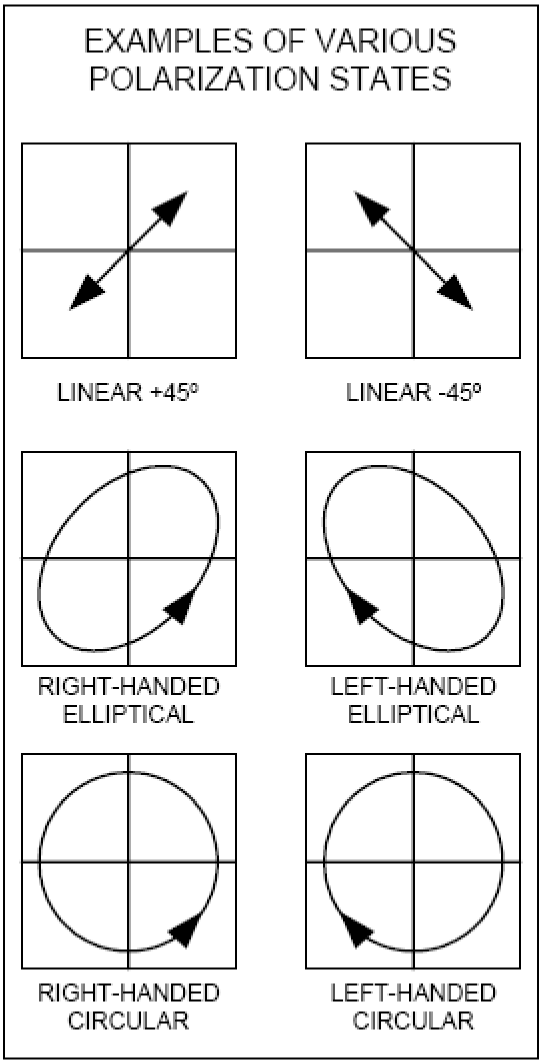

Figure 2-13. Different states of polarization for a lightwave traveling in z-axis.

Theory and experiments show that, whenever two pulses are orthogonally polarized at the input of an fiber transmission link , their orthogonality is maintained throughout the whole link, even in the presence of random *birefringence* and polarization dispersion [19] .In the absence of PMD and polarization dependent loss, if two independent pulses are sent in orthogonal polarizations they do not interfere with each other and both pulses can travel along the fiber doubling the capacity of the optical fiber link. Figure 2-14 shows a graphic interpretation of such a principle: two different pulses are sent in orthogonal states of polarization so that they reach the end of the fiber link in each polarization. If both polarizations are received independently, both pulses will be detectable.

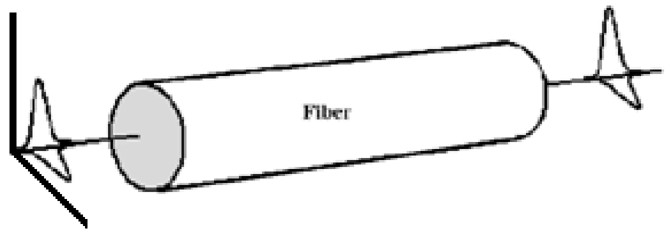

Figure 2-14. Ilustration of how two pulses are sent in different SOP's of a fiber link.

However, PMD, polarization dependent lost and birefringence exist in optical fibers, which deteriorate the ideal case before exposure. The presence of random carrying fiber birefringence will lead to an unpredictable polarization rotation of the SOP but the two orthogonal pulses launched into the fiber will remain orthogonal at the output. However, under such conditions, two data streams on two orthogonal polarizations will experience polarization crosstalk. Although polarization-multiplexing is considered interesting because it increases the transmission capacity, it suffers from decreased polarization-mode dispersion (PMD) tolerance, due to the polarization-sensitive detection used to separate the polarization-multiplexed channels. This greatly increases the effort of using polarization-multiplexing in commercial systems. PMD and polarization sensitivity is deeply examined later.

The polarization multiplexing architecture scheme is straightforward, requiring only a polarization beam combiner (PBC) to combine two channels with orthogonal polarizations at the transmitter and a polarization beam splitter (PBS) at the receiver. However, separating the two channels with acceptable cross-talk at the receiving end is not trivial because the polarization states of the two channels are no longer linear and change rapidly with time. This leads to channel cross-talk due to polarization misalignment between the channels and the polarization beam splitter (PBS) at the receiver side which is usually one of the limitations in studies that use this multiplexation technique. Other studies exist in the possibility of monitoring the cross-talk of the two channels in real time and then using the monitored information to dynamically control the states of polarization (SOP) of the two polarization channels [20] .

This polarization technique is used with single-mode fibers and is totally compatible with WDM, since polarization multiplexing can be used in each wavelength.

2.6 Degradation Effects in Optical Coherent Systems

In order to a better understanding of how a coherent receiver could be able of compensate some important fiber impairments a brief resume of such impairments is explained. As well, is shown how the impairments affect to a QPSK constellation, the modulation format that is used in the experimental part of the coherent receiver study.

2.6.1 Optical noise

As any other transmission system, optical transmission systems are affected by noise. The impact of different noise components is measured by their noise power. Noise leads to a degradation of sensitivity in the optical receiver, which is expressed through the *power penalty*. It is common to calculate the power of basic noise components first, and then to evaluate the impact of the individual noise components that have practical meaning in each specific case. Sometimes, other noise components can be neglected since their impact is minimal. In optical communications, the photocurrent given by the photodiode is a sum of the signal received and the noise contributions. Accordingly, it can be expressed as [9] :

$$I = I_s + i_{noise} = I_s + (i_{sn} + i_{dcn} + i_{the} + i_{beat} + i_{cross} + i_{\text{int}} + i_{jitt}) \tag{2.39}$$

Where I_s is calculated as the product of the incoming optical signal power P and the photodiode responsivity R. The noise components are expressed by the fluctuating portion of the total photocurrent around value I. This fluctuation includes quantum shot noise, dark current noise, thermal noise, beat noise components, crosstalk noise, intensity noise and timing jitter noise, respectively.

Table 4. Spectral Densities of Noise Components for Direct Detection

Noise Spectral Density [A^2/Hz]	PIN	APD
Dark Current	1.6×10^{-27}	0.8×10^{-24}
Thermal Noise	2×10^{-23}	2×10^{-23}
Shot noise without Preamplification	2.6×10^{-24}	1.28×10^{-21}
Shot Noise with Preamplification	2.6×10^{-22}	1.97×10^{-20}
Signal ASE beat noise	1.04×10^{-19}	0.52×10^{-18}

As an engineering reference Table 4 is included to consider the impact of noise components in different detection scenarios for direct detection receiver scheme. The power of individual noise component would be found by multiplying the spectral density given in the table with the optical receiver bandwidth.

The effects of optical noise in terms of optical signal to noise ratio (OSNR) over QPSK constellation are depicted in Figure 2-15. It denotes the undesirable effect that optical noise produces over a QPSK constellation as the OSNR of the received signal decreases leading to a higher BER. These figures are obtained from the designed system made in this work.

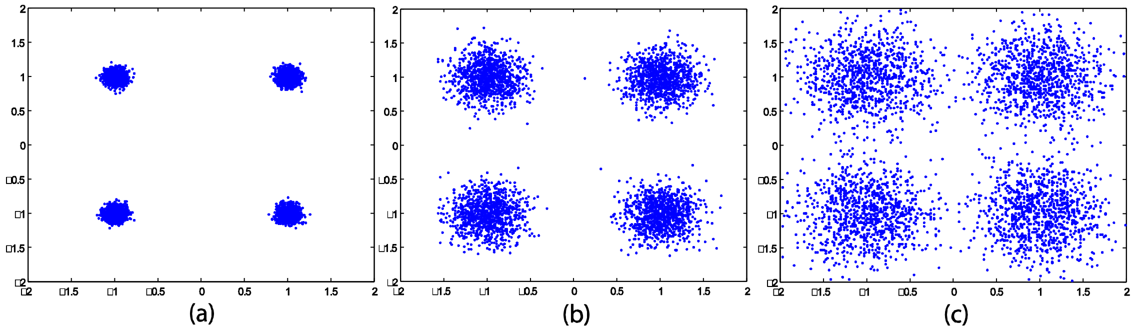

Figure 2-15. Effect of optical noise over QPSK constellation. (a) OSNR = 20 dB (b) OSNR = 10 dB (c) OSNR = 5 dB

2.6.2 Fiber Impairments

2.6.2.1 Chromatic Dispersion

Chromatic dispersion is a linear effect and is one of the most important impairments among optical fibers impairments. It is a variation in the velocity of the light that travel inside the fiber according to wavelength. It is caused due to the property that the refraction index of the silicon used in fibers fabrication is dependent of the wavelength of the light:$n(\lambda)$; therefore, as the velocity of the light that travels inside the fiber is strictly dependent of the refraction index of the fiber:$v = c/n(\lambda)$, the velocity of the light inside the fiber is also dependent of the wavelength of the light. Because do not exist ideal sources, the light sent by lasers has certain spectral width and therefore, different wavelengths that travel at different speeds inside the fiber. This leads to dispersion-induced pulse broadening that leads to ISI which effects are very important, even neglecting nonlinearities.

Mathematically, the effects of chromatic dispersion are accounted by expanding the mode-propagation constant in a Taylor series about frequency ω_0 at which the pulse spectrum is centered

$$\beta(\omega) = n(\omega)\frac{\omega}{c} = \beta_0(\omega_0) + \beta_1(\omega-\omega_0) + \frac{1}{2}\beta_2(\omega-\omega_0)^2 + \frac{1}{6}\beta_3(\omega-\omega_0)^3 ... \quad (2.40)$$

where

$$\beta_m = \left[\frac{d^m\beta}{d\omega^m}\right]_{\omega=\omega_0} \quad (2.41)$$

The parameters $\beta_1$and β_2 are related to the refractive index *n* and its derivatives through the relation

$$\begin{aligned} \beta_1 &= \frac{1}{v_g} = \frac{n_g}{c} = \frac{1}{c}(n + \omega\frac{dn}{d\omega}) \\ \beta_2 &= \frac{1}{c}(2\frac{dn}{d\omega} + \omega\frac{d^2n}{d\omega^2}) \end{aligned} \quad (2.42)$$

where n_g is the group index and v_g is the group velocity. A pulse envelope has group velocity $v_g = {}^{1}/_{\beta_1}$ while β_2 represents the dispersion of the group velocity. The parameter β_2 corresponds to pulse broadening due to frequency dependent group velocity which is known as group-velocity dispersion (GVD). There is a third parameter β_3 that accounts for the third order dispersion (TOD) which distorts ultra-short pulses.

The more commonly used dispersion parameter is given by

$$D = \frac{d\beta_1}{d\lambda} = \frac{-2\pi c}{\lambda^2}\beta_2 \approx \frac{\lambda}{c}\frac{d^2n}{d\lambda^2}\left[\frac{ps}{nm{\cdot}km}\right] \quad (2.43)$$

For standard single mode fibers $D = 0$ near 1.3 μm. Above 1.3 μm, where $D > 0$ $(\beta_2 > 0)$ is called anomalous dispersion; meanwhile, the region where $D < 0$ is known as normal dispersion. The third order dispersion parameter can be neglected except very close to the wavelength in which $D = 0$.

To show the effect of chromatic dispersion over a modulation constellation let's use QPSK modulation because it is used in the receiver designed. In presence of chromatic dispersion the four symbols sent would be very distorted due to the pulse spreading and they cannot be correctly detected inducing high BER. In Figure 2-16 is depicted in blue the four symbols sent just before entering the channel and in red is the signal sent when it has passed through an optical fiber of D= 13.32 ps/km·nm in which the output OSNR is 20 dB, other impairments as phase noise and nonlinearities are neglected. In figure (a) the length of the fiber is 50 km with a total dispersion affecting the signal of 666 ps/nm while in figure (b) the fiber has a length of 1000 km being the signal distorted by 13320 ps/nm. As it showed, the constellation obtained after the channel is very distorted by chromatic dispersion and would be impossible for the receiver to detect which symbol was sent.

Since chromatic dispersion is a linear impairment it can be equalized using digital filters. Later the properly filter for chromatic dispersion compensation is explained in chapter 3 being part of a whole coherent receiver, later its ability for compensating different amounts of chromatic dispersion is tested.

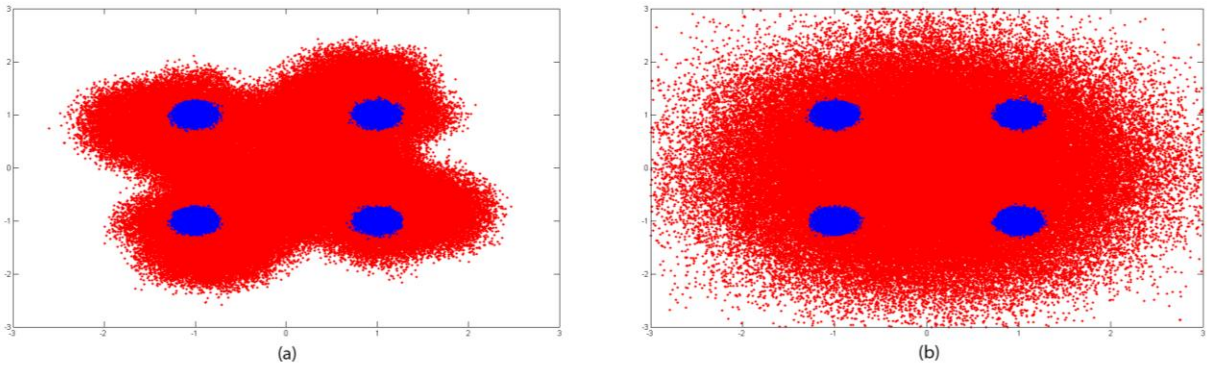

Figure 2-16. Chromatic dispersion effect on a QPSK modulation over (a) 50 km and (b) 1000 km of fiber length with D=13.32 ps/(nm·km) and OSNR = 20dB

2.6.2.2 Polarization Mode Dispersion

Polarization mode dispersion (PMD) effects are linear electromagnetic propagation phenomena occurring in single-mode fibers. PMD is a potential source of pulse broadening related to fiber birefringence that leads to a periodic power exchange between the two electric fields components of the polarization state.

For conventional single-mode fibers, birefringence varies along the fiber in a random way due to asymmetries in circular geometry of the core and stresses in the fiber core. In this case, the polarization state of light propagating in the fiber would change randomly along the fiber, and as result, light launched into the fiber with linear polarization quickly reaches an arbitrary state of polarization, an example of this effect is shown in Figure 2-17.

Moreover, different frequency components of a pulse acquire different polarization states, resulting in pulse broadening; this effect is the second order polarization mode dispersion. Polarization changes affect to the signal in coherent systems as these systems are sensitive to polarization as is studied in 2.6.3, however PMD is not caused directly by the random polarization change but by the pulse broadening induced by this periodical polarization changes.

Due to fiber birefringence, polarization state of a monochromatic pulse shows periodic evolution during propagation along the fiber with period:

$$L_B = \lambda / B_m \tag{2.44}$$

Where B_m measures fiber birefringence, typically its value is $B_m \sim 10^{-7}$. This period L_B is referred as *beat length*. The effect of this evolution in the polarization of the pulse is depicted in Figure 2-17 and it is the origin of PMD. From the figure can be seen how a pulse is sent into the fiber with linear polarization, then the polarization changes along the fiber due to birefringence. In this figure the length of the fiber link is exactly a beat length and therefore, at the end of the link, the polarization state of the pulse sent is exactly the same that was initially sent.

For a better comprehension of PMD phenomenon is needed the introduction of Principal State of Polarization concept. The term *Principal State of Polarization* was born in 1986 due to a phenomenon discovered by Poole and Wagner[21] . This phenomenon was based on the observation that for a linear optical transmission link there exist orthogonal input states of polarization for which the output states of polarization are orthogonal and showed to first order no wavelength dependence. They called to these input states of polarization, Principal States of Polarization. Because of its characteristics PSP are often used as principal axis, or reference axis of the fiber for the study of issues such as PMD. For example in Figure 2-17 the axis depicted as fast axis and slow axis, are the PSP of that fiber. From a physcical viewpoint, linearly polarized ligth remains linearly polarized only when it is polarized along one of the principal states axes. Otherwise, its state of polarization changes along the fiber length from linear to elliptical and then back to linear, in a periodic manner over the length L_B. This periodical behavior is exactly what shows Figure 2-17, since the linear polarization state of the pulse sent in the picture has an angle of 45º respect both PSP. Normally PSP have different group velocities which is indicated in the picture by the names “fast axis” and “slow axis”. If the input SOP excites both polarization components, it becomes broader as the two components disperse along the fiber because of their different group velocities. This phenomenon is called Polarization mode dispersion (PMD) and has been studied extensively because it limits the performance of modern lightwave systems operating at high bit rates [9] .

In Figure 2-18 is depicted an illustration of the PMD effect over one pulse sent through an optical birefringent fiber. The pulse is launched into the fiber with a SOP that has two component of the same amplitude in each PSP. This could be a linear polarization with an angle of 45º respect the PSP. As explained, the two principal states of polarization have different group velocities; therefore we have called the axis: Slow axis and Fast Axis. As each component of the main pulse will travel in each axe, they will travel at different speeds and therefore, at the end of the fiber both pulses arrive with a delay that causes the spread of the pulse sent. The time difference between two pulses arrival is called *differential group delay* (DGD) and it describes the impact of first order PMD, it is usually measured in picoseconds. Second order PMD is due to the variation of the PSP's of the fiber respect of the wavelength.

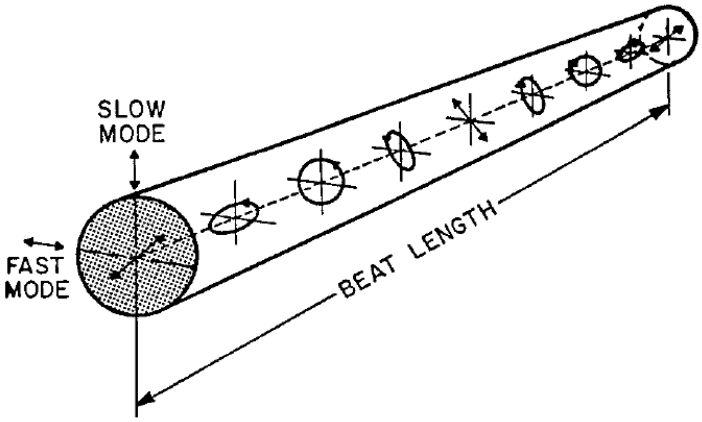

Figure 2-17. State of polarization of a pulse sent along a birefringent fiber of length L_B (beat length) . Input beam is linearly polarized at 45º with respect to the slow and fast axes.[9]

The birefringence varies along the fiber in a random manner, this variation also induces polarization mode coupling an effect that is not treated in this text. The treatment of PMD is quite complex because his statistical nature. A simple model divides the fiber into a large number of segments. In each segments the birefringence and the orientation of the principal axes remain constant for that segment but changes randomly from segment to segment, an illustration of this model is depicted in Figure 2-19. Long fibers are usually modeled as a concatenation of birefringent segments whose birefringence axes magnitude change randomly.

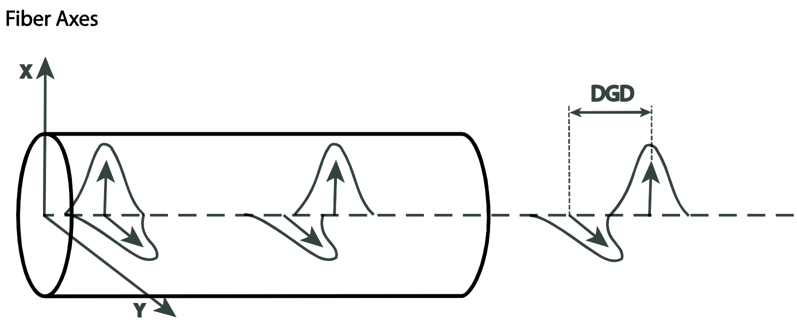

Figure 2-18. Time domain ilustration of how pulse components travels at different speeds inside a fiber affected by PMD.

Each section can be treated using a Jones matrix and the propagation of the entire fiber is then governed by a composite Jones matrix resulting from the multiplication of all the Jones matrixes defining each section. The composite Jones matrix shows that two principal states of polarization (SOP) exist for any fiber in where light propagates at different velocities from one to another.

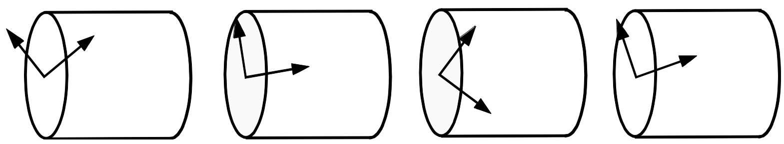

Figure 2-19. Concatenation of fiber elements with different principal axes due to birefringence.

Let's explain deeply the process of pulse broadening induced by polarization mode dispersion. For the explanation, Figure 2-20 extracted from [22] is used, as well as the model of concatenation of different birefringent sections for modeling an optical fiber. This model is an approximation of the reality because in real world birefringence modify PSP along the fiber without discontinuity.

Paying attention to first scheme of Figure 2-20 there are three axis: X, Y and a very long Z axis. The Z axis shows the direction of the fiber, meanwhile X and Y axes are the principal axis of the fiber for a first little piece of fiber, in other words the PSP for that little piece of fiber. If we continue the length of the Z axis it is found two more axes: P and Q. These two axes are no more than a rotated version of axis X and Y that belongs to the second segment of fiber. Therefore, it is depicted an scheme similar to the one depicted in Figure 2-19 just using two pieces of fiber, each one with its own PSP. At the beginning of the Z axis there are three electrical fields. The electrical field E is the pulse launched into the fiber, it defines the polarization of the light sent through the fiber. The fields E_X and E_Y are the decomposition of the resultant field E into the two given principal axis Y and X. In the example it is transmitted a rectangular pulse and therefore the components of the resultant field are rectangular pulses.

Should be noticed that one PSP is faster than the other because we are assuming PMD, in this case Y axis is faster than X and when the pulse arrives to the second piece of fiber the blue one in Y axis is ahead. Moreover, when the signal arrives to the second segment of optical fiber it is found that the principal axes of the new segment are a rotated version of the axes from the previous piece of fiber. At this point each component ϕ_X and ϕ_Y respect X and Y axis of the initial electric field E are again decomposed into the new axis P and Q resulting in an interference between the components. For example, each ϕ_X and ϕ_Y has a component in the axis P and exist an interference where both P components ϕ_X ϕ_Y are overlapped, the same occur for axis Q. This interference is shown in the following pictures, that shows the plane PZ and QZ respectively when the pulse arrive to the second fiber element. Here is also noticed that the blue components, the ones coming from the fast axis of the previous fiber element are ahead, resulting in a green final component composed by the overlap between the blue components (coming from the decomposition of the E_Y field) and pink components(coming from the decomposition into axis P and Q of the previous E_X field). As can be seen the final green and orange components are spread versions of the rectangular pulse sent which is the effect of PMD.

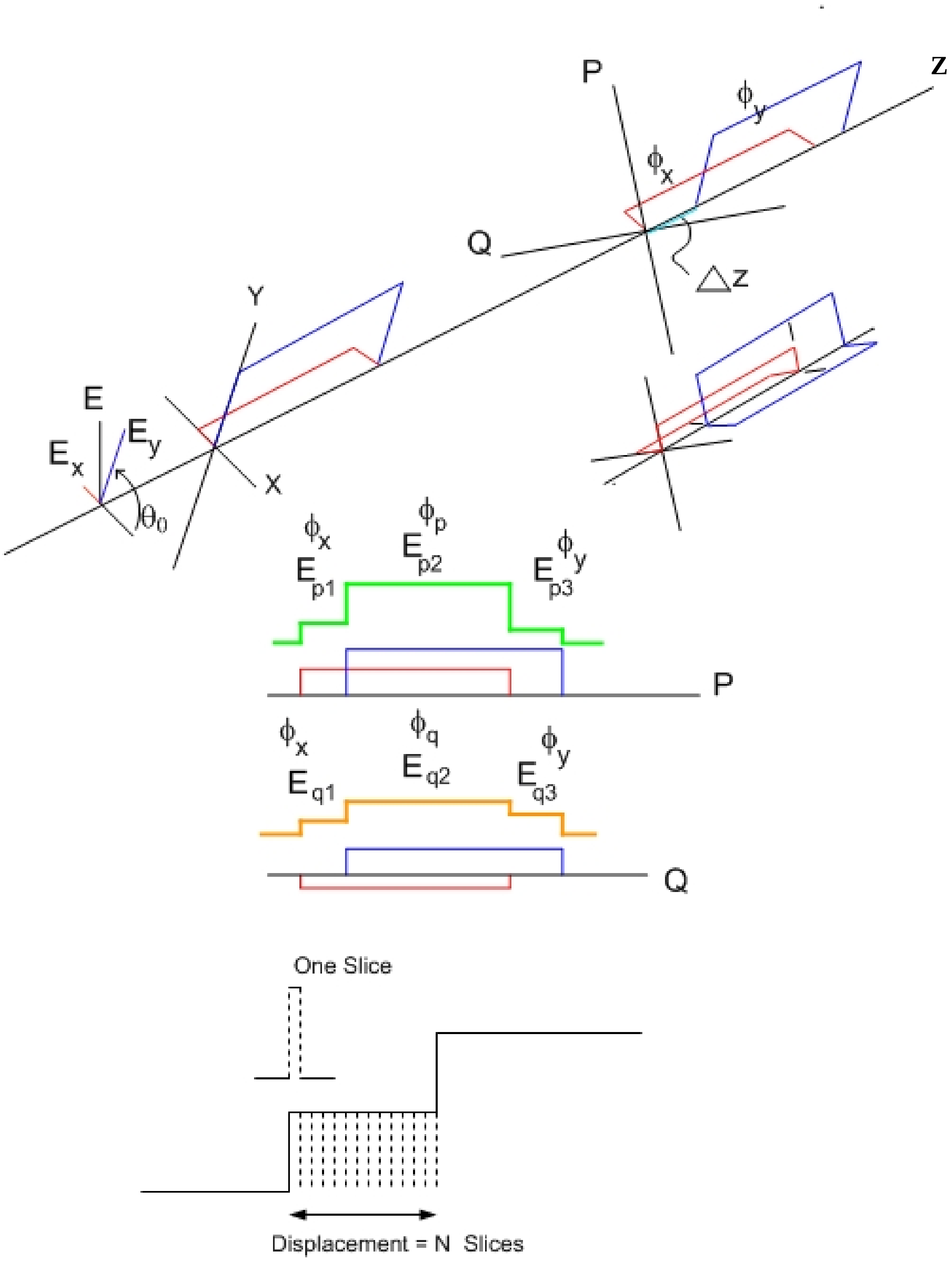

Figure 2-20. Detailed process of how pulse broadening is caused by PMD.

Previous explanation comes from a mathe matical model to work with polarization mode dispersion, but in real world there are no little segments of fiber and the rotation of the PSP are continuous. Moreover the effect of birefringence over the fiber are close related to external forces such bends, twists and stress, these external forces are time varying and makes the DGD also time varying causing even more difficult he compensation of PMD.

In Figure 2-21 is depicted the effect of PMD over a QPSK modulation when a DGD=$0.1\text{x}10^{-9}\frac{s}{\sqrt{Km}}$ affects the signal. There are three constellations for three different fiber lengths. To obtain such examples other impairments were neglected and the QPSK signal had an OSNR of 20dB when 20480 bits were sent at a bit rate of 10Gbps. The signal depicted is the QPSK signal sent in X polarization in a POL-MUX system when both signals were sent aligned with the PSP's of the fiber.

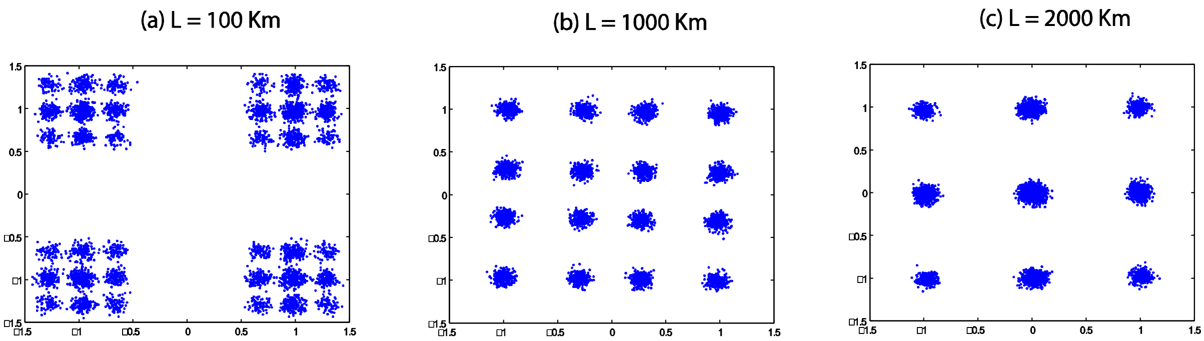

Figure 2-21. QPSK signals affected by PMD in fiber lengths of (a) 100 Km (b) 1000 Km (c) 2000 Km

In Figure 2-21 can be noticed how PMD affects QPSK constellations. In (a), the effect of PMD still let's detect the signal with 0 BER because the four decision regions are well delimited. The symbols spread but they are still inside them decision regions. On the other hand, (b) shows that each symbols of QPSK modulation has spread into four little symbols which are in the boundary of the decisions regions. In this case, the BER can still be 0 or a small BER can be present as this could be the limit case. In the last case, for a fiber length of 2000 Km, represented in (c), the QPSK symbols have passed the boundaries of its decision regions, in this case the BER is between 7% or 8 %, which is an important BER for a transmission system. Of course, the effect of PMD over the BER is worse if the bit rate is increased.

There are fibers with constant birefringence (e.g. polarization maintaining fibers), with these fibers the effect of first order PMD can be reduced to zero launching the light along one of the principal axes of the fiber. There are two mayor problems with such fiber, they need an improved transmitter to launch the signal perfectly aligned with one of the principal axes. The second problem is that these fibers are very expensive in comparison with general fibers and also have higher losses than conventional fibers. For that reason there are many studies in polarization mode dispersion compensation, in the present text it is proposed a digital equalizer that can compensate first PMD at the receiver once the signal has been converted into the digital domain.

2.6.2.3 Fiber nonlinearities

The dominant nonlinear impairments in fiber arise from the Kerr nonlinearity, which causes a refractive index change proportional to signal intensity. SPM (Self-phase modulation) and XPM (Cross-phase modulation) are the two most important nonlinear effects which originate from the intensity dependence of the refractive index.

SPM refers to the self-induced phase shift experienced by an optical field during its propagation in optical fibers due its own intensity. XPM refers to the nonlinear phase shift of an optical field induced by a co-propagating field at a different wavelength. Therefore, it is nonlinearity mostly present in WDM systems together with four-wave mixing (FWM), their impact can be reduced by allowing non-zero local dispersion. In the absence of ASE, and given knowledge of the transmitted data, all these nonlinear effects are deterministic, and it is possible, in principle, to pre-compensate them at the transmitter. At the receiver would be also possible to employ joint multi-channel detection techniques.

In long-haul systems, interactions between ASE noise and signal through the Kerr nonlinearity leads to nonlinear phase noise (NLPN). When caused by the ASE and signal in the channel of interest, this is called SPM-induced NLPN.

2.6.3 Polarization Sensitivity

The polarization state of the received signal plays no role in direct detection receivers. The photocurrent generated in such receivers depends only on the number of incident photons. This is not the case for coherent receivers, whose operation requires matching the state of polarization of the local oscillator to that of the signal received. To see this more clearly let's remind the notation used in section 2.1 where the use of E_S and E_{LO} implicitly assumed the same polarization state for the two optical fields. If we use $\hat{e}_S$ and $\hat{e}_{LO}$ for representing the unit vectors along the direction of polarization of E_S and E_{LO}, then the interference term in Eq. (2.5) has an additional factor $\cos\theta$,

$$i(t) = R(A_S{}^2 + A_{LO}{}^2) + 2RA_S A_{LO} \cos(w_{IF} t + \phi_S(t) - \phi_{LO}(t))\cos(\theta) \qquad (2.45)$$

where θ is the angle between $\hat{e}_S$ and $\hat{e}_{LO}$, in other words the angle between the polarization of the light sent and the polarization of the local oscillator lightwave. Since the interference term is used by the decision circuit to reconstruct the transmitted bit stream, any change in θ from zero reduces the received signal and thereby the receiver performance. In particular if the polarizations states of both signals are orthogonal to each other the signal completely disappears. Therefore, to obtain a received signal without distortion caused by polarization sensitivity we need at the receiver a local oscillator polarization aligned to the polarization state of the received signal.

Polarization state $\hat{e}_{LO}$ of the local oscillator is determined by the laser and remains fixed. This is also the case for the transmitted signal before it is launched into the fiber, however, as treated in section 2.6.2.2, because of fiber birefringence the polarization state of the signal received differs from the signal transmitted in a random manner. If such change were at least constant with time it would not be a problem because the polarization of the

LO could match the polarization of the incoming signal by simple optical techniques. Therefore, the source of the problem is polarization mode dispersion (PMD) or the fact that $\hat{e}_S$ changes randomly in most fibers because of birefringence fluctuations related to environmental changes.

Various solutions have been proposed for solving the polarization-mismatch problem. In one of them, the polarization state of the optical signal received is tracked electronically, and a feedback-control technique is used to match $\hat{e}_{LO}$ and $\hat{e}_S$ .There is other scheme in which polarization scrambling or spreading is used to force $\hat{e}_S$ to change randomly during a bit period. Exist other scheme based on the generation of a phase conjugated signal and many other but the most commonly used approach to solve polarization sensitivity problem is using a *polarization diversity receiver* architecture.

In polarization diversity receivers, the signal light arrives with an arbitrary SOP, generally elliptically polarized, and it is split into two orthogonal polarizations which are separately mixed with the local oscillator signal which has a constant SOP of 45º respect the receiver polarization. Polarization diversity receiver scheme front end uses an optical hybrid similar to the one depicted in Figure 2-7. The photocurrents at the output of the balanced receivers once they are in baseband are [24] :

$$\begin{aligned} r_I(t) &= \cos(\gamma) A_S \cos(\phi_S(t)) \\ r_Q(t) &= \sin(\gamma) A_S \cos(\phi_S(t)) \end{aligned} \tag{2.46}$$

where γ is relative to the receiver polarization, photodiode responsivity has been considered equal to one, A_s is the signal amplitude and $\phi_S(t)$ is the phase information as is considered a phase modulated signal. Last equations have been simplified considering baseband reception and phase matching. At this point the in-phase and quadrature components of the signals are then combined again.

One possible combination method is *maximal-ration combining*, that presents no penalty using polarization diversity receiver. In this method, combination is as follows

$$r_C(t) = \cos(\gamma) r_I(t) + \sin(\gamma) r_Q(t) \tag{2.47}$$

The simplest combining method may be *equal-gain combining* with a combining signal of

$$r_C(t) = r_I(t) + r_Q(t) \tag{2.48}$$

Selection-combining scheme is the third method in which the polarization component with higher power is chosen.

Another combining scheme can be used for either homodyne or heterodyne ASK. In this method the combined signal is

$$r_C(t) = r_I(t)^2 + r_Q(t)^2 \tag{2.49}$$

This method is known as *square-law combining*, because each signal is squared. It introduces only 0.4 dB degradation compared with *maximal-ratio combining* [25] .

If Polarization multiplexing is used, both polarization channels can be separated with maximum-ratio combination.

2.6.4 Phase & Frequency Noise

Laser phase noise is caused by spontaneous emission. Phase noise is an important source of sensitivity degradation in coherent lightwave systems as it impacts carrier synchronization. The values presented in Table 2 and Table 3 are considered neglecting phase fluctuations in both transmitter and local oscillator. To achieve such values phase fluctuations should be very small or phase noise should be compensated in the receiver side.

From eq. (2.10), a homodyne received signal and considering a phase modulated signal with phase information stored in $\phi_M(t)$ while $\phi_N(t)$ is the phase fluctuations due to phase noise difference of the transmitter and local oscillator we obtain the next equation:

$$i(t) = 2R\sqrt{P_S P_{LO}}\cos(\phi_M(t) + \phi_N(t)) \tag{2.50}$$

The phase fluctuations term $\phi_N(t)$ gives a certain spread to the spectrum even when no phase modulation is used. In absence of other impairments, phase noise results in a rotations of the received constellation, this effect over QPSK modulation can be noticed from Figure 2-22 in which any other impairment have been neglected.

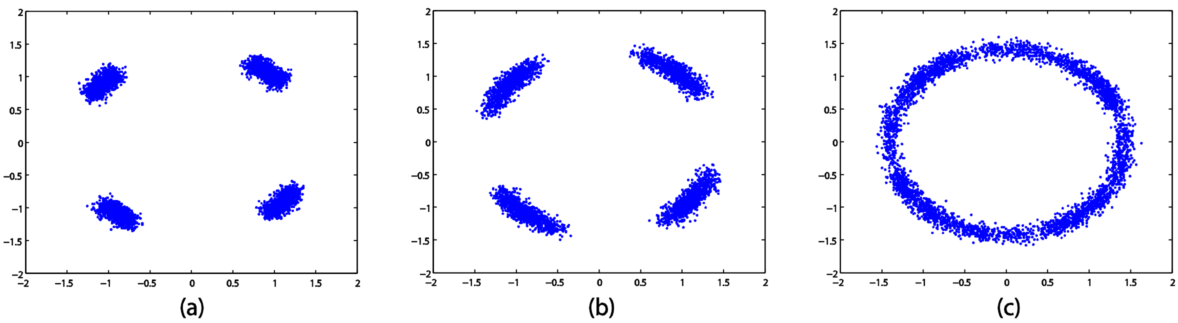

Figure 2-22. Phase noise effect over QPSK modulation: (A) $\Delta\upsilon = 10KHz$ h 10 KHz (B) $\Delta\upsilon = 100KHz$ (C) $\Delta\upsilon = 1MHz$

Phase fluctuations are independent in the transmitter and local oscillator, let's remind that we used in 2.1.3 $\phi_{S-N}(t)$ to name phase fluctuations of the transmitter while $\phi_{LO}(t)$ was used for the local oscillator. Now $\phi_N(t)$ is used for phase fluctuation of both transmitter and LO phase fluctuations. A measure of duration in which the laser phase remains relatively stable is provided by the *coherence time.* As the coherence time is inversely related to the laser linewidth $\Delta\upsilon$, it is common to use the linewidth-to-bitrate ratio, $\Delta\upsilon/Rb$ to characterize the effects of phase noise in the performance of coherent lightwave systems. As $\phi_{S-N}(t)$ and $\phi_{LO}(t)$ are independent $\Delta\upsilon$ is normally the sum of both laser linewidths: transmitter and LO.

The tolerable value of $\Delta\upsilon/Rb$ for which the power penalty remains below 1dB depends on the modulation format as well as on the demodulation technique. In general, the linewidth requirements are most stringent for homodyne receivers. Normally $\frac{\Delta\upsilon}{Rb} < 1x10^{-4}$ to realize a power penalty of less than 1dB [26] .

Linewidth requirements are relaxed considerably for heterodyne receivers, especially in the case of asynchronous demodulation. For synchronous heterodyne receivers $\frac{\Delta\upsilon}{Rb} < 5x10^{-3}$ is required [27] .

In Figure 2-22, 2048 bits were sent using QPSK modulation through a fiber of 500 km using a bitrate of 10Gbps. In this example the linewidth-to-bitrate ratio is therefore $1x10^{-6}, 1x10^{-5}$ and $1x10^{-4}$ in (a), (b) and (c) respectively. The OSNR is 20 dB and all the impairments are neglected except phase noise. As can be seen, the bigger the linewidth is the most the constellations rotate, making the symbols indistinguishable.

Since phase noise is a Wiener process with temporal correlation it can be mitigated by signal processing. A Traditional method for carrier synchronizations is PLL. It consists in a phase estimator that previously removed the data modulation $\phi_M(t)$, so that $\phi_N(t)$ can be measured. Then, the phase estimator output is an error signal that is passed through a loop filter as a controlling signal of the LO laser. Also exist optical PLL that are known as OPLL but normally an electrical PLL is superior to OPLL, however OPLL are preferable when the frequency drift of the laser is significant.

Another method has been widely studied for phase noise compensation: Feedforward Carrier Recovery. Instead of using a PLL to ensure that $\phi_N(t)$ is small, a FF phase estimator directly estimated the carrier phase and then de-rotates the received signal using the phase estimation. Therefore symbol decision can be made at low BER. Some results for both techniques are shown in Table 5 [29] .

Table 5. Linewidth requirements for various single-polarization modulation formats using PLL and FF carrier synchronizer at a target BER of 10^{-3} [29]

Modulation Format	OSNR per bit (dB)	Max. Linewidth using a PLL ($\Delta\upsilon/Rb$)	Max. Linewidth using a Feedforward ($\Delta\upsilon/Rb$)
4-QAM	7.79	$6.9x10^{-5}$	$1.3x10^{-4}$
8-QAM	10.03	$8.3x10^{-5}$	$1.3x10^{-4}$
16-QAM	11.52	$7.9x10^{-6}$	$1.5x10^{-5}$

From Table 5 can be inferred that FF carrier recovery technique lets wider laser linewidths for obtaining same BER than PLL under the same conditions. For example for 4-QAM with an OSNR equal to 7.79 dB if the transmission is made at 10Gbps PLL let a maximum linewidth of 690 KHz while FF let a maximum linewidth of 1.3MHz.

Frequency offset between the transmitter and the local oscillator laser also causes a phase shift in the symbols constellations similar to the one depicted in Figure 2-22. Let's consider a phase offset Δf between both lasers, therefore from equation (2.5), once the DC term has been filtered, considering that the current has been obtained using balanced detection and being ϕ_M the phase information due to QPSK modulation, the current obtained when other impairments have been neglected is:

$$i(t) = 2R\sqrt{P_S P_{LO}}\cos(w_{IF}kt + 2\pi\Delta ft + \phi_M(t)) \qquad (2.51)$$

From last equation should be noticed that we are dealing with a heterodyne receiver because we have an intermediate frequency. Because we have considered a phase offset between LO and transmitter we have a frequency offset term $2\pi\Delta f$ inside the cosine that can be seen as phase noise and thereby a phase shift in the QPSK constellation.

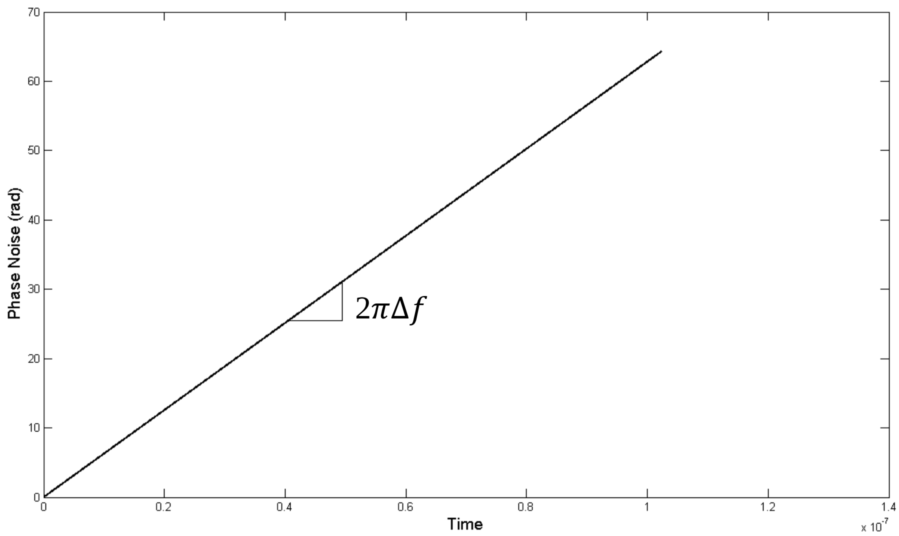

Figure 2-23. Phase noise due to frequency offset between transmitter and local oscillator lasers

Phase noise due to frequency offset has to be differenced from phase noise, phase noise is caused from small frequency drifts related to the coherence time or linewidths of lasers. On the other hand, frequency offset phase shift is related to a work frequency difference between local oscillator and the transmitted signal, in other words a difference between the carrier frequency and the frequency at which the local oscillator works. The frequency offset phase shift is linear as a function of time (Figure 2-23) if phase noise due to frequency drifts of laser is neglected. In reality, a frequency offset is always accompanied by frequency drifts and thereby by phase noise. QPSK constellation rotations due to frequency offset phase shift are showed in Figure 2-24.

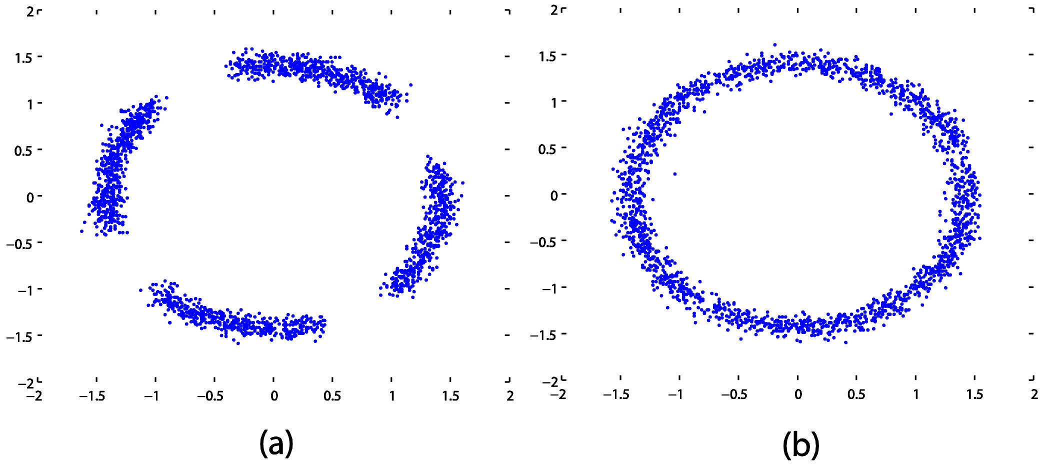

Figure 2-24. Constellation rotations due to frequency offset. (a) Δf = 10 MHz (b) Δf = 1 GHz

As well as phase noise, frequency offset can be compensated digitally in the receiver using feedforward techniques. This is interesting because it means that hardware issues as the work frequency of laser could be solver electronically at the receiver if necessary.

Chapter 3

3 Design of a Digital Coherent Receiver

In the practical part of the thesis we have implemented a digital coherent receiver for optical communication. This receiver uses the advantages that digital signal processing (DSP) brings to optical communications, compensating impairments as chromatic dispersion, polarization mode dispersion or classical difficulties in optical coherent systems like compensation of phase noise. Before the use of DSP, the electrical signal from the photodiodes has to be digitized, for such purposes a clock recovery circuit is needed for the correct sampling of the electrical signal. A clock recovery circuit is very important in any transmission systems since the incoming bit stream has to be sampled in the middle of each bit to obtain a useful digitized signal. Since DSP is able to compensate large amounts of chromatic dispersion, as we will show later, no compensation of CD before the receiver using dispersion compensating fibers (DCF) is needed like traditionally has been done. The disadvantage of this no pre-compensation is that the received signal is very distorted by chromatic dispersion making more difficult to obtain the clock signal. This issue is seen along the chapter. Afterwards the design of the different modules of the DSP in charge of impairments compensation is treated.

For an easy design and implementation the receiver was divided into three modules: clock recovery, equalization filter for CD and PMD compensation and frequency and carrier estimation. In this chapter the receiver is also divided into these three stages for a more easily comprehension.

3.1 Receiver Scheme

The receiver behind the front-end consists in three main components:

1. A clock recovery circuit in charge of obtaining the clock and the correct sampling point in the analog signal coming from the photodiodes.
2. A module in charge of the compensation of CD.
3. A module in charge of PMD compensation.

4. A last module in charge of phase noise estimation and compensation.

In the beginning of the implementation an entire optical transmission system, in which the receiver is embedded, was implemented in Matlab. It purposes is to check the functionality of the three modules of the coherent receiver during the implementation. The transmission system with the coherent receiver is depicted in Figure 3-1. In the figure, optical signals are drawn in orange while electrical signals are depicted in blue.

The receiver is designed to demodulate QPSK dual polarization signal, therefore a dual polarization QPSK system is implemented. PSK is chosen as modulation format since it is the most sensitivity modulation as shown in the previous chapter, moreover, dual polarization is chosen to double the capacity of the system. With this scheme the capacity of the fiber is then quadrupled compare to systems using direct detection. Therefore, the transmitter of this transmission system generates four binary sequences at the bit rate chosen Rb: two of them forming, in the first polarization, the in-phase and quadrature of the QPSK signal. The third and fourth sequences are for the in-phase and quadrature of the QPSK signal sent in the second polarization. For example if Rb is chosen to be 10 Gbps then four signals at 10 Gbps are generated obtaining an effective bit rate of 40 Gbps. Once the independent signals have been generated and modulated using QPSK, both QPSK signals are sent through the channel.

The channel was implemented adding optical noise, CD and PMD using the appropriate Jones Matrix and frequency response functions. As the entire transmission system has been created in a simulation environment, the impairments can be enabled or disabled for better study of the compensation technology inside the receiver.

After the transmission channel is where the coherent receivers lies. The signal passes through the receiver front-end where the optical signal is mixed with the local oscillator signal. This front end is also implemented in the transmission system model for simulating the entire systems. The front end implementation simulate a front-end formed by two phase diversity balanced detectors using a 90º optical hybrid like the one showed in Figure 2-7, forming in this way, a polarization diversity balanced receiver structure. These 90º optical hybrids preserve the optical power received by using balance detection and also give the in-phase and quadrature of the QPSK signal for each polarization. In these front-end is also implemented the phase noise and frequency mismatch between transmitter and LO that affects the performance of the system.

Once the optical signal has been mixed with the local oscillator in the front end, the in-phase and quadrature of both signals sent through both polarizations are sampled and then, process them digitally.

Once we have the signals in the digital domain they can be digitally processed to compensate the principal impairments that affects optical transmission. The compensation is performed in the module called equalizer in Figure 3-1. The module is designed to compensate CD, first order PMD and phase noise. The DSP module in charge of optical impairments compensation can be further seen in Figure 3-2. It is composed by two different modules that are treated independently in this chapter: Impairments compensation and Frequency Recovery.

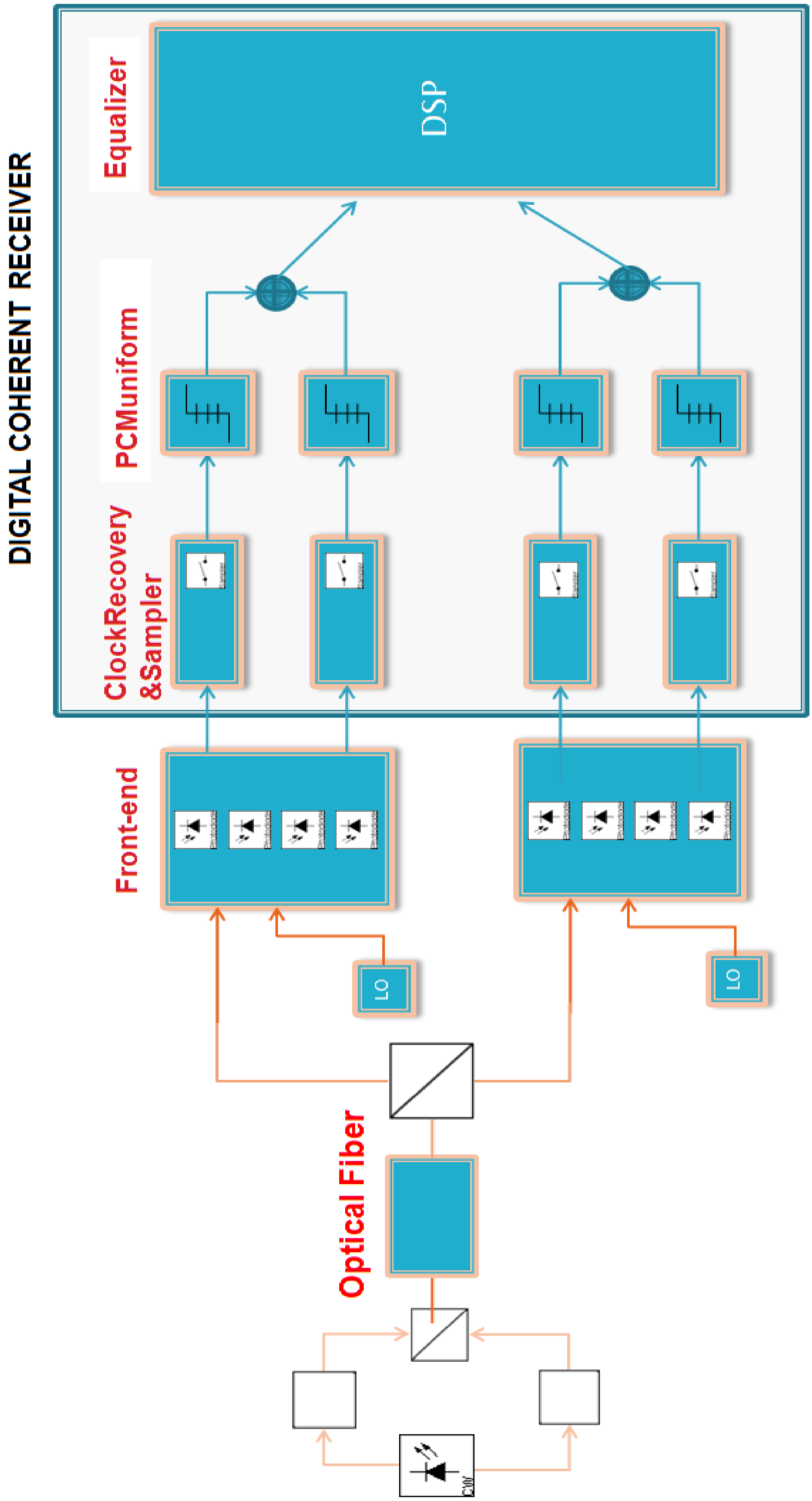

Figure 3-1. Transmission system with digital coherent receiver

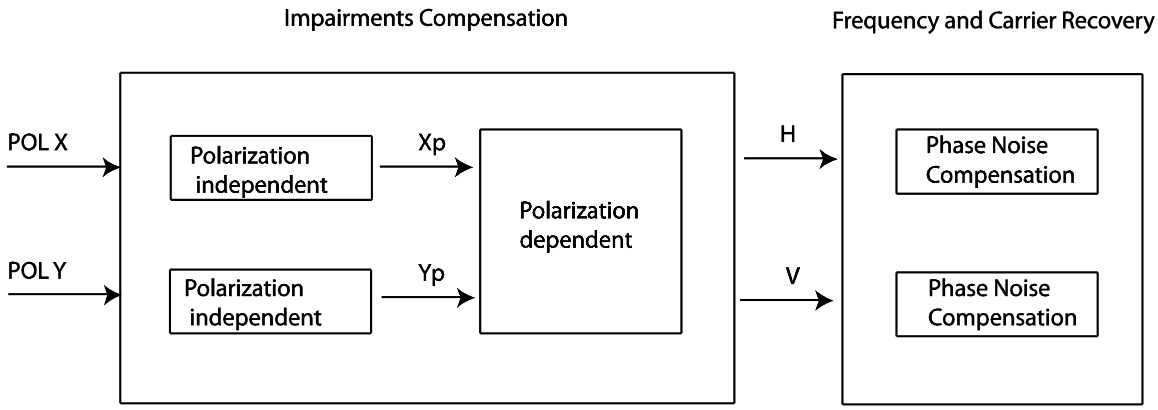

Figure 3-2. DSP module in charge of impairments compensation

The impairments compensation module is also formed by two modules: polarization independent and polarization dependent. These two modules are in charge of the compensation of chromatic dispersion and polarization mode dispersion respectively. For the frequency and carrier recovery module there are several architectures that can be used for phase noise compensation.

3.2 Clock Recovery

Behind the front-end architecture, once the signals have been converted into the electrical domain, the signals are filtered to reduce noise and then digitized using Analog to Digital Converter (ADC). The receiver has been implemented to choose the number of samples per bit wished in the sampling process and a clock recovery is used for finding the correct the sampling points.

Bits are not ideal and have a shape form similar to a Gaussian, therefore for a good sampling process the middle of the bit has to be found to try to sample the bit in the middle of it. If it is not found and the sampling is taken in wherever part inside the bit it could be sampled at the beginning or the end of it, where the value of it is almost zero even when the bit is a ONE. This sampling error would lead to an increased Bit Error Rate (BER). A common way to find out where are the middle of the bits, is to find out where are the edges of the transitions between ONE and ZERO bits. A problem using this method occurs if no transitions are present in the bit stream, in other words, if long sequences of only ONE’s (or only ZERO’s) have been sent, then is impossible to find the edges, since there are no edges. However long sequences of only ONE or only ZERO bits would not be often presents since normally channel coding is used; and even if they are present the bit stream that include this only ONES sequence is as large as the transitions presents in the stream are considered infinite.

There are many ways to find the edges of the signal, in this thesis a canny edge detector has been implemented.

To obtain the edges of the signals, or what is the same, the moments when transitions between ZERO and ONE occur, a canny edge detector is chosen [31] . A canny edge detector is a well known method in image processing for finding the edges of an image but it can also be used for one dimensional signals. It is characterized by a filter with an impulse response of the form

$$h(t) = \frac{t}{\sigma^2} e^{\frac{-t^2}{2\sigma^2}} \tag{3.1}$$

where sigma is an input parameter that can be chosen and changes the characteristics of the edge detection filter. Some function with different σ are depicted in Figure 3-3, where can be seen that σ has influence on the broadness of the impulse response h(t). According to [31] there are three characteristics for a step function h(t) in charge of edge detection:

i. Good detection. Should be a low probability of failing to mark real edge points, and low probability of falsely marking non-edge points. Since both these probabilities are monotonically decreasing functions of the output signal to noise ratio, this criterion corresponds to maximizing signal to noise ratio (SNR).

ii. Good localization. The points marked as edges by the operator should be as close as possible to the centre of the true edge.

iii. Only one response to a single edge. This is implicitly in (i).

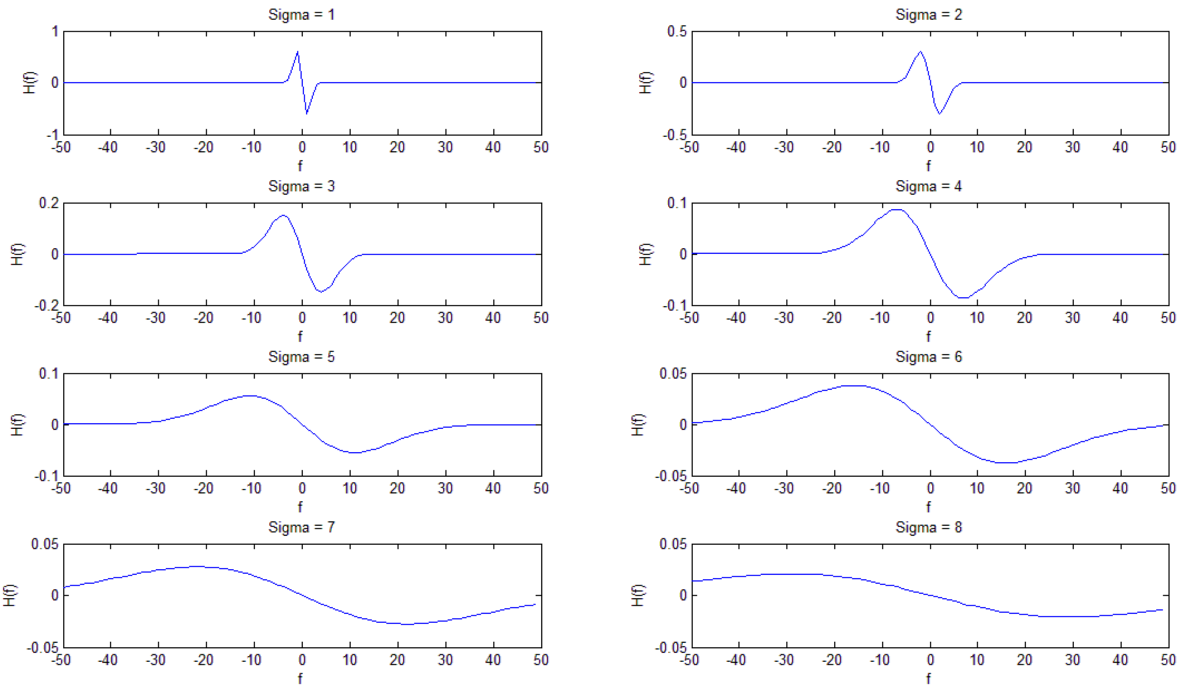

Figure 3-3. Different edge detection canny filter at different Sigma (σ)

The parameter σ, or the width of the impulse response has influence in both SNR (i) and localization (ii) simultaneously. Furthermore, the relation with localization is directly proportional; however, the relation with SNR is inversely proportional. Therefore, as sigma grows the localization of the edges is better; meanwhile, the SNR is worse and vice versa. This can be seen in Figure 3-4 that shows the bit stream before been affected by noise and then three different outputs of the edge detector for three different values of sigma: 1, 3 and 5. The bit stream is affected by noise with a finally SNR of 12. Looking closely at the three outputs can be seen how the SNR of the edge detection signal, depicted in red is getting better as σ grows. For $\sigma = 1$ the noise is important and some noise peak are close in amplitude to some true edges detected; in the edge detection signal when $\sigma = 3$ some noise peaks can still be found but are little peaks compared with those ones pointing the true edges; for $\sigma = 5$ the noise is practically disappeared.

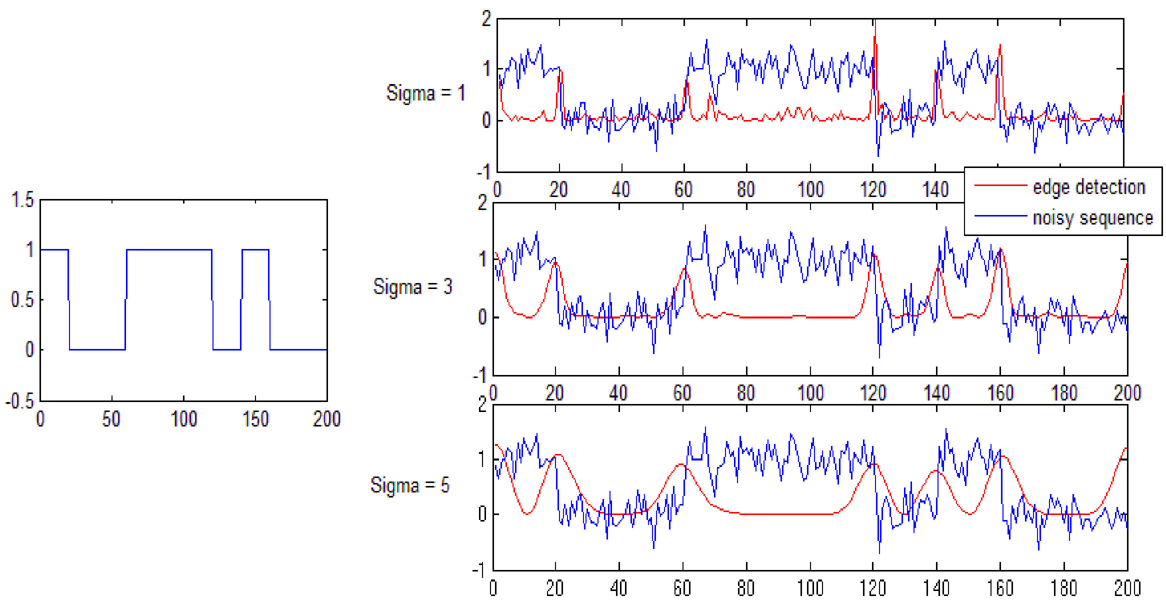

Figure 3-4. Outputs for different values of σ parameter of the step function impulse response h(t)

On the other hand, the localization of the edges is much better for $\sigma = 1$ where the shapes defining the edge are narrower than those in the edge detection signal when $\sigma = 5$ which are wider. When the peaks that define the edge are wider is more difficult to obtain the exact edge position. A better way to see how the localization could be influenced by the value of sigma can be seen in Figure 3-5 where the edges are extracted from an ideal bit stream without noise. We focus our attention on the first edge presented, where a black vertical stripe defines the maximum of the edge detection signal. It can be noticed that in (a) the black stripe exactly match the blue vertical line that shows the edge of the signal sent. In (b) the edge detected shape is wider and the maximum of it does not occur exactly at the same time that the real edge of the bit stream. Therefore can be inferred how the first edge is best located when sigma is low (a) than when sigma is high (b).

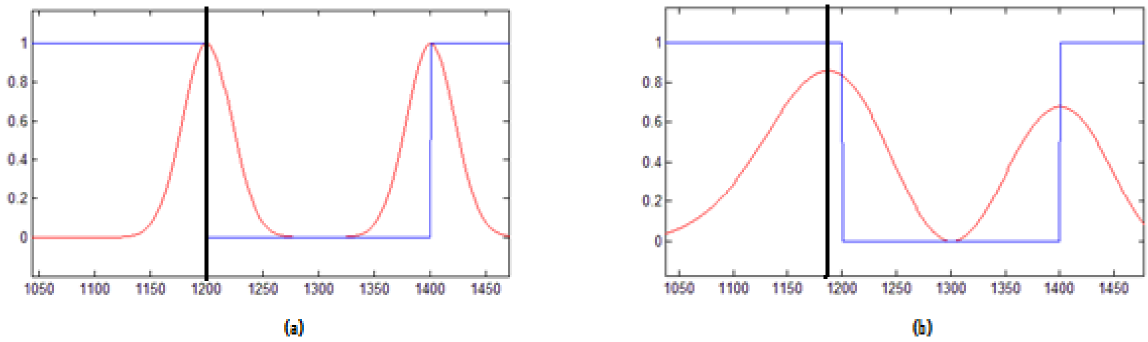

Figure 3-5. Influence of σ in the localization of the edges of a bit stream. (a) σ=1 (b) σ= 5

Because of these characteristics of the edge detection impulse response function, a decision has to be taken in function of the properties of the system, if the system has good SNR in reception is not extremely necessary to worry about the SNR of the edge detector, and better localization would be chosen; on the other hand if the SNR of the signal received is very low an edge detector operator with low σ has to be chosen. Since in coherent detection the power of the incoming signal is normally high enough, more precise localization is chosen in our design.

Once the edges are detected, the maximum value of the edges is extracted using an algorithm, the final purpose of the algorithm is to have an edges array with a ONE when an edge maximum is and ZEROS otherwise. This is done discarding all values below a threshold that depends on the SNR to prevent detection of noise peaks like edges of the bit stream. Once the noise is not taken into account each value is compared with the previous and the following one, if the value is bigger than both means that it is a maximum and therefore is where the edge has more probabilities to be. It can be seen in how the method is valid even under presence of hard noise. Both figures represent a bit stream of 64 bits sent at a bit rate of 10Gbps, no impairments are considered except noise, in (a) the SNR is 20 dB while in (b) the SNR is 0 dB; in red is represented the edges extracted using the model described using a impulse response with σ=BR/10 and the simulation is done with 32 samples per bit which is an assumption of that the bit stream is analog.

Once the exact position of the edges has been detected, the sampling process is carried out. Sampling is a periodic process with a sampling frequency chosen; therefore the edges signal found could not be used for the sampling because the edges are not periodic. Thereby, a sinusoidal signal is in charge of the sampling of the bit sequence received; let's call this sinusoidal signal the sampling signal. Each maximum of the sampling signal is in fact the sampling point, therefore, a sampling signal at least at the bit rate is needed, in such case one sample per bit of the bit stream is obtained. Of course the sampling frequency can be chosen higher than the bit rate to obtain more samples per bit and it is achieved by changing the frequency of the sampling signal. However, before the sampling itself the signal has to find where the edges are located since they are its reference for know where to sample, for that purpose the frequency of the sampling signal is set up to the bit rate for having one maximum per edge detected. If the sampling signal is first matched with the edges and then shifted half the bit time, the maximums of the sinusoidal signal fall into the middle of the bits. Then is when the frequency of the sinusoidal signal can be changed to the sampling frequency required for having the number of samples per bit wished.

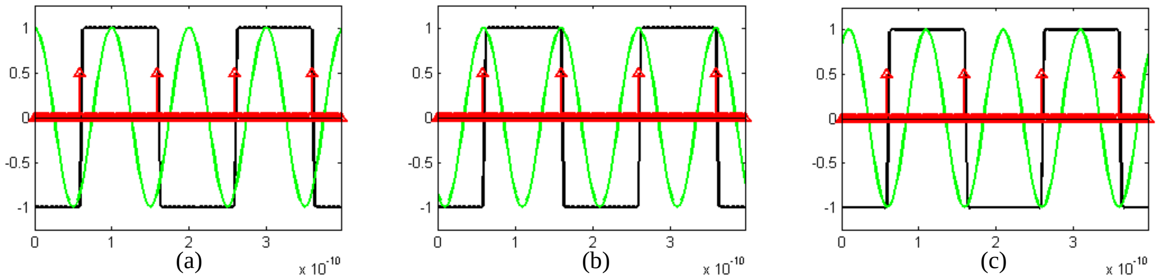

Figure 3-6. Sampling signal(green) with sampling rate = bit rate (a) before correlation with edges (b) after correlation with edges (c) after shift o T/2

The method for sampling at the correct point using the information given by the edges is as follow. Once the sampling signal is created it is shifted a little space of time and cross correlated with the edges. In each shift the cross correlation between both signals is stored. Finally the shifted sinusoidal signal that maximizes the cross correlation is chosen. In this moment a periodic signal with its maximums matched with the edges is obtained, see Figure 3-6-(b). Now if the sampling rate is chosen bigger than the bit rate, the frequency of the periodic signal is changed for having the required samples per bit. Because is said that the maximums are the sampling points and is required to sampling in the middle of the bit the sinusoidal signal is again shifted half the bit time, in this moment the sampling signal has its maximum or sampling points in the middle of the bits, see Figure 3-6-(c). In fact the signal has to be shifted half the bit time divided by the sampling rate, in this way if we have more than one sample per bit they fall into a correct position inside the bit. In Figure 3-6 are depicted the sampling signal in green, a part of a bit sequence in black and the edges in red.

From Figure 3-7 can be noticed that the noise is not a real problem for the edge detector since it can extract the edges with an excellent localization even when the SNR of the signal is low, moreover no false edges are present. But how does the edge detector behave with a distorted signal as consequence of chromatic dispersion or PMD?

Our intention is to implement a receiver able to compensate high values of chromatic dispersion using DSP, even for fiber lengths of thousand kilometers. Having such receiver mean that traditional chromatic dispersion pre-compensation along the fiber is not needed anymore, that is of course an advantage but mean that the signal arriving to the receiver will be very distorted, so how will the edge detector respond under high values of chromatic dispersion? In fact the edge detector response is chaotic, if the sigma parameter is chosen low many false edges are found giving wrong information for sampling; if sigma is chosen higher this false edges disappear, only few edges are found but at least they do not give false information.

This issue is an important problem in receivers with DSP equalization of impairments and the clock recovery can be important in such systems. Sampling the signal with the proper rate can avoid sampling time errors, the sampling frequency required to avoid sampling errors is in the order of the Nyquist rate of twice the bit rate that also is needed to completely reconstruct the signal.

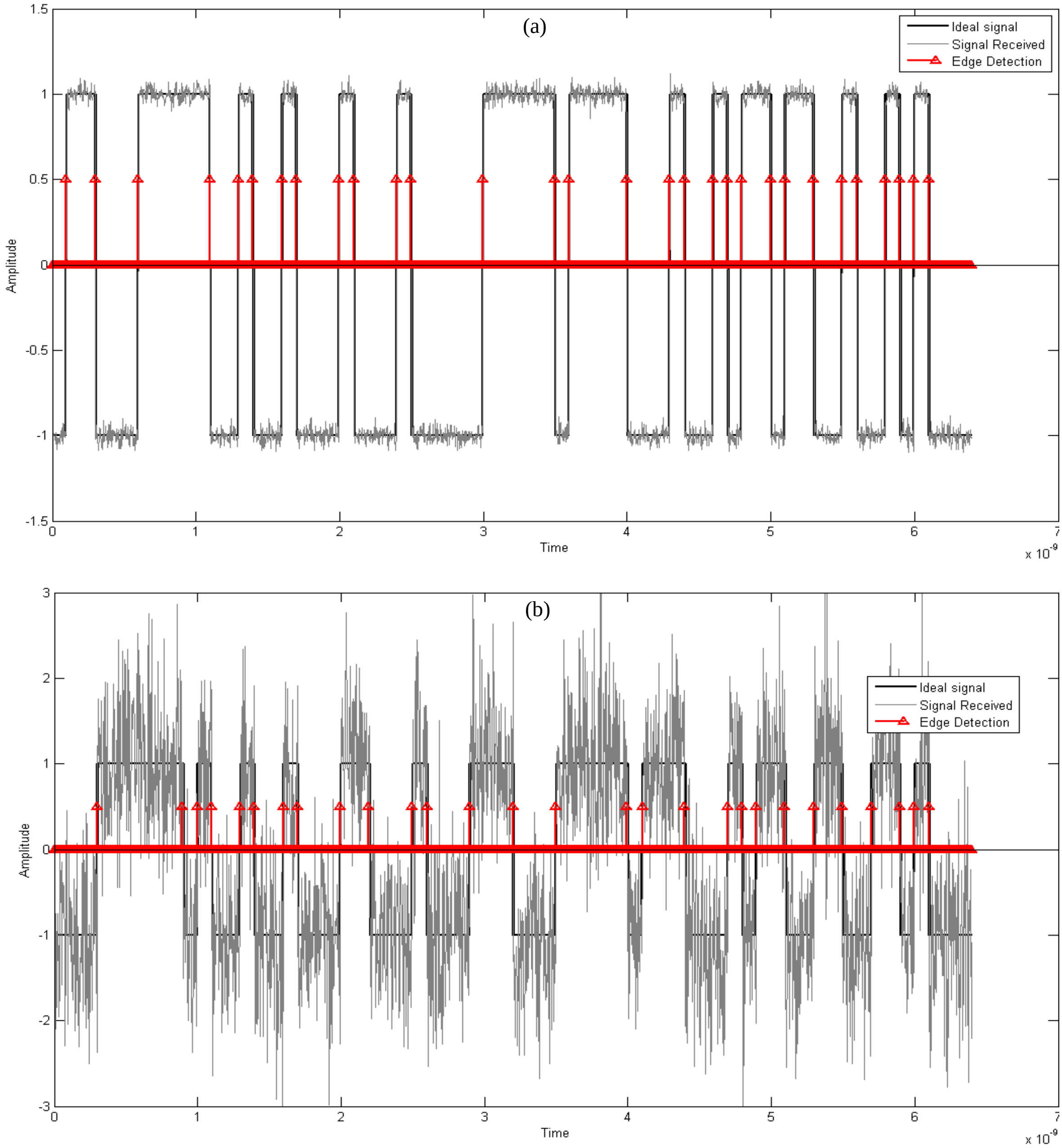

Figure 3-7. Edge detection for two bit stream of 64 bits sent at 10 Gbps, the edges extracted by canny edge detector with σ=0.1BR are represented in red. (a) SNR = 20 dB (b) SNR = 0 dB

3.3 Impairments Compensation

One of the most interesting parts of coherent receivers is the possibility of impairments compensation, such CD and PMD, because the information of the entire optical signal (phase and amplitude) is available. Phase noise and frequency mismatch between the transmitter and local oscillator laser can also be compensated digitally. Phase noise can also be considered impairment but its compensation is discussed in section 3.4, to simplify the reading.

The CD, PMD and polarization mismatch equalization carried out in our digital coherent receiver is explained in this point.

Electronic equalization can be used, if the fiber acts as a linear system, for compensating chromatic dispersion. PMD as well as polarization mismatch can also be equalized using adaptive filters [7] [8] . There are some difficulties performing both types of compensations. The main difficulty with both techniques is that they require fast electronic circuits which must operate at the bit rate, if not the receiver would work offline. In the case of CD compensation, DSP complexity increases exponentially with the number of bits over which an optical pulse has spread because of chromatic dispersion [9] . For PMD the filter design has to be adaptive since PMD is strongly time variant.

The design for the CD and PMD equalizer chosen follows the scheme showed in Figure 3-8 [7] . This scheme is inside the DSP block of Figure 3-1 following the PCM uniform, so it receive two signals x and y, one per each polarization of light due to polarization multiplexing technique. The equalization is divided into two blocks, the first one is for polarization independent impairments, this block is in charge of the CD compensation and because CD is independent of the polarization this block does the equalization of each polarization individually, and thus equalization of each polarization could be processed in parallel. For CD we have implemented two equalizers: one non-adaptive and an adaptive equalizer. The decision was to implement also an adaptive equalizer for CD because later four adaptive filters will be used for the PMD compensation equalizer. Therefore the CD adaptive equalizer implemented could be used for the PMD equalizer implementation and moreover, it can also be tested and compared with the non-adaptive version.

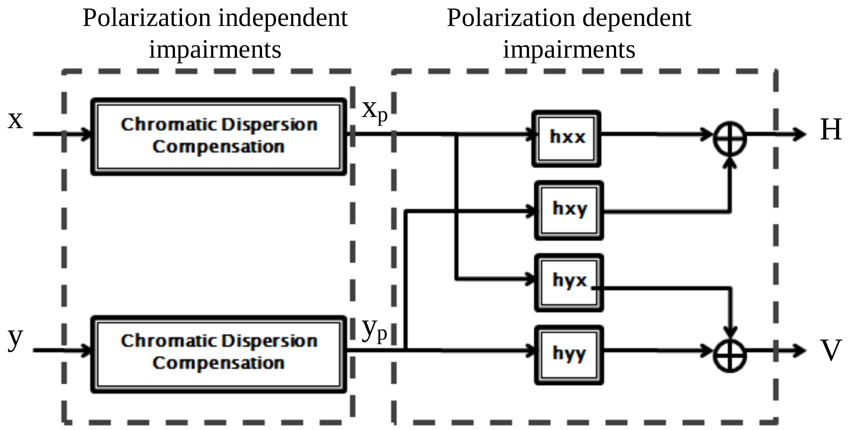

Figure 3-8. Block Diagram of the digital filtering stage.

The second block is for polarization dependent impairments and is able to compensate PMD and polarization mismatch. This block needs both polarization for equalize such impairments. For PMD and polarization mismatch compensation, the filter has to be adaptive since PMD and the polarization mismatch of the received signal due to fiber birefringence is time variant, and therefore, a solution with fixed taps is not valid.

Let's divide the explanation of CD and PMD compensation design in these two blocks and begin with polarization independent impairments. Nonlinearities are not taken into account all over this chapter.

3.3.1 Polarization Independent Impairments

The first block is in charge of polarization independent impairments equalization, which is mainly chromatic dispersion and tight filtering. Tight (optical or electrical) filtering leads to inter-symbol interferences and can also be mitigates using FIR filters. Validation of the CD equalizer proposed is further studied in section 4.2.

In the frequency domain chromatic dispersion can be represented as a scalar multiplication [8] being the transfer function:

$$H_{CD}(\omega) = e^{j(\frac{1}{2}\beta_2 L(\omega-\omega_S)^2 + \frac{1}{6}\beta_3 L(\omega-\omega_S)^2)} \tag{3.2}$$

where β_2 is the GVD, β_3 is the dispersion slope, L is the length of the fiber and ω_s is the signal carrier frequency. Long haul systems use DCF to compensate CD optically however, inexact matching between $\beta_2$and β_3 of transmission fiber and DCF dictates the need for terminal dispersion compensation at high bit rates, normally 40Gbps or higher [8] . In the implementation and simulations the considered chromatic dispersion parameter is $D = 13.32\, ps/(nm \cdot km)$ for all the fiber lengths used that is equal to a parameter $\beta_2 = 17^{-24}\, \frac{s^2}{km}$.

Knowing the transfer function of chromatic dispersion the compensation of it can be easily seen as a filter with a transfer function $G(\omega) = \mathrm{H_{CD}}(\omega)^{-1}$ in which the only parameters needed for obtaining it are the length and the dispersion parameters of the fiber, which are well known parameters in every optical system. For the compensation filter design we have chosen FIR architecture, presented in Figure 3-9. FIR filters can be implemented even if the filter function is not causal, if an additional delay is permissible. The coefficients of the FIR filter are usually called *taps weights* or taps coefficients and they define the degrees of freedom in the filter design. As more taps the filter has more degrees of freedom and more precisely the filter function is implemented but also more complex and slowly is the implementation in a DSP board. For that reason the number of taps wished on the filter designs is usually the minimum enough to obtain a certain result. Using the inverse of such transfer function and the enough number of taps any amount of chromatic dispersion can be compensated with this equalizer.

Therefore the minimum number of taps needed for CD compensation has to be found. Next is obtained a bound for the theoretical minimum number of taps needed for compensate a given value of dispersion. The CD equalizer must have at least the minimum number of taps determined by this theoretical bound for compensating a certain CD value. This theoretical bound is tested in chapter 3 using the results of the CD compensation equalizer.

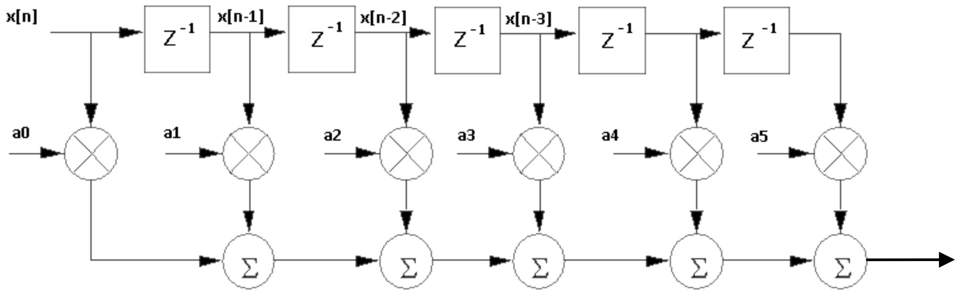

Figure 3-9. FIR filter architecture

The idea for obtaining the minimum number of taps needed for CD compensation is the following: to compensate a given dispersion value, the minimum number of taps needed is equal to the amount of samples affected by the overlapping caused by the spread of the pulse sent due to chromatic dispersion. In other words if the spread of a pulse overlap two neighbor bits we need the information of the overlapped bits for compensating the distortion caused by the spread symbol.

If the pulse spreading in time domain is given by

$$\Delta T = DL\Delta\lambda \tag{3.3}$$

where D is the dispersion parameter, L the length of the fiber and $\Delta\lambda$ is the range of wavelengths emitted by the optical source. Therefore the number of pulses affected by the spreading of one pulse is equal to the number of bits affected by the pulse spreading and we can calculate finding the number of pulse duration that enter in the pulse spreading time:

$$\frac{\Delta T}{\tau} \tag{3.4}$$

τ is the bit duration that is equal to de inverse of the bit rate. With the last expression the number of bits affected by the spread of the pulse due to chromatic dispersion is known, to know the number of taps needed by the FIR filter we should use the number of samples per bit. As the FIR filter works with samples and each bit is defined by the number of samples per bit, finally the number of taps needed by the FIR filter for compensating a given dispersion is

$$tapsCD_{\min} = \frac{\Delta T}{\tau}\left(\frac{f_S}{R_b}\right) = \frac{DL\Delta\lambda}{\tau}\left(\frac{f_S}{R_b}\right) \tag{3.5}$$

where the fraction $\frac{f_S}{Rb}$ is the number of samples per bit taken in the sampling process. Because the number of taps in a FIR filter is an integer number, if the result of the last expression is not an integer the ceil of the expression is used for describing the minimum number of taps needed for equalization of certain D dispersion over L km of fiber.

Next figure is an illustration of the number of bits, which are depicted as ceils, overlapped by the spreading of a pulse and the number of samples affected by this spreading. Therefore the theoretical number of taps needed for compensate CD are the number of neighbor bits affected by a pulse spreading multiplied by the number of samples per bit, which are drawn the figure by red circles.

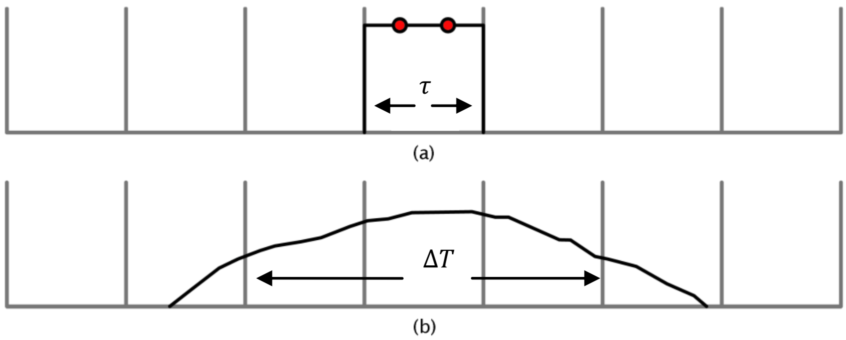

Figure 3-10. Spread due to chromatic dispersion.

For the FIR filter taps, Savory [7] has obtained a simple closed form solution for the tap weights that also provides an upper bound on the number of taps required for a given value of dispersion. The form of the taps is the following

$$a_k = \sqrt{\frac{jcT^2}{D\lambda^2 L}\exp\left(-j\frac{\pi cT^2}{D\lambda^2 L}\right)k^2} \;;\; -\left\lfloor\frac{N}{2}\right\rfloor \le k \le \left\lfloor\frac{N}{2}\right\rfloor \; and \quad N = 2\left\lfloor\frac{|D|\lambda^2 L}{2cT^2}\right\rfloor + 1 \tag{3.6}$$

where a_k are the taps weights, k is a sub-index indicating the number of the tap, c is the speed of light and T is the sampling time $T = 1/f_{s,}$. The operator $\lfloor x \rfloor$ means the integer part of x rounded towards minus infinite.

An adaptive equalizer for chromatic dispersion is also implemented. The adaptive equalizer adapts the taps of the filter dynamically and hence, even if the parameter of the fiber is unknown, the correct taps to equalize chromatic dispersion are found automatically. Therefore the adaptive equalizer has the advantage that the parameters of the fibers can be unknown and thus the receiver would operate for every kind of fiber, just choosing the number of taps used by the adaptive equalizer. This model has one important disadvantage:

require an initial time to converge to the optimal taps solution. At the beginning the taps are far away from the optimal solution and the adaptive filter needs some time to get closer to the solution.

A scheme of an adaptive equalizer is in Figure 3-11. In the figure *x(n)* is the incoming signal affected by chromatic dispersion, *d(n)* is the desired response, y(n) is the output of the adaptive filter and *e(n)* is the error signal defined as *e(n) = d(n)-y(n)*.

Mainly, the working process of a adaptive filter is as follows: the incoming signal *x(n)* enter to the digital filter which has an initial value for the taps ***a***. Then the output of the filter together with the desired response are used to obtain the error signal, which is the error between the output obtained and the output desire , that is the input of the adaptive algorithm in charge of changing the value of the taps. There are several adaptive algorithms, in this case, it has been implemented a receiver in which you can choose the adaptive algorithm between two well known algorithms: LMS and CMA.

Moreover the adaptive filter implemented can work a percentage of the time using one of the algorithms and the rest of the time using the other one. In this way are able to study the influence of the adaptive algorithm in the behavior of the adaptive equalizer.

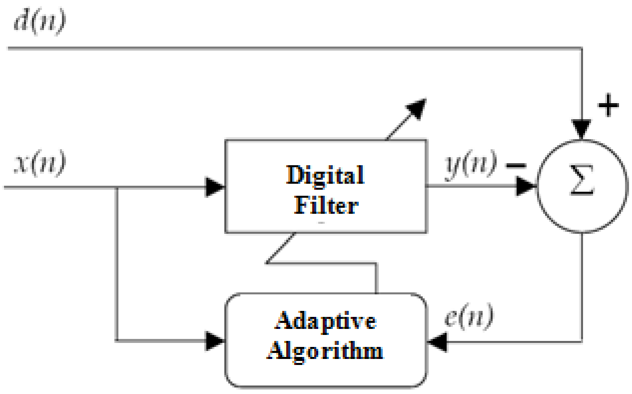

Figure 3-11. Adaptive filter scheme

Both the LMS (least mean square) algorithm and the CMA (constant modulus algorithm) have a similar form:

$$\begin{aligned} LMS:&\quad \overline{a_{k+1}} = \overline{a_k} + \mu e_k \overline{x_k^*} \\ CMA:&\quad a_{k+1} = \overline{a_k} + \mu e_k y_k \overline{x_k^*} \end{aligned} \tag{3.7}$$

μ is a constant term known as step parameter; $\overline{a_k}$ is the actual coefficient array and $\overline{a_{k+1}}$ is the next coefficients array; $\overline{x_k^*}$ is the conjugate of the input signal array while y_k is the last output of the adaptive filter. Lines over letters indicate that are arrays, in fact, the length of the array is determined by the chosen number of taps of the adaptive equalizer

The step parameter has an important influence on the adaptive filter behavior. In fact its influence is over the convergence speed and the error of the equalizer output. If the step size is big the algorithm will converge faster but its error will be bigger than if the step size is small. Otherwise, if the step parameter is chosen small then the convergence will be slow and the error will be large. This influence can be seen better using what is called learning curves of the adaptive equalizer. In a learning curve is depicted the mean square error in front of the time n. In a typical behavior of an adaptive equalizer the error begins high and it decrease as n is increased like a negative exponential as is showed in Figure 3-12.

The minimum error that an adaptive equalizer can achieve is the $e_{min,}$ the time needed to converge is depicted as t_{conv} and is known as convergence time. Convergence time is defined as the time needed for the adaptive algorithm to diminish the error to a 37% of its initial value.

If the step size μ is high then t_{conv} would be small as e_{min} would be big compare to the case in which μ is small, in such case t_{conv} is big and e_{min} is small. It is important to notice that in presence of different impairments such noise, PMD or nonlinearities the e_{min} has a floor value that the CD adaptive equalizer cannot improve.

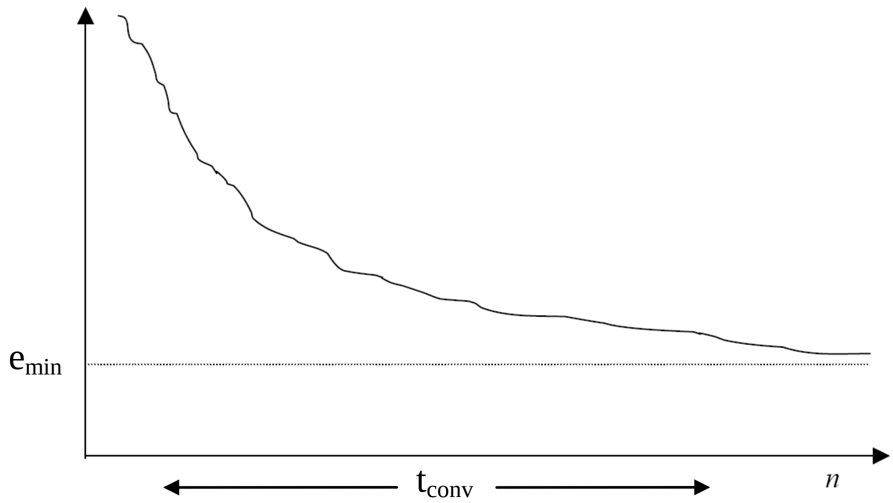

Figure 3-12. Learning curve of an adaptive filter

The difference between LMS and CMA lies in the signal *d(n)* from which the error signal is obtained. In LMS the *d(n)* signal is the closest symbol to the output of the adaptive algorithm, since we are working with QPSK the desire signal *d(n)* will depend on which quadrant lies the output of the adaptive filter *y(n)* and the symbol of the quadrant where *y(n)* fall into is chosen to be *d(n)*. In our case *d(n)* for the LMS algorithm can be one of the four options: 1+j, 1-j, -1+j and -1-j. In Figure 3-13 all this signal are represented for the two algorithms.

In the case of CMA only the modulus difference between the output of the adaptive filter y(n), and the desire signal d(n), is used. In the modulation case treated in this study, which is a QPSK, symbols are centered at 1+j, 1-j, -1+j and -1-j, so the d(n) signal used is $\sqrt{2}$. Then in CMA the error signal used is always: e(n) = $\sqrt{2}$ – |$\bar{y}$(n)|.

From Figure 3-13 can be noticed that LMS algorithm gives some phase information to the taps since the error signal is obtained from the difference of two vectors, on the other hand when CMA is used the error signal is only a real value that then is multiplied with $\bar{y}$ therefore no phase information is given to the taps adaptation since the phase information of the vector $\bar{e}\bar{y}$ is still being the phase of the vector $\bar{y}$.

In the case of adaptive filters the number of taps, like in the non-adaptive case, has to be chosen and moreover, the number of iterations of the algorithm. Since adaptive filter needs taps to converge to an optimal solution the algorithm needs some iterations to converge, this increase the computational cost of the adaptive design.

Due to this increment in the computational cost of the adaptive solution the non-adaptive option is the most suitable for chromatic dispersion compensation since both obtain the same good results referred to the quantity of chromatic dispersion that can be compensated. The fixed taps, or non-adaptive solution has in his favor that do not need time to converge to the solution since the taps can be introduced directly using Savory solution (3.6), or can be calculated using the transfer function of a dispersive fiber. The computational cost of equalize with non-adaptive equalizer is therefore less than using adaptive equalizer. In his favor the adaptive equalizer has the property that no information about the length or dispersion parameter of the fiber has to be known.

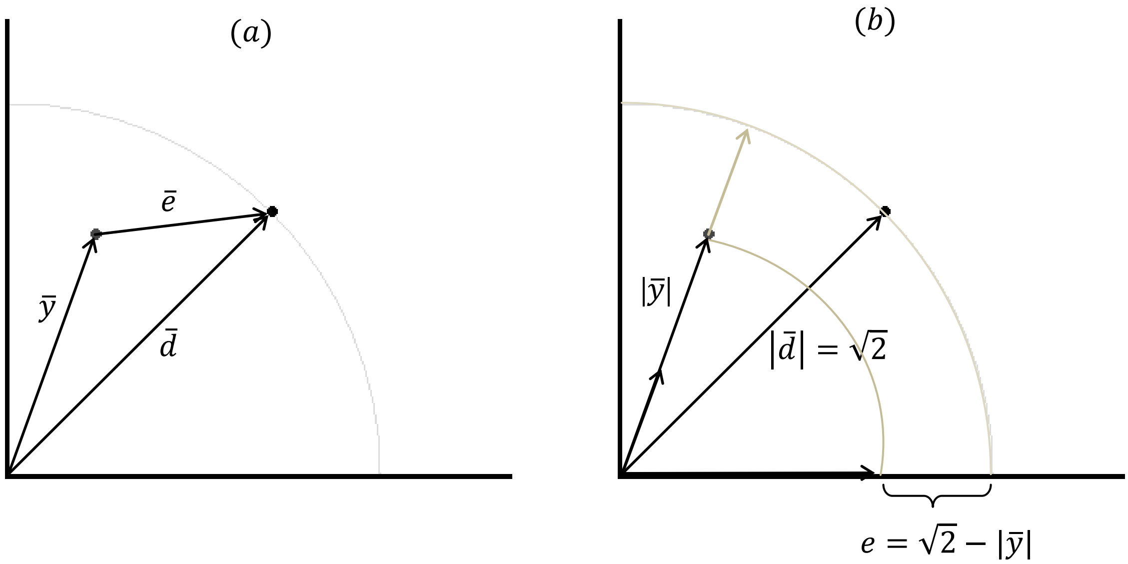

Figure 3-13. Graphical representation of error value in (a) LMS algorithm (b) CMA

Therefore, in this work two CD equalizers have been designed. A FIR based CD equalizer in which the taps are fixed and previously introduced in the filter. The taps are calculated in function of the parameter D of the fiber, using an equation given by Savory in [7] . The other CD equalizer designed is an adaptive equalizer in which the user can choose between two adaptive algorithms: CMA and LMS. At first sight, the FIR based CD equalizer is more suited for CD compensation than the adaptive CD equalizer however, both were implemented for later compare them performance in Chapter 4.

3.3.2 Polarization Dependent Impairments

Today's fiber exhibits PMD that can be smaller by orders of magnitude than older, currently laid-out fiber, which is mostly due to a much improved manufacturing process. Replacing old fiber, however, is very costly. Therefore understanding and compensating PMD is of great importance.

The second block of Figure 3-8 is in charge of polarization dependent impairments compensation. In this work polarization mismatch and first order PMD is taken into account in this module while second order PMS is neglected. The impact of polarization dependent effects on the propagation may be modeled by a Jones matrix, the task is therefore to estimate the Jones matrix and obtain the inverse of it for compensate for the impairments incurred. Some investigations throws that optical communications using polarization division multiplexing is analogous to wireless communications using multiple-input-multiple-output (MIMO) antennae and thus algorithms for channel estimation in wireless MIMO can be applied to optical polarization MIMO [30] [32] .

As told in chapter 2, due to environmental variations polarization of lightwave inside the fiber generally drifts with time, because the drift is generally much slower than the bit rate, the Jones matrix can be estimated.

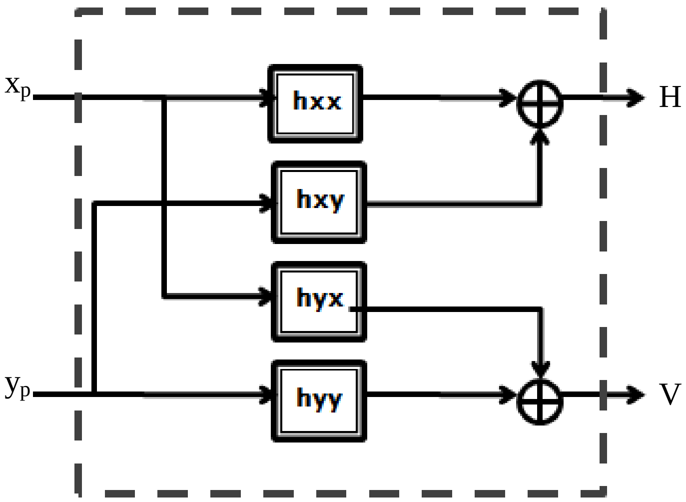

Figure 3-14. Adaptive filter architecture for polarization dependent compensation

For polarization dependent compensation four adaptive equalizers in the structure showed have to be used. All of them are FIR adaptive filters like the one designed for chromatic dispersion compensation depicted in Figure 3-11, their taps are denoted by hxx, hxy, hyx and hyy and they are adapted using again the LMS algorithm and CMA. Both algorithms are written in equation (3.8).

In equation (3.8) h is used to define the taps of each adaptive equalizer, line over letter indicates that are arrays, the sub-index k shows the actual value while k+1 means next value after taps adaptation.

$$
LMS: \quad \begin{aligned}
\overline{hxx_{k+1}} &= \overline{hxx_k} + \mu e_{xk} H \overline{x^*_{pk}} \\
\overline{hxy_{k+1}} &= \overline{hxy_k} + \mu e_{xk} H \overline{y^*_{pk}} \\
\overline{hyx_{k+1}} &= \overline{hyx_k} + \mu e_{yk} V \overline{x^*_{pk}} \\
\overline{hyy_{k+1}} &= \overline{hyy_k} + \mu e_{yk} V \overline{y^*_{pk}}
\end{aligned}
$$

$$
CMA: \quad \begin{aligned}
\overline{hxx_{k+1}} &= \overline{hxx_k} + \mu e_{xk} \overline{x^*_{pk}} \\
\overline{hxy_{k+1}} &= \overline{hxy_k} + \mu e_{xk} \overline{y^*_{pk}} \\
\overline{hyx_{k+1}} &= \overline{hyx_k} + \mu e_{yk} \overline{x^*_{pk}} \\
\overline{hyy_{k+1}} &= \overline{hyy_k} + \mu e_{yk} \overline{y^*_{pk}}
\end{aligned} \tag{3.8}
$$

If the taps of all filters are initialized with the same value then the 4 equalizers converge to the same output, corresponding to a singular Jones matrix which is not feasible. Therefore, the initial taps of the filters have to be all zeros except the central tap of hxx and hyy which are set to one.

Previously in chromatic dispersion compensation we have implemented two different equalizers: one adaptive and other non-adaptive. In case of polarization dependent impairments there is no choice and adaptive filter have to be used since polarization dependent impairments are time variant.

Therefore, the adaptive MIMO equalizer for PMD compensation has been implemented using two different adaptive algorithms: CMA and LMS. Later, in chapter 4 the performance of the equalizer is tested, first it alone and together with CD equalizer.

3.4 Phase Noise Compensation

Phase noise and frequency offset between transmitter and local oscillator laser can also be compensated using digital circuits in a DSP board when coherent reception is used. Let’s introduce how this compensation is done digitally in a digital coherent receiver.

As was shown in chapter 2, phase noise produces a rotation in the constellation sent, in our case on the QPSK constellation. The main idea behind phase noise compensation techniques is to make an estimation of the phase noise that affects the signal and once the estimation has been made the value obtained can be used to de-rotate the symbols.

3.4.1 Phase noise due to frequency offset

Let focus our attention in the case of phase noise present in the received signal when a frequency offset between transmitter and local oscillator laser is present. A frequency offset between transmitter and local oscillator is present creates a linear phase noise that can be compensated digitally. To illustrate such scenario just the information sent in one polarization is used, the results are analogous for the second polarization when polarization multiplexing is used.

As shown in 2.6.4, frequency offset produces a phase shift on the constellation that induces an increment in the BER. The increment on the BER depends in how much phase noise induced by frequency offset is present and therefore in the frequency offset between the transmitter and the local oscillator.

From equation (2.51), without the DC term because the current has been obtained using balanced detection, and ϕ_M denoting the phase information due to QPSK modulation, the current obtained when other impairments have been neglected, also phase noise, in the in-phase branches of X and Y polarization after the sampling process is as follows

$$i_I(kT_S) = 2R\sqrt{P_S P_{LO}}\cos(w_{IF}kT_S + 2\pi\Delta f kT_S + \phi_M(kT_S)) \tag{3.9}$$

where T_S is the sampling time, Δf is the frequency offset in hertz between local oscillator and transmitter laser, and k is a running index that denote the number of the sample taken by the sampler.

From last expression can be seen how the phase offset causes a phase shift $\Delta\varphi = 2\pi\Delta f kT_S$. Because phase noise due to frequency drift is neglected here and just frequency offset is present, the term Δf is constant and thereby, the phase shift induced is linear in function of kT_S with pendent $2\pi\Delta f$. Therefore, phase noise due to frequency offset between consecutives samples has always the same value:

$$\Delta\varphi = 2\pi\Delta f T_S \tag{3.10}$$

in which T_S is the sampling time. Therefore the idea is to find the value of the phase noise between consecutive samples and then use it to derotate each sample using the value estimated and the running index k of the sample. For that purpose has to be noticed that the phase information φ_M that each symbol contain because phase modulation has to be disccard. In fact, to estimate the phase shift $\Delta\varphi$ induced by a frequency offset without be blurred by phase information, a method to previously remove phase information has to be used. Let's explain deeply the method implemented at the receiver DSP module for frequency recovery.

For frequency offset compensation, the ***phase increment estimation algorithm*** proposed in [34] is implemented. This is a digital frequency estimator well known in wireless communication and it is simply enough to be implemented in a high-speed signal processor. The block diagram of the proposed algorithm is depicted in Figure 3-15.

Let's explain how the frequency estimator implemented works. The signal that arrives to the frequency estimator is QPSK modulated signal, a complex value which real part is the in-phase photocurrent and its imaginary part is the quadrature photocurrent. Therefore the complex value arriving to frequency estimator is

$$H_k = 2R\sqrt{P_S P_{LO}}\exp(j(w_{IF}kT_S + 2\pi\Delta f kT_S + \phi_M(kT_S))) \qquad (3.11)$$

To obtain the phase shift between consecutives samples, the frequency estimator obtain first the phase difference between consecutives samples then, the phase modulation is removed. Finally, the resultant phase is averaged over a large number of samples to obtain an averaged estimation Δφ.

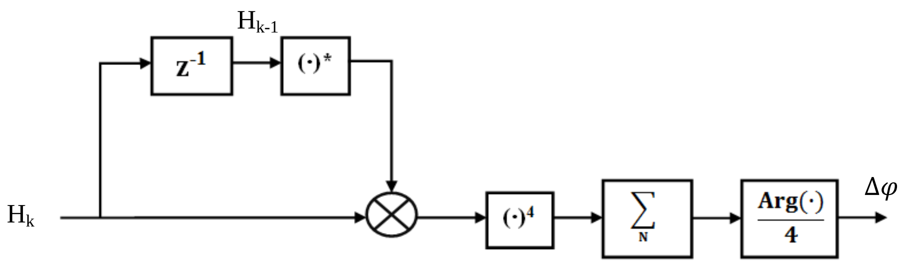

Figure 3-15. Block diagram of a frequency estimator [34]

To realize such algorithm the received signal is retarded, depicted as H_{k-1} in Figure 3-15, and then conjugated, afterwards, H_{k-1}^* is multiplied with the signal without been retarded H_k. This means that every sample is multiplied with the conjugate of the previous sample, obtaining in this way, a complex number whose phase is the phase difference between two consecutives samples, see eq (3.12).

$$H_k H^*{}_{k-1} = 4R^2 P_S P_{LO}\exp[j(\Delta\varphi + (\phi_{M_k} - \phi_{M_{k-1}}))] \qquad (3.12)$$

where ϕ_{M_k} is the phase modulation of the symbol k at time kT_S and Δφ is the phase noise due to frequency offset between consecutive samples as was shown in eq. (3.10). Now we have the phase difference between consecutives symbols and therefore an estimation of Δφ, the problem is that at this point, the difference of the phase information of both symbols $\phi_{M_k} - \phi_{M_{k-1}}$ introduces an error in the estimation of Δφ and therefore the phase modulation must be removed. For that pourpose the nth power of the complex value has to be taken, being n the number of costellations points, in our case for QPSK n= 4.

Can be simply seen why taking the fourth power of (3.12) the phase information is removed: in QPSK the phase information is one of these four option: $\frac{\pi}{4}, \frac{3\pi}{4}, \frac{5\pi}{4}, \frac{7\pi}{4}$, therefore the phase information difference of two symbols will always be $2n\frac{\pi}{4}$ $n\in[-3,3]$. When a complex value is powered to four is the same than multiply the phase of the complex value by 4, thereby the phase information difference will always be a $2n\pi$ with $n\in[-3,3]$ and the phase shift caused by the frequency offset $\Delta\varphi$ is not blurred by the phase information difference between the consecutive symbols.

$$(H_k H^*{}_{k-1})^4 = (4R^2 P_S P_{LO})^4 \exp[j(4\Delta\varphi + 2n\pi)] = (4R^2 P_S P_{LO})^4 \exp[j4\Delta\varphi] \quad (3.13)$$

We should notice that the desired $\Delta\varphi$ is also multiplied by 4 due to the nth power operation and thereby phase estimation should be divided by four to obtain the correct phase estimation, this operation is done later.

Now we have a valid estimation of $\Delta\varphi$ without phase modulation information and now the results are summed up over a large number of samples, essentially to average the phase difference between samples and therefore have a better estimation of $\Delta\varphi$. The number of symbols to be averaged N, has to be chosen and, as bigger N as better the average value obtained. A decision concerning the number of symbols over the averaging is taken has to be made, if N is chosen small more simple and faster the DSP board will be but worse estimations would be obtained. N needs to be as large to at least have an enough low BER. For our results ,if it is not indicated, N is chosen to be 500. It is a large number that should be enough to completely compensate phase noise due to frequency offset.

Once the averaged value has been obtained it has to be divided by four to compensate the earlier power-of-four operation. Finally, at the end of the block diagram represented in Figure 3-15 we have the averaged $\Delta\varphi$ caused by the frequency offset between transmitter and local oscillator laser. Once this value has been obtained it can be used for correcting the phase noise induced by a frequency offset. For that purpose each sample k has to be multyplied by the phase estimation scalated by k. This is due to the fact shown in chapter 2.6.4 that phase noise due to frequency offset is completely linear as a function of time. Therefore each sample k that arrives to the frequency estimator is finally derotated by multiplying it with an exponential having as phase the estimated value done by the frequency estimator multiplied by k:

$$\phi_k = k\Delta\varphi \quad (3.14)$$

being φ_k the phase that has to be derotated each sample H_k to compensate for phase noise due to frequency offset and $\Delta\varphi$ the averaged phase estimation done by the frequency estimator.

The explained method is usefull when phase noise is linear, as in the case of a frequency offset between transmitter laser and LO, however when phase noise due to frequency drifts in lasers is present, which is not linear, then last method is not valid. Frequency recovery method can be used for phase noise induced by frequency offset but another technique has to be implemented for phase noise due to frequency drift. At this point if phase noise due to frequency drift is taken into account, symbols should be compensated using phase estimation techniques.

3.4.2 Phase noise due to frequency drifts

The lases involves in the optical tranmission systems have certain linewidht and do not work at a fixed frequency, the working frequency drifts causing phase noise. This phase noise is not linear as was the phase noise due to frequency offset. A random phase noise due to frequency drift of the lasers depicted in Figure 3-16.

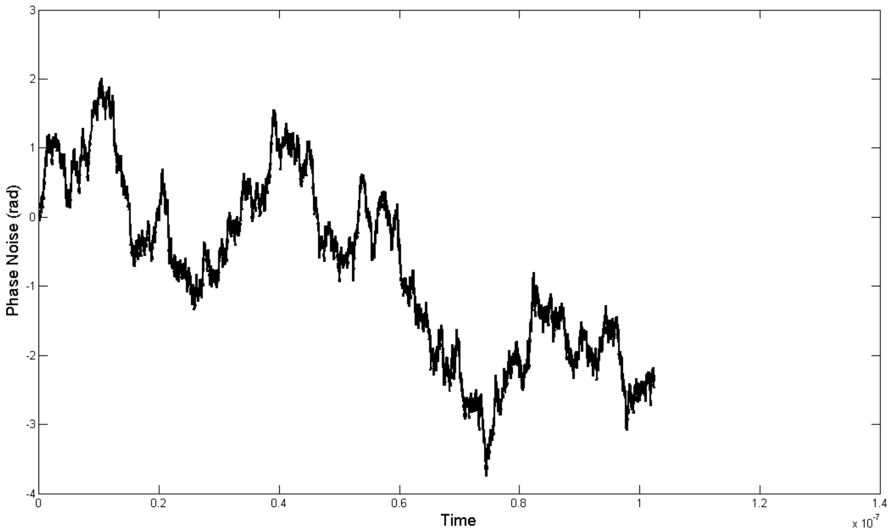

Figure 3-16. Phase noise ϕ_{IF} (t) due to linewidth of the laser

Laser peak contains unwrapped phase noise $\phi_{IF}(t)$ such $\phi_{IF}(t) = \phi_{IF}(t-\tau) + w(t)$ where w(t) is a zero mean Gaussian noise having variance

$$\sigma_w^2 = 2\pi\tau\Delta\upsilon \tag{3.15}$$

where τ is a differential of time and $\Delta\upsilon$ is the sum of the linewidths of the transmitter laser and local oscillator. The received signal arriving to the phase estimator is a complex sampled signal received using balanced detection, after the sum of the sampled in-phase and quadrature components the incoming signal is the following

$$H_k = 2R\sqrt{P_S P_{LO}}\,\exp(\,j(w_{IF}kT_S + \phi_{IF}(kT_S) + \phi_M(kT_S))) \tag{3.16}$$

In las equation has been discarded phase noise due to frequency offset. In this way it is only ilustrated when just carrier phase noise affects the signal. Since the incoming signal has been sampled, the carrier phase noise is also sampled beeing

$$\phi_{IF}(kT_S) = \phi_{IF}((k-1)T_S) + w(kT_S) \tag{3.17}$$

where $w(kT_S)$ is a zero mean gaussian noise with variance $\sigma_w{}^2 = 2\pi T_S \Delta\upsilon$. In this case phase noise is not linear as it was in the case of phase noise due frequency offset and thereby, it draws a picture similar to the one depicted in Figure 3-16.

In this work, two different carrier recovery methods have been implemented: *soft estimation carrier recovery*, and *hard estimation carrier recovery*. Let's begin with **soft estimation**.

The technique employed for soft phase estimation is very similar as the described for frequency estimation, the main difference reside in that no phase difference between symbols is used. The block diagram of the methos used is on Figure 3-17 and is based in [36] , phase unwrapping function is obtained from [37] .

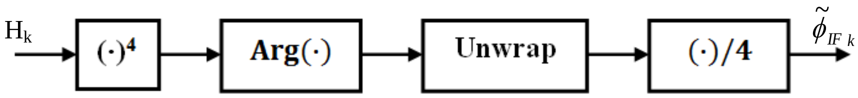

Figure 3-17. Block diagram of a NDA Soft Phase Estimator for QPSK modulation

The structure depicted in Figure 3-17 is a Soft Phase Estimation technique known as ***NDA (Non-Data Aided)***. It is a technique that exploit the M-fold rotational symmetry of an M-PSK constellation.

The technique, needs again to remove the phase information due to the modulation therefore, H_k is raised to *n*th power as was explained for the frequency estimator. In this way, the phase modulation does not affect anymore to the carrier phase that is wanted to be estimated.

At this point, the argument of the complex value raised to the *n*th power is taken. From equation is implicit that carrier phase noise has to be an unwrapped value but the function arg(·) of Matlab gives wrapped values in the range $-\pi$ to π therefore, phase unwrapping has to be implemented accordingly to [37] . This unwrapping is done in the module Unwrap of Figure 3-17. In the last module, the unwrapped phase has to be divided by n to compensate for the *n*th power previously taken and, the estimation of the carrier phase is finally obtained.

Therefore the NDA soft estimator obtains an estimation of the phase of every symbol, in frequency estimator the estimation was the phase difference between consecutive symbols.

Furthermore what is very interesting from this compensation scheme is that, theoretically it can also detect phase noise due to frequency mismatch between the transmitter and the LO laser. In the presence of both frequency mismatch and carrier phase noise in a homodyne receiver the phase estimation of the NDA soft estimator of every symbol k would be

$$\tilde{\phi}_{IF\,k} = \phi_{IF}(kT_S) + 2\pi\Delta f k T_S \tag{3.18}$$

If this phase estimated is substracted from each symbol k it would be compensated for both frequency offset phase shift and carrier phase noise. Therefore NDA soft estimator can theoretically be used for the estimation of both. So, using this NDA soft phase estimator no frequency offset estimator is needed.

The **hard estimation carrier recovery** implemented was the ***two-stage iterative carrier phase estimator***, depicted in Figure 3-18. In a hard estimation model, after the soft decision phase estimation a hard decision phase estimator is used. The hard decision phase estimator is no more than a Wiener filter W(z) whose output is the minimum mean square error of the actual carrier phase estimation obtained by a soft phase estimator.

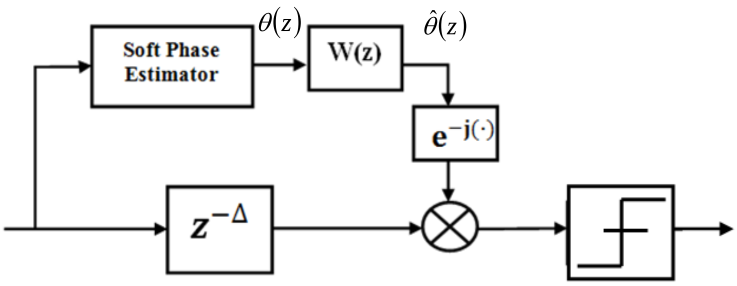

Figure 3-18. Two-stage iterative carrier phase estimator and compensator

The zero lag Wiener filter calculated is in terms of its z-transform is

$$\hat{\theta}(z) = \frac{1-\alpha}{1-\alpha z^{-1}}\theta(z) \tag{3.19}$$

Where

$$\alpha = \frac{\sigma_w^{\ 2} + 2\sigma_p^{\ 2} - \sigma_w\sqrt{\sigma_w^{\ 2} + 4\sigma_p^{\ 2}}}{2\sigma_p^{\ 2}} \tag{3.20}$$

and $\sigma_p^{\ 2}$ is the variance of gaussian noise introduced by the channel.

The Wiener filter having lag of D symbols is

$$\hat{\theta}(z) = \frac{(1-\alpha)\left(\alpha^D + (1-\alpha)\sum_{k=1}^{D}\alpha^{D-k}z^{-k}\right)}{1-\alpha z^{-1}}\theta(z) \tag{3.21}$$

The finite lag filter gives better results than the zero lag filter because it considers D symbols into the future as well as the infinite past in making its estimate. Filter taps of the zero lag Wiener filter and finite lag filter are schematically depicted in Figure 3-19 (a) and (b) respectively.

The application of equations (3.21) is expected to give very accurate phase estimate since the Wiener filter is the least mean square error linear estimate, and the approximations applied have been minor. However, the equations cannot be implemented directly in DSP that uses parallel architecture because they involve feedback of the immediately precedent result. The equations can be recast using a look-ahead computation so as to refer to feedback of a distant past result, L symbols in the past, by multiplying numerator and denominator by a polynomial . The zero lag estimate equation becomes

$$\hat{\theta}(z)=\frac{1-\alpha}{1-\alpha^{L}z^{-L}}\sum_{k=0}^{L-1}\alpha^{k}z^{-k}\ \theta(z) \tag{3.22}$$

The finite lag equation can be recast in a similar way. In this work it is implemented the non look-ahead version since this project has purpose of demonstrate the viability of the proposed algorithms to compensate phase noise and the look-ahead version of this phase estimator is left for future studies. Real implementation of such algorithms in DSP boards should be studied apart and could be a good extension of this thesis.

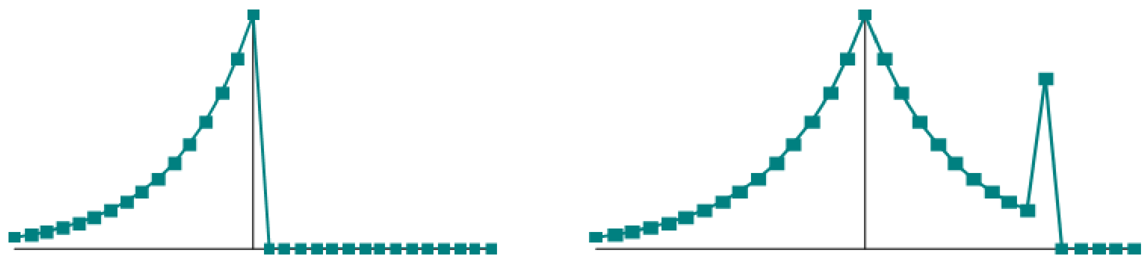

(a) (b)

Figure 3-19. (a)Taps of the zero lag Wiener filter. (b) Taps of the finite lag filter.

To finally compensate phase noise the symbols must be multiplied by and exponential which phase is the phase estimation result of phase estimator. Last block of the estimator would be a decision threshold to finally decide which symbol was sent.

The two-stage iterative carrier phase estimator was implemented but not finally studied in the whole receiver, being the NDA soft phase estimation the algorithm in charge of the compensation of the phase noise due to frequency drifts of the lasers. This decision was made due to the better results that were obtained by the NDA soft estimator in terms of phase noise compensation. The NDA algorithm is even simpler than the two-stage iterative and therefore NDA was chosen for being used in the whole receiver.

Ressuming this section, there are two main sources of phase noise: frequency offset and lasers linewidths. For the first source a ***phase increment estimation algorithm*** to compensate phase noise is proposed. For the second phase noise source the ***NDA*** is finally chosen. Moreover NDA is also able to compensate phase noise due to frequency offset. Therefore, both methods have been compared when compensating frequency offset phase noise in Table 6.

Table 6. Comparison of frequency estimator and phase estimator techniques in presence of phase shift due to frequency offset

$\tau_s\Delta f$					
Method \ Δf	1Mhz	10Mhz	100Mhz	1Ghz	10Ghz
Theoretical	0.0001	0.001	0.01	0.1	1
Frequency estimator	9,21E-05	9,91E-04	0.01	0.1	-0.4378
Phase Estimator	9,21E-05	9,91E-04	0.01	0.1	-0.4379

Table 6 represents the value of $\tau_s\Delta f$ for different offsets and for different estimation techniques. First row is the theoretical value, no more than the value of $\tau_s\Delta f$, second and third row are the estimation of that theoretical value obtained when using frequency estimation and phase estimation method respectively. The results of the table were obtained in simulations with 4x10240 bits using dual polarization QPSK at 20 Gsymbol/s in each polarization with a SNR of 10 dB in a model where no other impairments as phase noise, CD and PMD were present. For the frequency estimator the value obtained was averaged over the entire signal of 10240 giving therefore its best estimation. Under this conditions can be inferred that NDA soft phase estimation is as good as frequency estimation to obtain the phase shift due to a frequency offset between the transmitter and local oscillator, in fact both methods give exactly the same results when N is large in Frequency estimator method. Can also be noticed that the estimations are very precise results under ideal conditions where no impairments are present, but even under ideal conditions none of them can give a good estimation for frequency offsets that are close to the bit rate, in our case 10 Ghz. Therefore these two digital techniques cannot be used for large offsets near to the bit rate, if large frequencies offsets are wanted to be compensated PLL are required.

Chapter 4

4 Experimental Study

This chapter has the finality of describe the capability of the designed digital coherent receiver. First is described the systems in which the receiver is tested, for later validate its functionality. In the receiver validation, the purpose of each module is tested individually to find the boundaries in its functionality. Several test results are shown along the chapter to find the parameters of the receiver implemented as how much dispersion is capable to compensate the CD equalizer, how much phase noise is able to compensate or even to compare different techniques that can be used in the DSP module of the digital coherent receiver.

Once each module has been tested individually, the whole system is then tested to describe the transmission performance that it can achieve using the receiver designed. Here the tolerance of the whole system to linewidths, signal power, chromatic dispersion or PMD is described.

4.1 System specification

To test the behavior of the receiver implemented the VPI Transmission Maker tool is used. The whole transmission system is created in VPI TM, in the schematic created with TM the digital coherent receiver implemented with Matlab code is included using a special module of TM.

The transmission system designed with VPI Transmission Maker that is used to validate the receiver designed is an optical coherent system that uses QPSK dual polarization transmitting at 10 Gsymbols/s in each polarization for a total bit rate of 40 Gbps. The schematic used is depicted in Figure 3-1. All the components of the transmission system belong to the VPI TM library having a realistic behavior.

In the system designed, MZ external modulators [38] are used at the transmitter for the modulation of the two independent signals from two different lasers. Both lasers send information at 1550 nm in two perpendicular polarizations, which are combined using a PBS beam combiner just before the fiber. The PBS combiner is denoted in Figure 3-1 by the name MUX.

The output of the fiber is connected to a PBS beam splitter to separate both polarizations. Then each polarization arrives to two different 90º optical hybrids that uses the same local oscillator. The output of the local oscillator also passes through a beam splitter to have the local oscillator signal with 45º respect the signals that arrives to each 90º optical hybrid. The receiver front end is a balanced phase and polarization diversity receiver, in this way the signals are lineally converted to the electrical domain and are suitable for the DSP circuits in charge of impairments compensation.

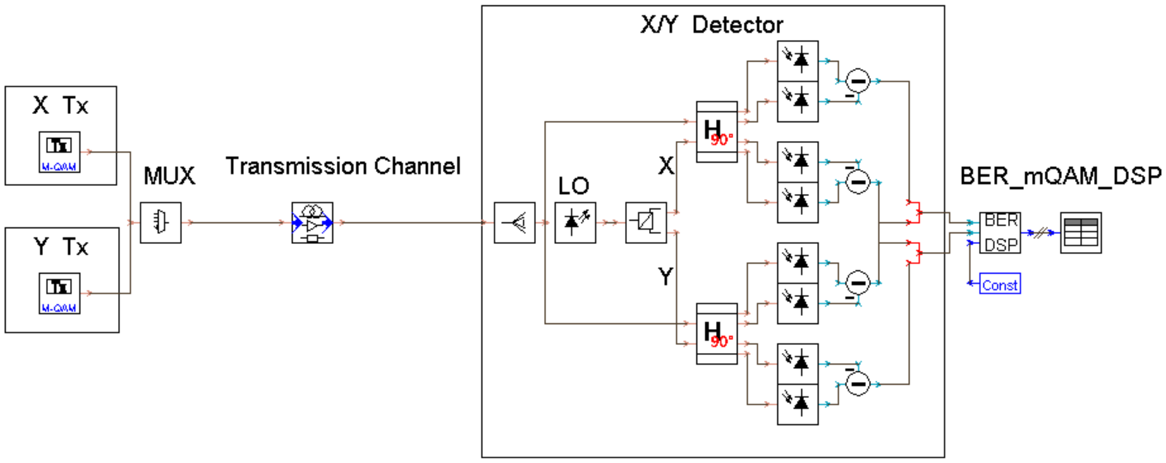

Figure 4-1. Optical Transmision system for testing of the digital coherent receiver.

The analog signals used in the system are simulated using 16 samples per bits, sending in the in-phase and quadrature of each polarization 10240 bits, achieving a total transmission of 40960 bits. For that amount of bits and due to Monte Carlo method we are able to report BER until 0.001 which is our reference boundary in terms of BER. When chromatic dispersion is studied, a fiber with dispersion parameter of D=13.3286 is used, and the length of the fiber is modified to see the behavior of the receiver under different dispersion values. In case of PMD, the DGD value adopted is $0.1\text{x}10^{-9}\frac{s}{\sqrt{Km}}$.

Resuming, these are the main characteristics of the system created in VPI TM, where the receiver is tested.

- Analog signals simulated using 16 samples/bit
- 40960 bits sent. 10240 bits in the in-phase and quadrature of each polarization.
- A/D with 2 Samples/bit.

These characteristics can be modified for some simulations if required, if any of these characteristics is modified it is indicated along next sections.

4.2 Receiver validation

In this section the robustness of each part of the digital coherent receiver is tested. First of all, the functionality of the receiver in absence of impairments is checked when the clock recovery based on canny filter is used taking two samples per bit. The section continues testing the behavior of the DSP impairments compensation modules independently, first chromatic dispersion, then polarization mode dispersion and finally phase noise compensation.

First of all the system functionality had to be checked, for that purpose a total number of bits of 40960 bits were sent through the system using polarization multiplexing. The analog signals were simulated using 16 samples per bits. For this simulation all the impairments were neglected except optical noise because we just wanted to test if the system was working properly, if the bits sent were received without error when the OSNR was high enough and also at which OSNR the BER begins to differ from 0. Therefore, DSP module is not needed in this simulation. In this ideal system the results are noise-limited and the constellation receive under such conditions are analogous to those depicted in Figure 2-15.

From this simulations it is demonstrated that the system is capable of sent and receive information using polarization multiplexing and QPSK modulation format achieving a bit rate of 40Gbps. From several simulations it is found that, in this ideal system without impairments the BER is maintained behind $1x10^{-3}$ for values equal or higher than 5 dB of OSNR. Therefore, in this study is adopted an OSNR of 5 dB as the reference for power penalty needed to obtain BER values behind $1x10^{-3}$.

CD equalizer validation:

Here the behavior of the chromatic dispersion equalizer design is tested. We talk in section 3.3 about the chromatic dispersion equalizers implemented. When the inverse of the transfer function is implemented with the equalizer, any quantity of chromatic dispersion can be compensated if the enough number of taps is used. This module is tested sending again 10240 bits in each in-phase and quadrature of the two QPSK modulations sent in both polarizations for a total number of bits of 4x10240.

In this test the dispersion slope is not taken into account, this mean β_3=0. The linewidth of the transmitter is chosen to be $\Delta\lambda = 0.1\ nm$ and the dispersion parameter of the fiber is D=13,3286. Before the equalization the signal has been sampled at twice the bit rate having in this way two samples per bit. Next is a resume of the CD equalization simulations characteristics:

- Dispersion parameter D=13.3286 $\frac{ps}{\mathrm{nm.km}}$
- Dispersion slope β_3=0.
- Linewidth of lasers $\Delta\lambda = 0.1\ nm.$
- Other impairments neglected.

In the next simulation the SNR of the signal in reception is chosen to be 200 dB neglecting in this way optical noise since our intention here is to check the ability of the equalizer to compensate chromatic dispersion impairment. Moreover, other impairment are neglected including nonlinearities. Under this characteristics can be shown that any amount of chromatic dispersion can be compensated just using the proper number of taps in the equalizer. In Figure 4-2 is depicted the effect of CD equalization over the signal QPSK sent in X-Polarization. In this simulation the signal was sent through a 500 km link and a 15 fixed taps CD equalizer was used. From the figure can be seen qualitatively how the symbols are distinguishable after the equalization having a very low BER, in this case the BER obtained over 20480 bits sent through X-Polarization was below $1x10^{-3}$.

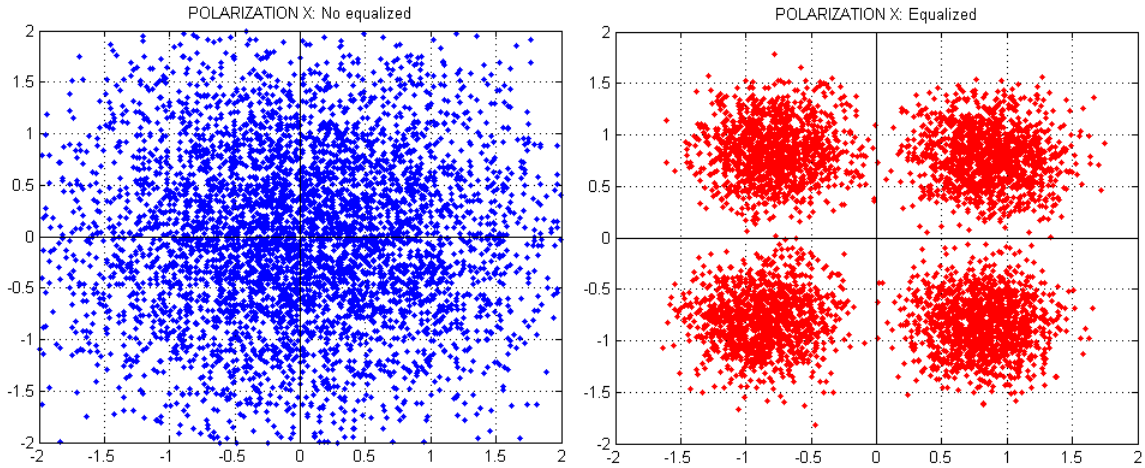

Figure 4-2. CD Equalizer effetc over QPSK constellaltion. (a) Before CD Equalization (b) After CD Equalization

When more taps are used in the equalizer to mitigate the same dispersion value then, better results are obtained from the equalizer. In next figures are presents the two signals sent in both polarization and shows qualitatively how the equalization is improved when more taps are used. There are present two rows one per polarization. In each polarization 20480 bits are totally sent using QPSK modulation. The three columns are the QPSK constellation after CD compensation, from left to right they depicts the constellation compensated using a non-adaptive CD compensator with 2, 3 and 5 taps respectively.

From Figure 4-3 can also be noticed that two QPSK signals sent in orthogonal polarizations are received correctly in the coherent receiver. It is perceived that both signals have practically the same form and the small difference comes from the fact that in each polarization independent signals were sent. From the figure can be also inferred that the number of taps used in the CD equalizer has a tangible effect in the CD compensated constellation. From left to the right the number of taps used in the equalizer is incremented having a much better result in the constellations most at the right which were compensated with 5 taps non-adaptive CD equalization. In the figure most at the left just 2 taps were used for CD equalization having a BER higher than 0,001 which is our reference BER. In the figures of the middle a 3 taps CD equalizer is employed giving a BER below 0,001. The figure most at the right does not suffer of error decisions as its symbols do not enter in other decision regions. Can be noticed how the number of taps have influence in the radio of the constellation symbols, when more taps are used the radio of the symbol is smaller and thereby the symbols do not enter in other decision regions giving higher BER.

Furthermore, when less taps are used in the equalizer a certain rotation in the constellation is present because less taps equalizers cannot completely compensate CD that affects the signal. This effect is present in the constellations compensated with 2 and 3 taps equalizers.

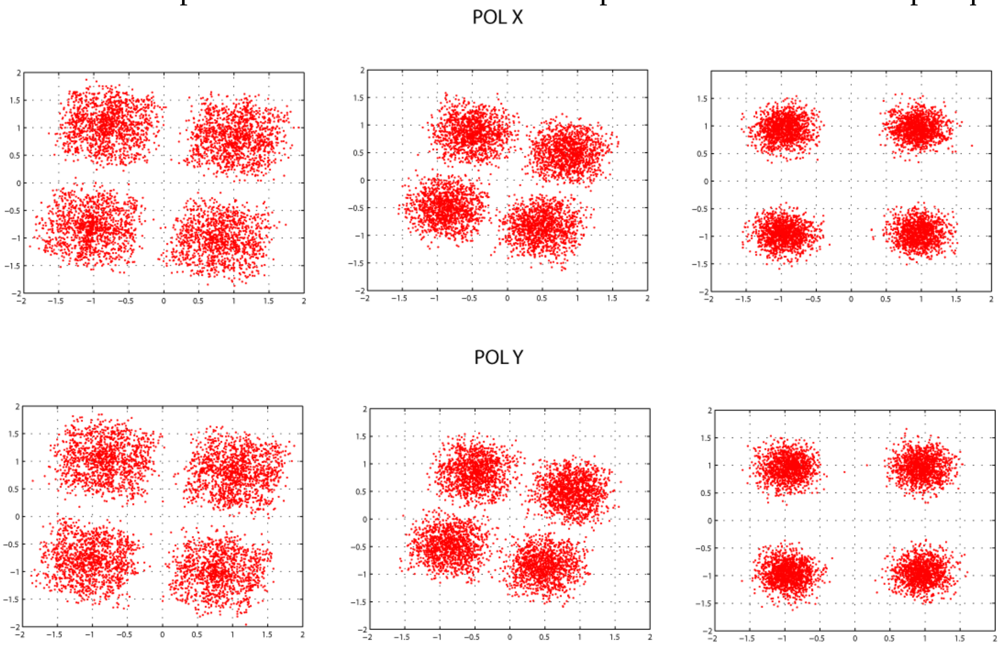

Figure 4-3. Non-adaptive CD equalization of L=100 km fiber for both polarizations in a polarization multiplexing system and three different taps values of the CD equalizer: 2, 3 and 5.

Of course arbitrary number of taps cannot be used, the number of taps used in the equalizer has an important influence in the complexity of the equalizer and the speed of it when implemented in a DSP board. As the optical systems are very fast they need fast receivers, in this context faster and less complex equalizers are preferable. For that purpose the minimum number of taps to compensate CD with a certain BER has to be found. For example, in last figure the constellation obtained after 3 taps CD equalization has a BER below 0,001 which is a result that could be desirable, also the 5 taps CD equalizer obtained a BER lower than 0,001 but this last equalizer uses more taps which can result in a slower DSP implementation of the equalizer. Therefore the compensation capacity of the equalizer and the equalizer complexity must be taken into account in the design of the equalizer. In this work the implementation of the receiver in a DSP board is not tackled and the speed of such equalizers in a DSP board is not obtained, its study is proposed for future works.

Because the number of taps are therefore a very important parameter of the equalizer, some simulations were carried out to check the minimum number of taps needed to obtain a $BER<1x10^{-3}$ for different CD values. Because the dispersion parameter is fixed, the variation of the fiber length implies a variation in the total dispersion that affects the signal. The OSNR is still 200 dB as in previous simulations. Simulation results are shown in Figure 4-4 in which is included the theoretical minimum number of taps needed based in eq. (3.5) and therefore they are compared with the minimum number of taps that were found in simulations.

From Figure 4-4 is found that the theoretical minimum number of taps is bigger than the minimum number of taps that were needed in simulations for obtaining a $BER<1x10^{-3}$. This fact comes from eq. (3.5) that is an equation that provides an approximation to the minimum number of taps needed for totally compensate CD meanwhile the experimental results obtained are the minimum number of taps to achieve a BER below 0.001. Can be also find out that any chromatic dispersion can be compensated when enough taps are used, even CD due to 5000 km fiber (66600 ps/nm). What make this long distance compensation not feasible is the total amount of taps required in the receiver, in order of hundred taps. For such long distances the use of inline DCF can relax this taps requirements for compensating the residual CD.

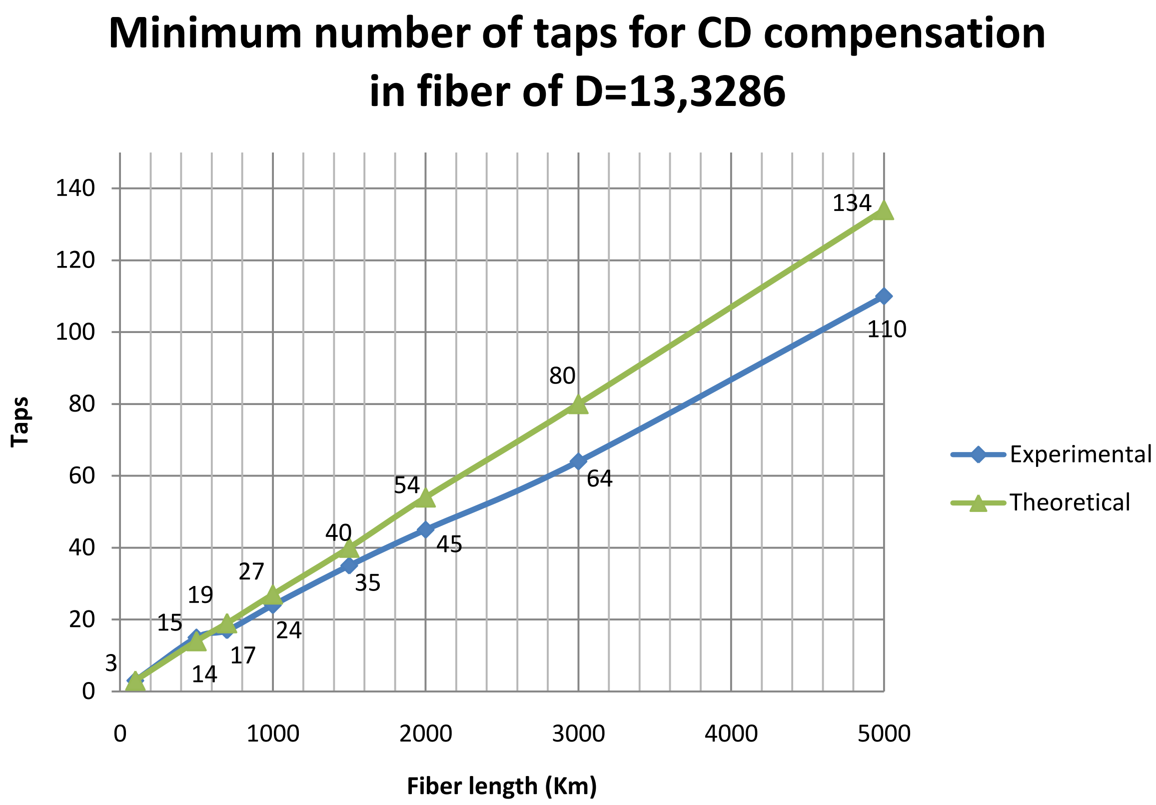

Figure 4-4. Minimum number of taps for CD compensation in fiber of D=13,3286 to obtain BER below $1x10^{-3}$

The CD equalizer can also be studied in terms of power penalty, or the OSNR needed to obtain a certain BER value. For the elaboration of the next chart, the CD equalizer was tested for 5 different taps length equalizers. Figure 4-5 present a graphic that depicts the OSNR of the signal in reception versus the length of the fiber. This graphic can be also seen as the amount of CD that different non-adaptive equalizers can compensate and which power is required for that compensation to achieve a BER below 0,001.

From Figure 4-5 can be noticed that CD compensation does not imply much power penalty and can work perfectly behind 20 dB of OSNR in reception. Of course that the lines that represents the equalizer with less taps are shorter than the ones that describes longer taps equalizer. For example the 3taps CD equalizer is just able to compensate CD due to 100 km fiber length and does not mind with how much power the signal is sent. To compensate the same dispersion value the equalizers with more taps needs less OSNR in reception. It is important to notice that larger taps equalizers have a OSNR penalty close to the reference of 5 dB, this mean that the CD is practically compensated with such equalizers and the BER comes from the optical noise and not from CD effects.

In chapter 3 was also present the design of an adaptive equalizer for chromatic dispersion with two different algorithms for taps adaptation: CMA and LMA. Now the adaptive version of the equalizer is tested and compared with the non-adaptive version.

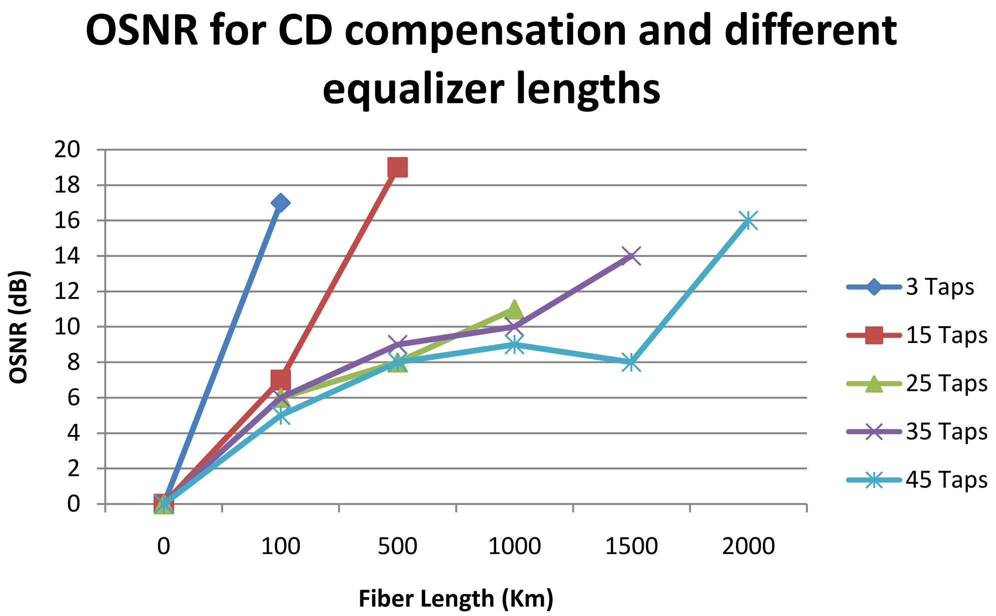

Figure 4-5. Power penalty to compensate different dispersion values for different non-adaptive CD equalizers.

The adaptive option has two possibilities depending in which equation is used for taps adaptation: CMA and LMS algorithm. With CMA algorithm we have obtain no CD compensation, it is a not valid adaptation algorithm for polarization independent impairments therefore we discard this algorithm for the adaptive CD-equalizer and we focus our attention in the LMS algorithm.

CD adaptive equalizer using LMS algorithm for taps adaptation was tested in a system of the characteristics described at the beginning of this section, with the difference that the OSNR is 20dB in reception. The adaptive CD equalizer was used with a step size μ equal to 0,001.

From the results obtained can be inferred that adaptive CD equalizer with LMS algorithm obtains better results than non-adaptive equalizer in terms of BER achieved when using the same number of taps than the non-adaptive equalizer. It also showed an improvement in the minimum number of taps needed to obtain a certain BER value. The non-adaptive equalizer showed that it needed less taps to obtain BER below 0,001 than the non-adaptive version. These conclusions are extracted from Figure 4-6 in which four charts are depicted, each chart is for a different dispersion value affecting the fiber. Each chart has two sequences, one in blue that describes the CD adaptive equalizer with LMS algorithm and the other sequence in red for the non-adaptive equalizer.

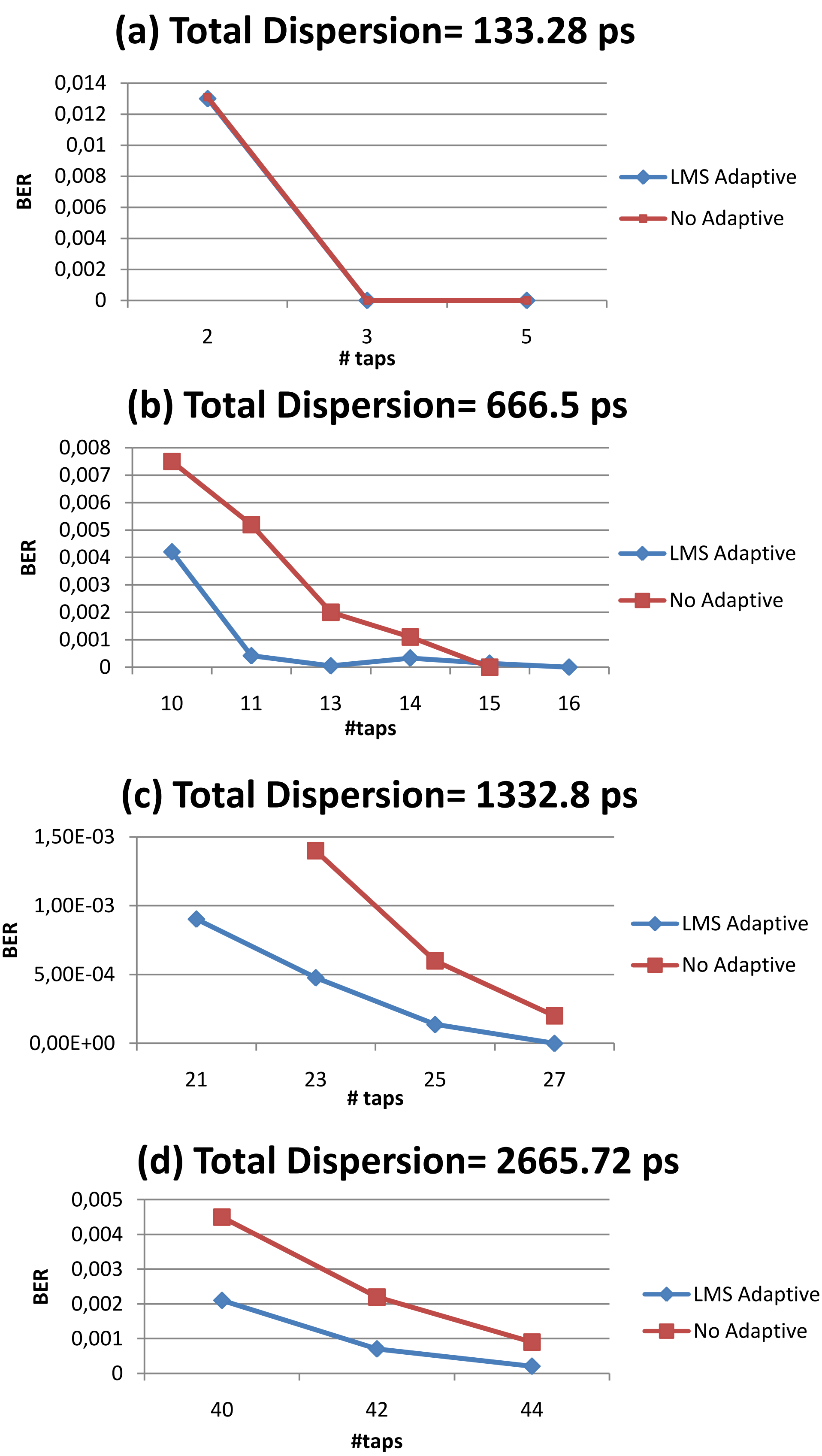

Figure 4-6. BER after signal compensation for four different chromatic dispersion values when using CD adaptive compensation and CD non-adaptive compensation. (a) Fiber Length 100 km (b) Fiber Length 500 km(a) Fiber Length 1500 km (b) Fiber Length 2000 km

In each chart is drawn the BER obtained by the system versus the number of taps used for CD equalization. Therefore this figure is a direct comparison between non-adaptive and adaptive CD equalizers.

Chart (a) is for a fiber length of 100 km with a total dispersion affecting the signal of D=133.28 ps. In this case both equalizers have practically the same behavior and both need 3 taps to obtain a BER below 0.001 which were the number of taps announced by eq. (3.5). In Chart (b) is for first time noticeable the improvement in the BER of the adaptive equalizer over the non-adaptive version. In this chart the length of the fiber is 500 km. The same improvement is present in the two following graphics for 1000 km and 2000 km respectively. These results were expected as the adaptive version is able to find the best taps weight for CD compensation while non-adaptive have fixed taps that try to be as close as possible of the ideal taps solution.

The differences in the number of taps used by both equalizers to obtain a BER less than 0.001 are: 0, 4, 5 and 2. This is not a real big difference when we are dealing with equalizer that uses a high number of taps like 20 or forty that are needed to equalize thousands of CD ps. It could be a difference to take into account for the equalizers used in second chart, for 1000 km of fiber. It would be interesting to investigate the difference in performance in a DSP board of the equalizers as a function of the number of taps. We leave this investigation as a proposal for next studies.

At first sight, it seems that adaptive equalizers are a better solution for chromatic dispersion equalization. The disadvantage of adaptive-equalizer are that they need some time to converge to the optimal taps solution, this time conversion made this equalizers little bit slower than non-adaptive, on the other hand the adaptive version needs less taps than the non-adaptive. Another undesirable effect of using adaptive equalizers for polarization independent impairments is that each polarization is treated independently and both equalizers (one per polarization) do not necessarily converge to the taps solution at the same time. The equalizer could be designed to let the compensated signal out as soon as the error signal of the adaptive equalizer achieves some desirable value however, this solution would make the two outputs get out the compensator at different times with high probability. Another option for the adaptive CD equalizer is to use the same time t_{conv} (remain Figure 3-12) for both polarization branch. This time has to be long enough to let both branch arrive to an error value small enough for compensate CD. In this way both branches will arrive at the same time.

The most important aspect that we have found from using adaptive equalization for CD compensation is the fact that LMS algorithm is not possible when the signal is affected by polarization mode dispersion effects. Until here the CD compensator has been tested neglecting other impairments, but the CD equalizer is going to work in a system affected by PMD.

For the complete receiver design we should take into account that the fiber is going to be affected by PMD and therefore is completely necessary use the fixed taps CD equalizer since both adaptive equalizers (CMA and LMS) are not useful when the signal is affected by PMD. Therefore the non-adaptive equalizer is the one used in the final design of the receiver.

PMD equalizer validation:

Now is turn to the check the robustness of the PMD equalizer. For that purpose CD and phase noise are neglected, the OSNR chosen is 20 dB in reception. Both signals consist in two QPSK modulations of 20480 bits each sent in orthogonal polarization. Listed is a resume of the main characteristics for next simulations.

- Just first order PMD is taken into account with DGD = $0.1\text{x}10^{-9}\frac{s}{\sqrt{Km}}$.
- Other impairments are neglected.
- OSNR = 20dB
- Step parameter $\mu = 0.001$ for PMD adaptive equalizers.

If any of these simulation characteristics are changed in any simulation along this section it is indicated. Now we are dealing with polarization of the signal and should be take into account that the PMD distortion of the signal will depend on the angle of the orthogonal polarization respect the PSP of the fiber which are set at 0º and 90º. When the signal are sent through the PSP of the fiber PMD is less important than when both QPSK signal are sent with certain angle from the PSP. Therefore, the distortion of the signal depends on the angle between the launched signal and the PSP of the fiber. Following, in Figure 4-7 is depicted the effect of PMD when there is an angle PHI between the PSP and the signals sent through the fiber.

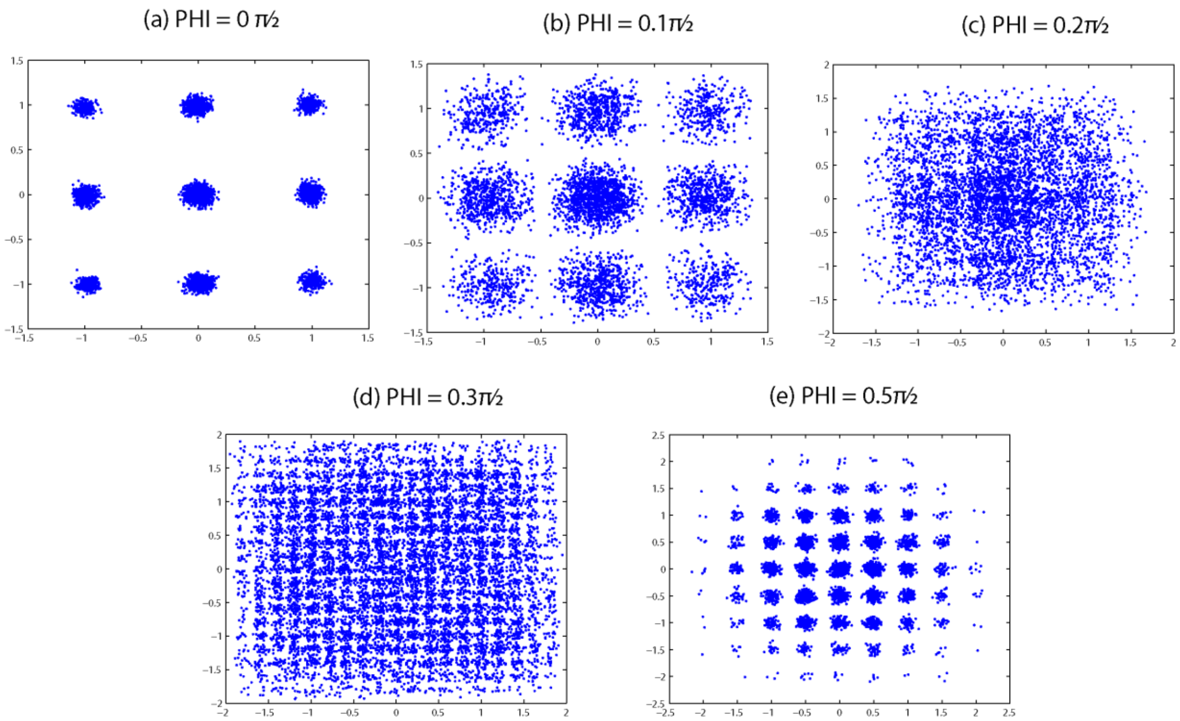

Figure 4-7. PMD distortion effect in function of the angle between the PSP and the launched signal.
(a) BER = 0.077 (b) BER = 0.139 (c) BER = 0.189 (d) BER = 0.21 (e) BER = 0.32

The five constellations presented in Figure 4-7 are the QPSK constellations received after fiber lengths of 2000 km. Each one corresponds to a constellation received when a certain angle between the launched signals and the PSP of the fiber is present. The angle is written on top of each constellation in function of $\frac{\pi}{2}$ and it is called PHI. When the angle PHI is zero it represent the better case as well as $n\frac{\pi}{2}$ where n represent any natural number, in such cases the signals were launched aligned with the PSP of the fiber. The worst case occurs when the signal are launched with and angle of $\frac{\pi}{4}$ respect the PSP, in this case the power transfer between the signals sent using polarization multiplexing is maximized and the BER is increased. Therefore, when these constellations are decoded the BER obtained increases in function of the angle between the launched signal and the PSP. The BER reaches its maximum when PHI is exactly $\frac{\pi}{4}$ and it decreases again in the same manner. If the BER is drawn in function of the angle it is ideally symmetrical respect $\frac{\pi}{4}$ and periodical with period $\frac{\pi}{2}$. Because this behavior and for simplicity in this work it is assumed that the angle PHI is always between 0 and $\frac{\pi}{4}$. The importance of the angle PHI over the BER can be noticed from next figure, in which the BER respect the fiber length for different PHI angles is depicted. From the figure is extracted that the BER arises with fiber length as well as with PHI. It is important to notice that in these results no PMD equalization was used.

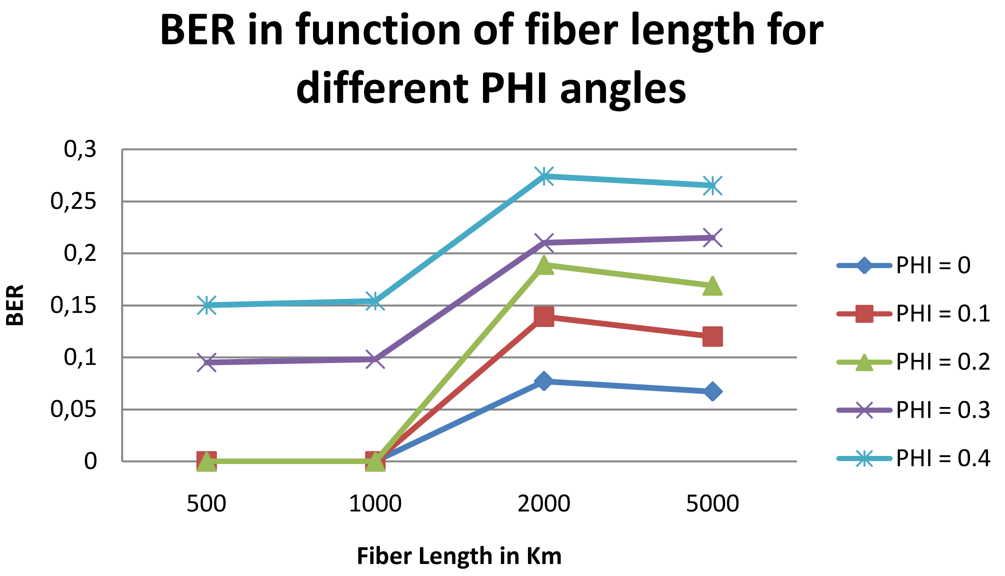

Figure 4-8. BER of QPSK signal affected by PMD for different PHI angles depicted versus the length of a fiber with DGD = $0.1\text{x}10^{-9}\frac{s}{\sqrt{Km}}$.

Now that the effect of PMD over QPSK constellation is a little bit clearer let us talk about the equalization of PMD. Because the PMD equalizer solution described in chapter 3 uses adaptive equalizers we have again two different options to study that depend on the adaptation algorithm used: LMS or CMA.

When LMS adaptation algorithm is used for the equalizer proposed the following result are obtained. LMS cannot compensate PMD when the angle between the launched signal ant fiber PSP are in order of $0.4\frac{\pi}{2}$, therefore when this solution is chosen for PMD equalization the signals must be sent with an angle respect the PSP of the fiber inside the range $\left[0, 0.4\frac{\pi}{2}\right[$. Another important aspect found is that PMD equalizer with LMS needs just few taps for the equalization. The number of taps to compensate PMD depends again on the angle PHI and the DGD affecting the signals. In this case, because the DGD chosen in this study is fixed, the total DGD that affects the signal is in function of the length of the fiber. It is found that for obtaining a BER below 0.001 just few taps between 2 and 4 are needed. In Table 7 there are the taps found that are able to compensate PMD to achieve a BER below 0.001. In green there are the values of PHI and length of the fiber in which the BER before PMD compensation is already below 0.001. Inside these green cells there is also a tap number, these number taps achieves BER better than 0.001. Red cells indicate that for that PHI angles and fiber lengths the BER is worse than 0.001 and cannot be compensated using the equalizer designed.

Table 7. Taps needed to achieve BER<1x10^{-3} in PMD compensation when other impairments are neglected.

	Fiber Length(Km)			
PHI x $\frac{\pi}{2}$	500	1000	2000	5000
0	2	2	2	2
0,1	3	3	2	2
0,2	3	3	2	2
0,3	4	4	3	3
0,4				
0,5				

The PMD constellations after PMD equalization are depicted in Figure 4-9. The four constellations presented in the figure correspond to the PMD compensated version of those constellations that are depicted in Figure 4-7.

Therefore is shown that PMD equalizer together with LMS algorithm can compensate PMD when the angle PHI is inside the range $\left[0, 0.4\frac{\pi}{2}\right[$ by using 3 or four taps in each adaptive equalizer that forms the PMD compensator.

The PMD equalizer when CMA algorithm is used has been tested under the same conditions than the LMS version obtaining similar results. It cannot compensate PMD when the angle PHI is between $\left[0.4\frac{\pi}{2}, 0.5\frac{\pi}{2}\right]$ and the number of taps needed to compensate the different values of PMD under BER of 0.001 are exactly the same than those of Table 7. Therefore CMA adaptive algorithm does not obtain any improvement over LMS when other impairments except PMD are neglected.

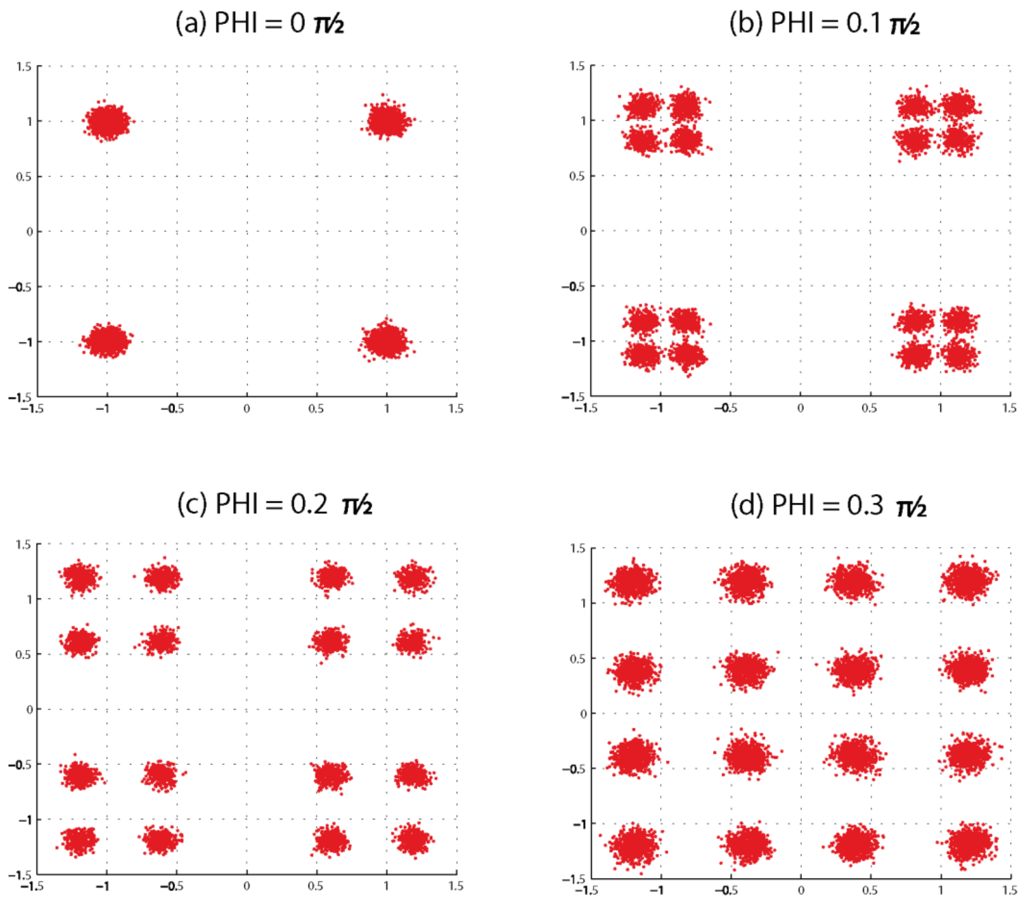

Figure 4-9. QPSK constellation after PMD compensation. (a) BER<0.001 with 2 taps (b) BER<0.001 with 2 taps (c) BER<0.001 with 2 taps (d) BER<0.001with 3 taps

Phase Noise compensator validation:

There are two main phase noise impairments to deal with: frequency offset between transmitter laser and LO and the second one is phase noise due to frequency drifts in lasers. In chapter three were proposed two solutions: frequency estimator circuitry, which can compensate frequency offset but cannot compensate phase noise; the second option is phase estimator which is able to compensate both. The idea is to choose one solution between the following two options: use both DSP techniques (frequency and phase estimator) together or just use carrier recovery to compensate both impairments. Without take any test the second option seems preferable because it is simpler, but we should validate both options and find which is better for phase noise compensation.

Let's begin to check the behavior of both estimators to compensate a certain frequency offset. In Table 6 of chapter 3 was shown that both estimator can compensate frequency offset but the values obtained in that table for the frequency estimator were obtained after averaging the phase difference between symbols along the entire signal sent, it means that the values given by the frequency offset were averaged by N=10240 symbols. On the other hand phase estimator does not need any averaging module because it just obtains the phase of each symbol directly using the function arg. Therefore, phase estimator results when frequency offset is present are the same that those presented in Table 6, however, for the frequency estimator, those results of Table 6 are the best results that it can achieve when 10240 symbols are sent because it estimates the frequency offset averaging the estimation using the entire signal sent N=10240. Now the behavior of the frequency estimator is checked when the average is obtained using different N values, being N the number of phase difference values used to obtain the final frequency estimation.

In this test no phase noise was taken into account and just frequency offset. The results obtained are shown in Figure 4-10. From that figure can be notice that frequency estimator just need to average the frequency offset with N=500 values to obtain a BER<0.001 for the 4 different frequency offset that we have used in the study.

In the case of the phase estimator, the BER obtained when only frequency offset is present is always below 0.001. Different compensated QPSK constellations when phase estimator and frequency estimator is used are shown in Figure 4-11 as well as the QPSK constellation affected by frequency offset before compensation.

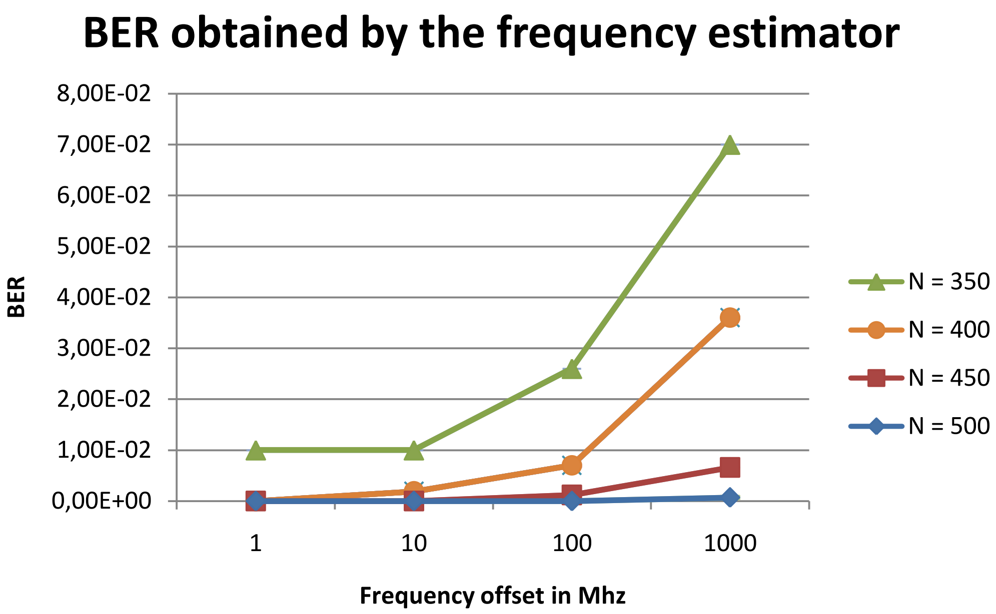

Figure 4-10. BER obtained by the frequency estimator for different frequency offset and different values of N

Constellations depicted in Figure 4-11 have been affected by 10 and 100 Mhz offset (Figure 4-11 (a) and (d) respectively). Then, the figures (b) and (e) are the compensated constellations after frequency estimator with N=350 and N=500 respectively. Finally the figures (c) and (f) are the constellations (a) and (d) respectively after phase estimator compensation. From the figure can be noticed the improvement of the frequency estimator when N is increased and the great performance of the phase estimator when just frequency offset is present.

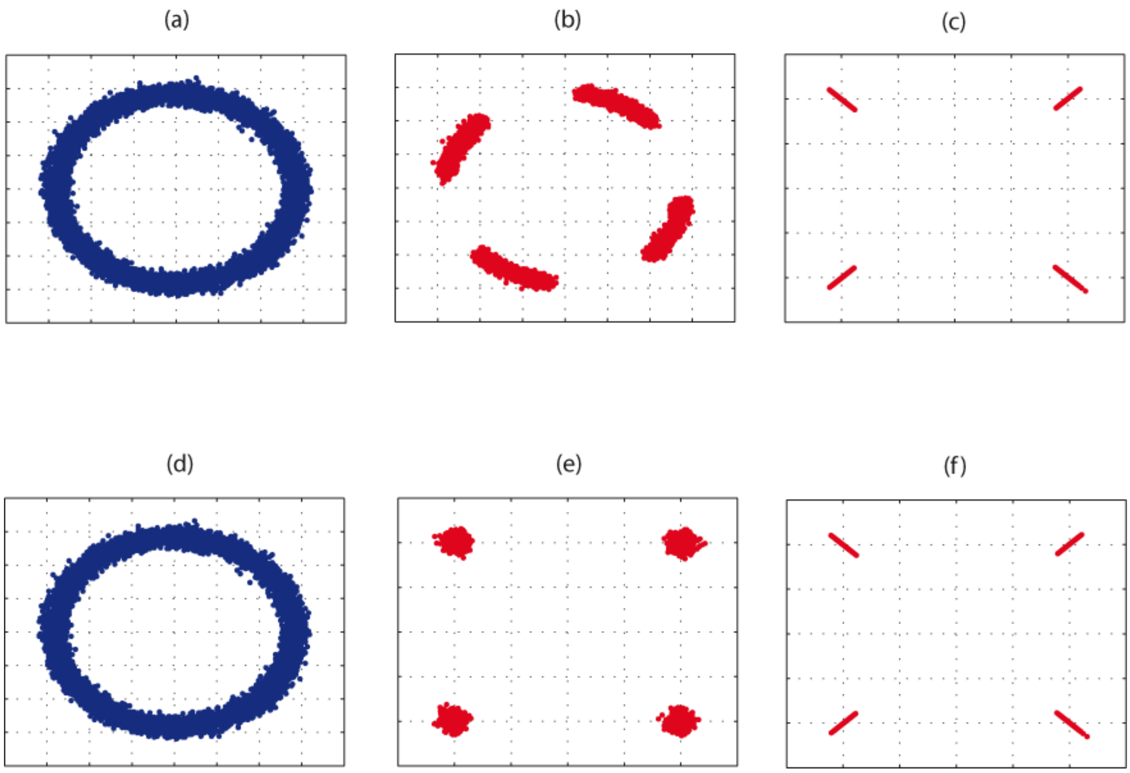

Figure 4-11. QPSK constellations affected by frequency offset and then compensated by frequency estimator and phase estimator. (a) QPSK constellation affected by 10 Mhz offset. (b) QPSK constellation from (a) after frequency estimator compensation with N=350. (c) QPSK constellation from (a) after phase estimator compensation. (d) QPSK constellation affected by 100 Mhz offset. (e) QPSK constellation from (d) after frequency estimator compensation with N=500. (f) QPSK constellation from (d) after phase estimator compensation.

From this study the functionality of both techniques when only frequency offset is present has been validated. It is shown that phase estimator achieves an excellent performance and frequency estimator can also achieve that performance by averaging the estimation along enough number of symbols N. In this case we have obtained that the frequency estimator technique can achieve similar performance than the phase estimator by using N = 500.

Should be taken into account that frequency offset always comes together with phase noise due to frequency drift of the lasers involves in the system. The phase estimator compensator is able to compensate phase noise in a range of noise variance (remember eq. (3.15)) from $[1_x10^{-5}, 1_x10^{-2}]$ achieving the objective BER under 0.001 when other impairments are neglected. This phase estimator just uses soft phase estimation, no hard estimation is utilized.

When both frequency offset and phase noise affects the signals there are two options for compensating both impairments, to use just the phase noise estimator or to use frequency estimator together with the phase noise estimator. Of course the use of just phase estimator is a simpler solution and seems preferable at first sight however, we checked if the combination of both estimators introduces an improvement over just phase estimator.

First of all, the behavior of the phase estimator was checked all over the possible combinations of frequency offset and phase noise in absence of other impairments as CD and PMD. From that point of view the phase noise estimator had an incredible performance achieving BER<0.001 in all the tests made except when the frequency offset is higher than 1Ghz and or the phase noise variance is higher than 1_x10^{-3} ,this is represented in Table 8. The combination of both frequency estimator and phase estimator did not improve the results obtained by phase estimator option. The range in which both methods can achieve BER<0.001 are shown in Table 8.

Table 8. Ranges of frequency offset and phase noise at which phase estimator and frequency estimator+phase estimator can achieve BER<0.001

	Frequency offset (Mhz)					
Noise variance σ_w^2	0	1	10	100	1000	10000
0	BER<0.001	BER<0.001	BER<0.001	BER<0.001	BER>>0.001	BER>>0.001
0.00001	BER<0.001	BER<0.001	BER<0.001	BER<0.001	BER>>0.001	BER>>0.001
0.0001	BER<0.001	BER<0.001	BER<0.001	BER<0.001	BER>>0.001	BER>>0.001
0.001	BER<0.001	BER<0.001	BER<0.001	BER<0.001	BER>>0.001	BER>>0.001
0.01	BER>>0.001	BER>>0.001	BER>>0.001	BER>>0.001	BER>>0.001	BER>>0.001
0.1	BER>>0.001	BER>>0.001	BER>>0.001	BER>>0.001	BER>>0.001	BER>>0.001

Therefore, phase estimator is chosen for phase noise compensation because both methods achieves practically same results and using just phase estimator we obtain a simpler phase noise compensator module.

4.3 Transmission performance

Until here the performance of each module involved in the receiver has been checked, for that purpose each module was tested neglecting the impairments that are not associated with the module tested. In this case, the functionality of each module has been validated however the functionality of the entire receiver when the three modules are involved is not already tested. This is the purpose of this chapter.

Now in this section the whole receiver functionality is tested. For simulations in this section the transmission system from Figure 4-1 is used with same specifications of section 4.1. Next is included a resume of the main characteristics of the system where the receiver and its modules are tested.

- Analog signals simulated using 16 samples/bit
- 40960 bits sent. 10240 bits in the in-phase and quadrature of each polarization.
- A/D with 2 Samples/bit.
- CD affecting the signal with parameter D=13.3286 $\frac{ps}{\text{nm.km}}$ and Dispersion slope β_3=0.
- First order PMD DGD = 0.1x10$^{-9}\frac{s}{\sqrt{Km}}$.

Finally the DSP used in the digital coherent receiver was a fixed taps CD equalizer, a PMD equalizer using LMS algorithm and a phase noise estimator at the end of the DSP before the symbol decision. A scheme of the three DSP modules of the coherent receiver is next depicted, in Figure 4-12 the scheme of the DSP modules are accompanied by four figures obtained from one simulation over 2000 km of fiber. Figure 4-12 shows how the DSP works to equalize the blurred constellation that arrives to the digital coherent receiver to finally obtain a QPSK constellation able for the symbol decision.

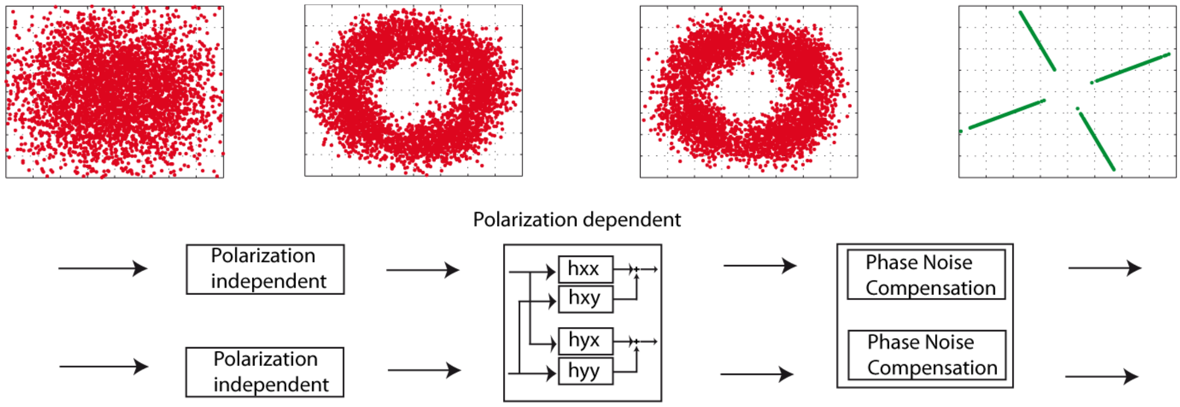

Figure 4-12. Scheme of the DSP modules involved in the receiver. Above the arrows are depicted the QPSK constellations extracted from a simulation over a 2000 km of fiber. From left to right the first figure correspond to the constellation before being equalized. Second figure is the first figure once it has been equalized in the CD equalizer using 40 taps. Third figure is after 8 taps PMD equalization. Last figure is after the phase noise estimation.

Under previous characteristics, the receiver showed that was able to compensate CD, PMD and Phase Noise under certain conditions. When these three impairments are present in the system the CD and PMD equalizers need more taps to obtain similar results to those obtained when the system was just affected by one of these impairments. Even if phase noise is neglected, an increase in the number of taps of both CD and PMD equalizers is needed to achieve BER<0.001. In Figure 4-13. Number of taps for CD and PMD equalizers for obtain BER<0.001. This results were obtained for an OSNR=20.Figure 4-13 are depicted the taps that were found necessary to obtain such BER value. The taps are depicted in function of the parameter PHI. Can be noticed that in the chart the maximum PHI angle is 0.2, was found that with the angle PHI higher than 0.2 BER<0.001 was unreachable. When the angle PHI is zero the taps needed for CD compensation are practically the same than those obtained in the validation of the CD equalizer while the number of taps needed is increased when the PHI angle is bigger than zero. The same happens to the number of taps used in the PMD equalizer, with PHI=0 then number of taps is increased by one to obtain BER<0.001 when PHI is increased the number of taps is also increased to obtain BER below 0.001.

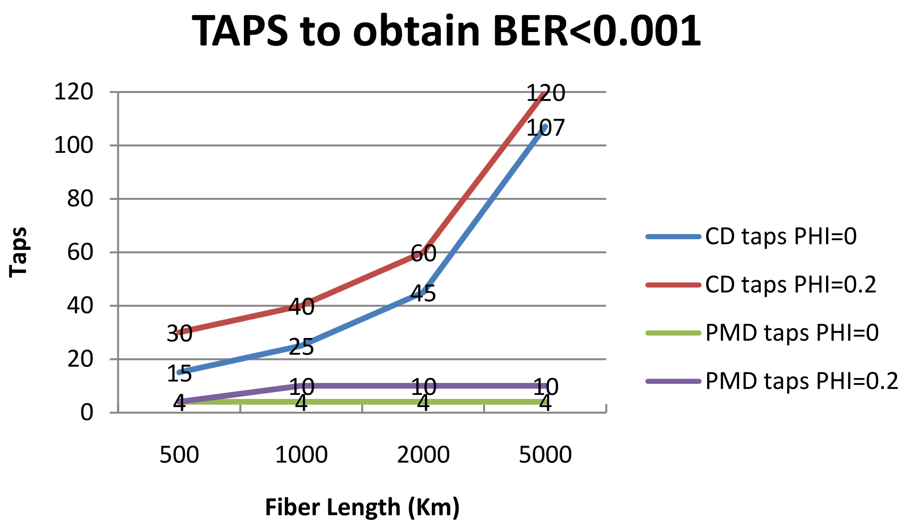

Figure 4-13. Number of taps for CD and PMD equalizers for obtain BER<0.001. This results were obtained for an OSNR=20.

In the case of Phase noise estimation, was found that the previous equalization of CD and PMD, which directly affects the phase of the incoming signal, has an influence in the estimation made by the phase noise estimator. This influence lead to an error in the estimation furthermore, the error is traduced in a rotation of the final QPSK constellation. If such rotation is bigger than $\pi/4$ then, the BER obtained is increased. The rotation of the final QPSK constellation can be noticed from Figure 4-14. In the simulations run to obtain these figures the linewidth of the laser was varied, being 1Mhz, 10 Mhz and 100Mhz respectively. For 1Mhz, in figure (a) the QPSK constellation present no rotation, and as the linewidth of the laser grows the constellation rotates, in this case to the right. In (b) the rotations is still slight and every point of the constellation is still in the correct decision region obtaining BER<0.001. On the other hand we have the figure (c) in which the rotation is bigger than $\pi/4$ and therefore the BER increases.

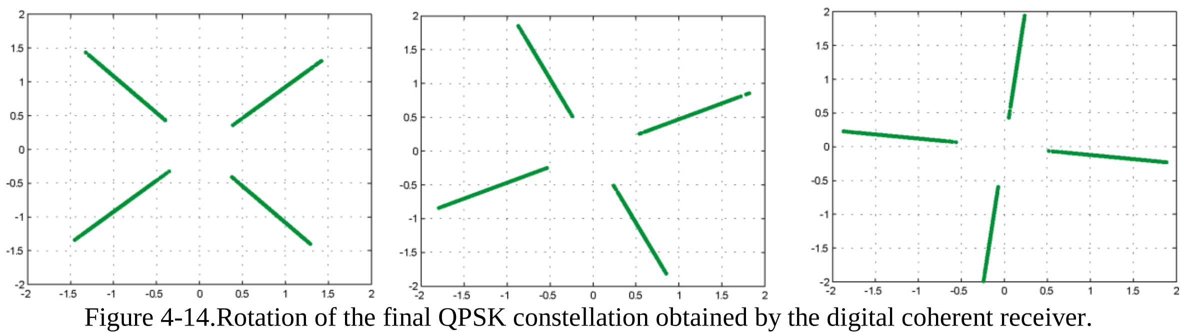

Figure 4-14.Rotation of the final QPSK constellation obtained by the digital coherent receiver.
(a) $\sigma_w^2 = 0.00001$ (b) $\sigma_w^2 = 0.0001$ (c) $\sigma_w^2 = 0.001$

This error can be prevented reducing the linewidth of the lasers involved and controlling the frequency offset between the laser and the LO are decreased to be not bigger than 100Mhz. Therefore the capability of the whole receiver compensating phase noise is reduced.

The digital coherent receiver designed, therefore is able to obtain BER < 0.001 when the linewidth of the lasers are not bigger than 100Mhz, if the polarization angle PHI is between$\left[0, 0.2\frac{\pi}{2}\right[$ and the frequency offset between transmitter and local oscillator is not bigger than 100 Mhz. Under these conditions we can report BER below 0.001 using the equalizers previously described with the number of taps indicated in Figure 4-13 for fiber lengths until 5000 km that have DGD = $0.1\text{x}10^{-9}\frac{s}{\sqrt{Km}}$ and dispersion parameter D=13.3286 $\frac{ps}{\text{nm.km}}$. Has to be taken into account that in this report the simulated fiber didn't have third order PMD not fiber nonlinearities either.

Chapter 5

5 Conclusions and Future Work

In this work a study of coherent receivers for optical transmission has been made. Along the text was presented today's technology in the field and was also presented some digital techniques for optical transmission impairments equalization. Afterwards a digital coherent receiver has been designed and tested using the information previously presented. The digital coherent receiver designed tried to show how coherent receivers could improve the performance of optical communications taking advantage of coherent communications properties.

With coherent receivers for optical communications we are able to receive the phase of the signal by using 90º Hybrid and balanced detection front-end architecture. Balanced detection is today a must in coherent detection because it gives twice the power that non-balanced detection gives. Once we have obtained the entire signal we can convert it into the digital domain. In the digital domain, using DSP techniques, we are able to compensate the main impairments that affect optical communications. This work pays special attention to this part of the receiver, the digital design of the coherent receiver, finally obtaining a digital coherent receiver.

Because the digital coherent receiver needs to convert the incoming signal from analog to digital, the first idea to point out is the fact that clock recovery and retiming plays an important role in digital coherent receiver when DSP is used for impairments compensation, moreover when it is affected by high values of CD. Using DSP, the chromatic dispersion affecting long hauls system can be compensated digitally at the receiver making traditional inline pre-compensation not needed. Of course this is an advantage, however it brings an important problem: because the signal is not inline pre-compensated it arrives to the receiver very distorted and therefore it makes very difficult to obtain the clock from the signal. If the clock signal obtained is not accurate enough the digital signal obtained in the A/D is going to be the main source of error in the system. Because of that, CD inline pre-compensation using dispersion-compensating fiber (DCF) could be a good solution. Using these fibers the CD that affects the signal could be maintained under a certain value small enough to obtain a valid clock signal. To find such value was not the purpose of this work, some authors assumed 2% under compensation in its investigations [29] of the DSP taps needed for CD compensation. In this investigation no pre compensation was assumed and thereby, the number of taps obtained to achieve a BER<0.001 is higher than if we would have assumed pre-compensation. Moreover, sampling times error can be avoided by oversampling the signal with sampling rate $1/T = M/KTs$ where M/K is a rational oversampling ratio. Along this work oversampling has been used with $M/K = 2$ with no errors in the sampling stage.

The DSP module is able to compensate CD, PMD and Phase Noise. The simulations of this work were made sending a total of 40000 bits through the system therefore, following Monte Carlo method we can report BER until 0.001.

The CD equalizer was designed adaptive and non-adaptive. In the adaptive version of the equalizer we can choose between two adaptive algorithms: CMA and LMS. Was found that CMA is not useful for CD equalization. On the other hand, LMS obtained good results in CD equalization but cannot be used when polarization dependent impairments as PMD affects the signal. The other option investigated for CD equalization has been a fixed taps equalizer. A digital coherent receiver designed with an adaptive CD equalizer can be used for any fiber despite of the amount of CD that affects the fiber, in case of non-adaptive CD equalizer (or fixed taps equalizer) the dispersion parameter of the fiber should be measured to use the proper taps in the equalizer, however the dispersion parameter is normally a well known parameter of the fiber. LMS based adaptive equalizer, obtained slightly better results than the CD equalizer with fixed taps but fixed taps implementation was chosen for the digital coherent receiver because LMS cannot be use when polarization dependent impairments affects the signal.

For fixed taps CD equalizer there is a close taps equation that depends on the dispersion parameter of the fiber, implementing this equation with a FIR filter CD can be compensated. Fixed taps CD equalizer is able to compensate chromatic dispersion accumulated in very long fibers, for example was found that CD accumulated in 5000 km of a fiber with D=13.3286 $\frac{ps}{\text{nm.km}}$, which is a total dispersion of 66643 $\frac{ps}{\text{nm}}$, was compensated with almost 100 taps. Was also found an expression that gives an approximation to the minimum number of taps the filter needs to compensate CD, this expression acted as a boundary for the minimum number of taps needed by the equalizer. In the simulations was found that fixed taps CD equalizer never used more taps than those indicated by this expression.

The digital coherent receiver designed also has a block in charge of PMD equalization. Because PMD is time variant the equalizer must be designed with adaptive equalizers. The PMD equalizer is therefore formed by four adaptive equalizers in a MIMO structure and it is able to compensate PMD accumulated in fiber lengths from 500 km to 5000km when the DGD of the fiber is $0.1\text{x}10^{-9}\frac{s}{\sqrt{Km}}$. In our simulations the PMD equalization is in function of the angle between the PSP and the signal sent through the fiber. The equalizer can compensate signals with PHI angles in the range $\left[0, 0.4\frac{\pi}{2}\right[$ when no other impairments are present in the system. The number of taps needed to achieve the equalization of PMD when the PHI angle is between the given range is between 2 and 4 taps per adaptive equalizer.

The last module of the DSP of the digital coherent receiver is in charge of the equalization of the phase noise. The phase noise come from the frequency offset between the transmitter and the LO and also from the linewidth of the laser involved in the transmission system. For such purpose two kind of compensators were designed: frequency estimator and carrier recovery. The first one is able to compensate just frequency offset and has to be used together with carrier recovery. Carrier recovery can compensate both phase noise sources. In the simulations the use of both systems achieve practically the same results and therefore carrier recovery was chosen for the whole receiver scheme since it is simpler and would make the DSP of the coherent receiver faster.

Finally the whole receiver was tested being found that when all the compensators are together in the DSP stage of the receiver and the three impairments that can be compensated affect the signal the system loses some capabilities. The number of taps needed to compensate the impairment to obtain a BER<0.001 grow, and the requirements of the system are more exigent. For example we said that PMD compensation can be done with the PMD equalizer if the signal was sent with an angle PHI in the range $\left[0, 0.4\frac{\pi}{2}\right[$, that's true when the PMD equalizer was tested just with PMD affecting the signal and therefore not equalizing CD in the previous step of the DSP. When the whole receiver is assembled, the PMD equalizer needs the angle PHI to be between$\left[0, 0.2\frac{\pi}{2}\right]$. Also the taps of the PMD equalizer need to be incremented as well as the taps of the CD to achieve the CD equalization needed to obtain the BER required. The same happens to the phase noise estimation and compensation. In this case, when the three modules of the DSP are assembled, the phase estimator obtains certain error in the estimation that leads to an increase in the BER. To prevent the BER increase because the phase estimator, the frequency offset between transmitter and local oscillator cannot be bigger than 100Mhz and the linewidth of the laser just can be of 100Mhz

However the taps and the requirements of the system with coherent transmission and the digital coherent receiver can be achieved transmission along 5000 km of fiber without amplification along the link. Not amplification along the fiber would increment the speed transmission however the speed of the coherent receiver has to be checked when the receiver is implemented on a DSP board. The implementation of the receiver should be the next step in the study of digital coherent receivers.

Until here is known and showed that digital coherent receivers brings great opportunities to optical communications. Coherent detection without DSP already brings an improvement in the sensitivity of the receivers but the real advantage would be the capability of such receivers to compensate the main impairments in the digital domain. The possibility of equalization of the main impairments in optical communication like CD and first order PMD or phase noise is enough reason to think in coherent receivers as a real option. But still exist a question about the capability of implementing the DSP block of digital coherent receivers in a DSP board. The DSP block will suppose to the whole system a bottle neck since the DSP clock speed is slower than the symbol rate of optical communications. A solution would be to force the DSP to operate in parallel but this would suppose that the algorithms employing feedback would be compromised. The implementation of the DSP into a board needs a previous study and many tests after the implementation, it could be a great continuation of the present work.

The digital coherent receiver designed here is just a baby of what digital coherent receivers will be in the future. It just uses QPSK modulation with POL-MUX , however coherent detection is already able to use more complex modulations as 8-PSK or better, coherent receivers can even be used together with WDM to maximize the spectral efficiency. Coherent receivers could bring to the optical communication the possibility of exploit the optical fiber to its maximum.

References

[1] T. Okoshi and K. Kikuchi, “Coherent optical fiber communications”, Kluwer Academic Publishers, Springer, 1988.

[2] E.E. Basch and T.G. Brown, “Introduction to coherent optical fiber transmission”, IEEE Commun. Mag., vol. 23, pp. 23-30, May 1985.

[3] Kazuro Kikuchi, “Coherent Detection: Born Again?”, Lasers and Electro-Optics Society, 2006. LEOS 2006. 19th Annual Meeting of the IEEE.

[4] K.-P. Ho and J. M. Kahn, “Ultimate spectral efficiency limits in DWDM systems”, in *OFC*, Anaheim, CA, 2002, Paper 12B22-1.

[5] Yan Han and Guifang Lee, “Theoretical Sensitivity of Direct-Detection Multilevel Modulation Formats for High Spectral Efficiency Optical Communications”. IEEE Journal of Selected Topics in Quantum Electronics, Vol.12, No. 4, July/August 2006.

[6] M. Ohm and J. Speidel, “Differential optical 8-PSK with direct detectin (8-DPSK/DD),” in Voträge der 4. ITG-Fachtagung Photonische Netze Leipzig, Germany, pp. 177–181, May 2003.

[7] S.J. Savory, “Digital filters for coherent optical receivers”, Optics Express, vol. 16, no.2, pp.804-817, 2008.

[8] Alan Pak Tao Lau, Daniel J.F. Barros, Joseph M. Kahn, “Coherent Detection in Optical Fiber Systems”, Optics Express, Vol. 16, Issue 2, pp. 753-791, 2008.

[9] Govind P. Agrawal, “Fiber-Optic Communications Systems (Third Edition)”, John Wiley and Sons, 2003.

[10] J. R. Barry and E. A. Lee, "Performance of Coherent Optical Receivers", *Proceedings of the IEEE,* vol. 78, no. 8, pp. 1369-1394, August 1990.

[11] T. G. Hodgkinson, R. A. Harmon, and D. W. Smith, *Electron. Lett*. 21, 867, 1985.

[12] Matthias Seimetz, “Phase diversity receivers for homodyne detection of optical DQPSK signals”, J. Lightwave Technology, vol. 24, pp. 3384-3391, 2006.

[13] Leonid G. Kazovsky, Lyn Curtis, William C. Young, and Nim K. Cheung, "All-fiber 90° optical hybrid for coherent communications," Appl. Opt. **26**, 437-439, 1987.

[14] A. Yariv, Optical Electronics. New York: Holt, Rinehart and Winston,(Third Eddition).

[15] J. Salz, “Coherent lightwave communications,” *AT&T Tech. J.,* vol. 6***4,*** no. 10, pp. 2153-2211, Dec. 1985.

[16] Satoshi Tsukamoto, Kazuhiro Katoh, Kazuro Kikuchi, “Coherent Demodulation of Optical Multilevel Phase-Shift-Keying Signals Using Homodyne Detection and Digital Signal Processing”, IEE Photonics Technology Letters. Vol. 18, No. 10, May 2006.

[17] Claude Herard and Alain Lacourt, "New multiplexing technique using polarization of light," Appl. Opt. 30, 222-231, 1991.

[18] Krzysztof Perlicki, “3x2.5 Gbit/s Polarization Division Multiplexing Transmission”, 12th WSEAS International Conference on Communications, Heraklion, Greece, July 23-25, 2008.

[19] C. de Angelis, S. Wabnitz, “Interactions of Orthogonally Polarized Solitons in Opticals Fibers”, November 1995.

[20] X. Steve Yao, L.-S. Yan, B. Zhang, A. E. Willner, Junfeng Jiang, “All-optic Scheme for Automatic Polarization Division Multiplexing” Optics Express, vol. 15, Issue 12, pp.7407-7414, 2007.

[21] C. D. Poole and R.E. Wagner, “A phenomenological approach to polarization dispersion in long single-mode fibers,” *Electron. Lett.***,** vol. 22, no. 19, p. 1029, 1986.

[22] http://www.cirl.com

[23] T. Okoshi, J. Lightwave Technol. 3, 1232, 1985.

[24] Keang-Po Ho, “Phase-modulated optical communication systems”, Springer Science-Business Media, 2005.

[25] S. Ryu, S. Yamamoto, Y. Namihira, K. Mochizuki, H. Wakabayashi, “Polarization diversity techniques for the use of coherent optical fiber submarine cable system”, J. Lightwave Technology, vol. 9, n. 5, 1991.

[26] L.G. Kazovsky, “Decision-directed phase-locked loop for optical homodyne receivers: Performance analysis and laser linewidth requirements”, J.Lightwave Technolog. 3, 1238, 1985.

[27] L.G. Kazovsky, “Balanced phase-locked loop for optical homodyne receivers: Performance analysis, design considerations and laser linewidth requirements”, J. Opt. Commun. 7, 66 (1986); J. Lightwave Technolog. Vol. 4, 182-195, 1986.

[28] T.G. Hodgkingson, “Receiver analysis for synchronous coherent optical fiber transmission systems”, J. Lightwave Technolog. 5, 573, 1987.

[29] Ezra Ip, Alan Pak Tao Lau, Daniel J.F. Barros, Joseph M. Kahn, “Coherent Detection in Optical Fiber Systems”, Opt. Express, vol. 16, Issue 2, pp. 753-791, 2008.

[30] Y. Han and G. Li, “Coherent optical communication using polarization multiple-input-multiple-output”, Opt. Express 13, 7527-7534, 2005.

[31] John Francis Canny, “Finding edges and lines in images”, June 1983.

[32] Zhu Z, Sadjadpour H. R., Blum R. S., Adrekson P. A., Li T. J., “Performance of a single-input multiple-output decision feedback equaliser for polarisation mode dispersion compensation”, Optoelectron., Vol. 1, Issue 5, p.233–240, October 2007.

[33] Ezra Ip and Joseph M. Kahn, “Carrier synchronization for 3 and 4-bit-per-Symbol Optical Transmission”, Journal of Lightwave Technology, vol. 23, no. 12, December 2005.

[34] Andreas Leve, Noriaki Kaneda, Ut-Va Koc, Young-Kai Chen, ”Frequency Estimation in Intradyne Reception”, Optical Fiber Communication and the National Fiber Optic Engineers Conference, 25-29 March 2007, pp. 1 – 3.

[35] H. Meyr, M. Moeneclaey, and S. Fechtel, “Digital Communication Receiver. New York: Wiley, 1998, ch. 8.2.2.

[36] Ezra Ip and Joseph M. Kahn, “Feedforward Carrier Recovery for Coherent Optical Communications”, Journal of Lightwave Technology, vol. 25, no. 9, September 2007.

[37] M. G. Taylor, “Accurate digital phase estimation process for coherent detection using a parallel digital processor”, ECOC 2005 conference, Glasgow, UK, paper Tu4.2.6, Sep. 2005.

[38] Ling Liao, Dean Samara-Rubio, Michael Morse, Ansheng Liu, Dexter Hodge, Doron Rubin, Ulrich Keil, and Thorkild Franck, "High speed silicon Mach-Zehnder modulator," Opt. Express 13, 3129-3135, 2005.

[39] D. van den Borne, N. E. Hecker-Denschlag, G.-D. Khoe and H. de Waardt, “Cross phase modulation induced depolarization penalties in 2x10Gbit/s polarization-multiplexed transmission”, in Proc. ECOC 2004, Mo4.5.5, pp. 1-3.

[40] Chris R. S. Fludger, Thomas Duthel, Dirk van den Borne, Christoph Schulien, Ernst-Dieter Schmidt, Torsten Wuth, Jonas Geyer, Erik De Man, Giok-Djan Khoe, and Huug de Waardt, "Coherent Equalization and POLMUX-RZ-DQPSK for Robust 100-GE Transmission," J. Lightwave Technol. 26, 64-72, 2008.

[41] H. Louchet, K. Kuzmin, C. Arellano, I. Koltchanov, A. Richter, “Modeling of Ultra-High Speed Optical Transmission Systems”. Optical Transmission, Switching, and Subsystems VI. Proceedings of the SPIE, Volume 7136, pp. 713632-713632-10, 2008.

Anexos

A.Traducción de la introducción y las conclusiones

De acuerdo a la normativa de la EPS, los capítulos de introducción y de conclusiones se incluyen también en castellano.

1.Introducción

En el presente proyecto vamos a realizar el diseño y testeo de un receptor digital coherente para comunicación óptica. Estos receptores, como detallaremos más adelante, presentan una serie de ventajas sobre los receptores de detección directa que se vienen utilizando históricamente en comunicación óptica. Entre las ventajas más interesantes que presenta el receptor digital coherente está la posibilidad de utilización de diversas técnicas de procesamiento digital de señales. Haciendo uso de dichas técnicas se diseña un receptor digital coherente capaz de compensar digitalmente dos de los tradicionales efectos adversos de las comunicaciones ópticas como son la dispersión cromática y la dispersión por modo de polarización.

El esquema del sistema de transmisión donde se incluirá el receptor diseñado será por lo tanto coherente, siendo la señal a enviar por el canal una señal modulada en fase. Una simplificación del esquema de transmisión está presente en la ilustración 1. Además el esquema de transmisión hará uso de una técnica de multiplexación, multiplexación por modo de polarización (POL-MUX), permitiendo enviar información en cada modo de polarización. Por lo tanto se enviarán dos señales moduladas en fase por la línea de transmisión, cada una en un modo de polarización distinto. El receptor diseñado será capaz de detectar ambas señales moduladas. El presente estudio finalizará poniendo a prueba la robustez del receptor, testeando su comportamiento en cuanto a BER o capacidad de compensación de los efectos adversos bajo distintas condiciones, como pueden ser distintas longitudes del canal, distintos valores de dispersión cromática o desfase entre modos de polarización.

La idea de sistemas coherentes para comunicación óptica no es nueva y data de la década de los 80. Sin embargo la tecnología no estaba lo suficientemente adelantada por entonces para su implantación comercial. Además aparecieron nuevas tecnologías que dotaban a los sistemas de transmisión óptica por detección directa de gran potencial, evitando de esta manera la aparición comercial de los sistemas coherentes.

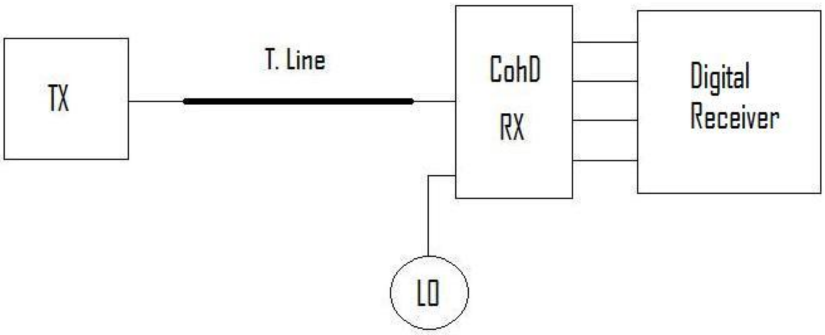

Ilustración 1: Esquema de un sistema de transmisión genérico con un receptor coherente. Tx – Transmisor encargado de la modulación de la señal. T. Line – Línea de transmisión, en nuestro caso una fibra óptica.CohD - detector coherente con LO – oscilador local. En el extremo final el receptor digital, encargado de llevar a cabo el trataminedo digital de señales.

En comunicaciones ópticas, hay por lo tanto dos grupos de receptores: receptores de detección directa y receptores coherentes. Los receptores de detección directa reciben este nombre debido a que la señal recibida es aplicada directamente al fotodiodo encargado de transformar la onda luminosa en una señal eléctrica. En los receptores coherentes, en cambio, hay un estadio intermedio en el cual se mezcla la señal recibida con una onda luminosa proveniente de un oscilador local. Esta suma es lineal lo que permite recuperar también la fase de la señal cosa que no es posible con un receptor de detección directa, el cual solo capta la amplitud de la señal en recepción.

Los receptores coherentes poseen importantes ventajas sobre los de detección directa, sin embargo, éstos últimos son los que tradicionalmente han sido utilizados en los sistemas de transmisión óptica, debido a su mayor sencillez y a que las mejores introducidas por los receptores coherentes no han sido necesarias. El ancho de banda que proporcionaban los sistemas de fibra óptica equipados con detección directa satisfacía, con creces, la demanda de ancho de banda de la época. En los últimos años, la cada vez mayor demanda de ancho de banda y los avances en otras tecnologías están fijando de nuevo la atención de los investigadores en los receptores coherentes.

En los siguientes capítulos de esta introducción damos un breve repaso a la historia de las comunicaciones ópticas para enmarcar la aparición de los receptores coherentes y dilucidar por qué la supremacía de la detección directa pese a las ventajas de los receptores coherentes. Más tarde en *Motivaciones* enunciamos las principales ventajas de dichos receptores y las nuevas posibilidades que éstos ofrecen para más tarde fijarnos los objetivos del presente proyecto. Terminaremos describiendo la organización del proyecto.

Perspectiva Histórica

La fibra óptica se ha convertido en el medio preferido para las comunicaciones digitales de alta capacidad y larga distancia debido a sus importantes ventajas: enorme ancho de banda, baja atenuación, inmunidad frente a interferencias y alta seguridad. El estudio de los sistemas de comunicación ópticos comenzó alrededor de 1970 y la historia de su evolución se divide en generaciones. Cada generación ha introducido un cambio fundamental que ha permitido incrementar sustancialmente la capacidad de los sistemas de fibra óptica.

La *primera generación* fue utilizada durante los años 70. Se usaban fibras multimodo a longitudes de onda bajas, en torno a los 850 nm. Esta primera generación sufría tres importantes limitaciones: atenuación alta, dispersión cromática (o dispersión intramodal) y dispersión modal. La atenuación para longitudes de onda cercanas a 850 nm era de 2 B/km, lo que es una atenuación relativamente alta en comparación con las atenuaciones que la fibra óptica ofrece en otras ventanas. Por otro lado la dispersión de la fibra limita la velocidad a la que podemos transmitir la información. Esto es debido a que la dispersión provoca el ensanchamiento en el tiempo de los pulsos enviados, de manera que los pulsos contiguos interfieren entre sí generando errores en la detección del pulso, es lo que se conoce como interferencia entre símbolos(ISI). Existen dos tipos de dispersión: cromática y modal. La dispersión cromática es debida a que las diferentes frecuencias viajan a distintas velocidades dentro de la fibra óptica. De manera similar, la dispersión modal es debida a que los distintos modos de la luz viajan a distintas velocidades. En esta primera ventana la dispersión cromática es alta y el uso de fibras multimodo provoca la aparición de dispersión modal. En los sistemas de primera generación se operaban a una tasa binaria de 45Mb/s.

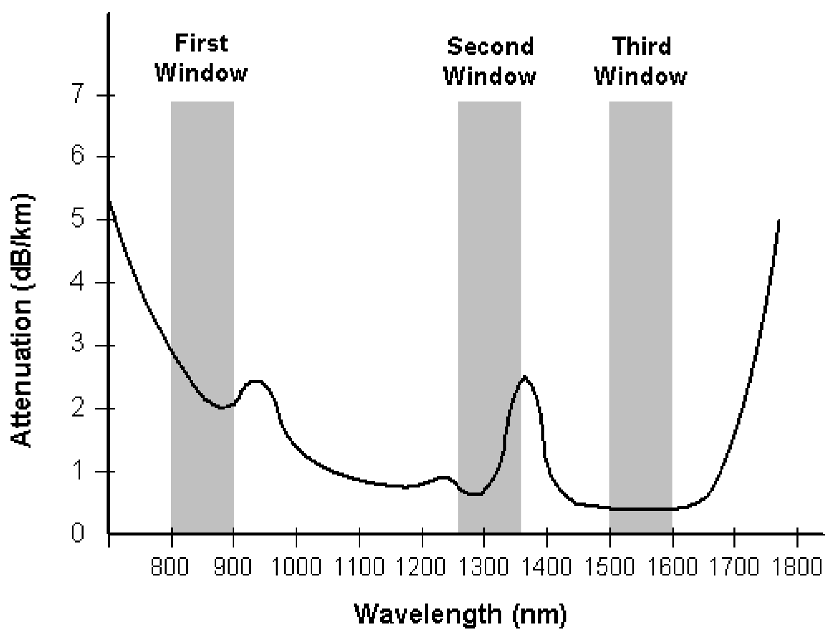

Ilustración 2: Atenuación frente a longitud de onda en fibra óptica de Silicio.

Los sistemas de *segunda generación* fueron introducidos a principios de 1980. El principal avance fue que evitaban la dispersión cromática operando a 1300 nm, la ventana de menor dispersión cromática. Una segunda ventaja era que a esta longitud de onda la atenuación disminuía hasta los 0.5 dB/km (observar ilustración 1). De nuevo esta generación utilizaba fibras multimodo y continuaba sufriendo dispersión modal, pero esta limitación fue superada a mediados de los años 80 con el uso de fibras monomodo. Las fibras monomodo son fibras cuyo radio del núcleo se escoge para que solo pueda transmitirse un modo a través de ellas, evitando así la dispersión modal. Los sistemas comerciales de segunda generación basados en fibras multimodo alcanzaban tasas binarias de 100Mb/s mientras que los basados en fibra monomodo llegaban hasta 1.7Gb/s.

La mínima atenuación de una fibra óptica, cercano a 0.2 dB/km, se encuentra entre 1450 y 1650 nm. Para explotar esta bajísima atenuación aparecieron los sistemas de *tercera generación* trabajando en la tercera ventana a 1550 nm(observar ilustración 1). En estos sistemas, gracias a la baja atenuación se incrementó la distancia entre repetidores. Son capaces de transmitir a 10Gb/s.

La *cuarta generación* hace uso de amplificación óptica mediante amplificadores de fibra dopada con erbio (EDFA) y de multiplexación por división de longitud de onda (WDM). Estas tecnologías conjuntamente permiten el envío de información por varios canales dentro de la misma fibra. En este caso la capacidad de la fibra se incrementa tanto como canales WDM se usen. Por ejemplo un sistema de 16 canales actuando a 10 Gb/s permite una tasa binaria total de 160 Gb/s.

El esquema de recepción utilizado en estas cuatro generaciones era detección directa. La detección óptica coherente aparece en los años 80 siendo intensamente estudiada con resultado de las siguientes propiedades principales[1] :

1. La sensibilidad límite del receptor debido al ruido de descarga (shot noise) puede ser alcanzada ajustando la potencia del oscilador local.

2. Habilidad de los receptores coherentes de recuperar la fase de la señal.

Ambas ventajas aumenta la sensibilidad del receptor, lo que permite aumentar la distancia entre los repetidores. La segunda ventaja permite la utilización de modulaciones multinivel, lo que incremente la capacidad de la fibra. Además al recuperar la fase de la señal tenemos información suficiente para que utilizando técnicas de procesado digital de señales se puedan compensar efectos indeseables introducidos por la fibra, como la dispersión cromática o la dispersión por modo de polarización.

A pesar de estas ventajas, la detección coherente no se llevó a la práctica debida principalmente a la llegada de los EDFA y de la tecnología WDM a principio de los años noventa. Con estos amplificadores de fibra dopada con erbio es posible amplificar la señal en el dominio óptico, la distancia entre repetidores crece y la primera mejora de los detectores coherentes se hace menos significativa. Además el uso de WDM aumenta la capacidad de la fibra sin necesidad de utilizar otros métodos como pueden ser las modulaciones multinivel que ofrecía la detección coherente.

Por lo tanto las dos principales mejoras proporcionadas por el esquema coherente eran cubiertas por éstas dos nuevas tecnologías de una manera más eficaz y también más económica debido dificultades técnicas inherentes a los receptores coherentes en los años 80. Esto hizo que el esquema de modulación IM/DD siguiera siendo utilizado pese a la superioridad del esquema coherente.

Actualmente se vuelve a enfocar la mirada hacia estos receptores por las ventajas ya descritas, por la excelente sociedad que podría formar junto a WDM y por la característica de que en muchos casos, dependiendo de la longitud de canal, el esquema coherente solo necesitaría, para implantarse, modificaciones en el emisor y en el receptor.

Motivación y Objetivos

MOTIVACIÓN:

La continua y creciente demanda de ancho de banda ha vuelto a acaparar la mirada de los investigadores en los receptores coherentes. Los sistemas WDM que primero retrasaron la llegada de los receptores coherentes ahora aceleran el interés en dichos receptores. Con la llegada de WDM la eficiencia espectral se ha convertido en tema clave de estudio por parte de los investigadores. En este contexto las ventajas de los receptores coherentes vuelven a ser muy atractivas para alcanzar los límites de eficiencia espectral. Además el esquema coherente, aprovechándose de las ventajas en otros campos, ofrecen nuevas posibilidades como la capacidad de filtrar canales WDM densamente empaquetados mediante filtros digitales o el post-procesado de las señales recibidas para compensar efectos indeseables como Dispersión Cromática.

La detección coherente es la gran aliada de los sistemas WDM en el contexto de la eficiencia espectral. Haciendo uso de detección coherente se han demostrado las mayores eficiencias espectrales como se puede observar en la siguiente figura[4]

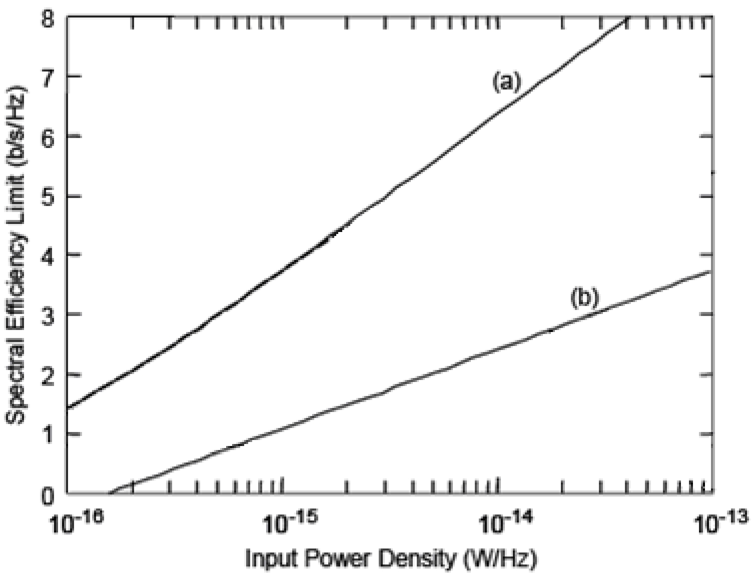

Ilustración 3. Límites de eficiencia espectral en función de la densidad de energía de entrada en sistemas WDM amplificados: (a) detección coherente en régimen lineal, (b) detección directa en régimen lineal, asíntota de SNR alto[4]

Para lograr las más altas eficiencias espectrales se debe hacer uso de modulaciones multinivel las cuales aumentan la capacidad de la fibra sin necesidad de aumentar el ancho de banda. Se han investigado maneras de introducir modulaciones multinivel en sistemas que usan DD [5] [6] , pero estos receptores pierden sencillez y se vuelven complejos y costosos. En cambio, los detectores coherentes presenta una arquitectura simple para este tipo de modulaciones. Otra manera de incrementar la eficiencia espectral es mediante multiplexación por polarización. Con esta tecnología se puede enviar información en ambas polarizaciones de la luz duplicando de esta manera la capacidad.

Mediante recepción coherente se ha demostrado que se puede demultiplexar eléctricamente señales multiplexadas por polarización [7] [8] .

Además los receptores coherentes poseen la propiedad de tener una resolución en frecuencia muy alta lo que les permite separar canales WDM muy cercanos mediante filtros en el dominio eléctrico. Esto permite empaquetar los canales WDM muy juntos de manera que quepan mas canales en un ancho de banda dado.

Otro gran atractivo que brinda la detección coherente es que abre la puerta al Procesamiento Digital de Señales (DSP) en los sistemas de transmisión óptica. Gracias a los avances en circuitos integrados digitales de alta velocidad y a la preservación de la fase de la señal por parte de los receptores coherentes se pueden procesar la información recibida. Mediante el procesado digital se puede hacer un seguimiento de la fase y polarización de la señal recibida o mitigar el impacto de efectos indeseables de las comunicaciones ópticas como pueden ser la Dispersión Cromática (CD) o la Dispersión por Modo de Polarización (PMD). Además el DSP proporciona una gran flexibilidad a estos receptores al ser capaz de compensar inexactitudes a nivel hardware como por ejemplo un cierto offset entre el láser transmisor y el oscilador local.

OBJETIVOS:

Una vez detalladas las motivaciones expuestas como las ventajas que un receptor coherente puede aportar a las comunicaciones ópticas, el presente proyecto tiene como principal objetivo el diseño, implementación y simulación de un receptor digital coherente. El receptor diseñado, principalmente debe ser capaz de recibir señales previamente moduladas en fase en el transmisor y multiplexadas por polarización. La modulación en fase junto a la multiplexación por polarización hacen que la capacidad de la fibra se vea incrementada notablemente. El uso de multiplexación por polarización hará que nuestro canal de transmisión tenga el doble de capacidad. Si enviamos además señales moduladas en cada polarización la capacidad de la fibra aumenta aún más. Originalmente si una fibra tiene una capacidad C, con multiplexación por modo de polarización la capacidad será 2xC. Si además hacemos uso de modulación QAM en cada canal multiplexado por polarización, obtendremos finalmente una capacidad total para la fibra de 4xC. La mejora es por lo tanto, de cuatro veces la capacidad inicial.

Con respecto al diseño del receptor se tienen los siguientes objetivos: se implementará un circuito recuperador de reloj. El receptor es digital por lo que se encarga de la conversión A/D tras la fase de recuperación de reloj. Tras la conversión A/D y a partir de aquí será capaz de demultiplexar canales multiplexados por polarización y compensar Dispersión Cromática junto con Dispersión por Modo de Polarización. Haciendo uso de DSP será también capaz de hacer un seguimiento de la fase de la señal para recuperarla. Debe trabajar con modulación QPSK que junto con multiplexación por polarización cuadriplica la capacidad una fibra.

El receptor es implementado en Matlab lo que luego permite incluirlo dentro de la herramienta de simulación VPI Transmisión Maker para estudiar su robustez mediante simulación. Se estudia la capacidad de compensación tanto del ecualizador de dispersión cromática como del ecualizador de PMD y el compensador de ruido de fase, primero por separado y finalmente cuando se encuentran todos juntos. Se caracteriza esta capacidad de compensación obteniendo el mínimo número de taps de los filtros, necesarios para compensar distintos valores de dispersión, se obtendrá la cantidad de potencia de penalti necesaria para obtener BER < 0.001, el cual será nuestro valor de referencia para el BER.

En este proyecto no abordamos la construcción del receptor en circuito impreso de alta velocidad. Este sería un magnífico tema de investigación que traería la continuidad al presente estudio sobre el receptor digital coherente.

Organización de la memoria

El proyecto comienza presentando las bases de la comunicación óptica coherente y una serie de conceptos importantes que serán utilizados a lo largo del proyecto. Primero detallamos un receptor coherente genérico y diferenciamos entre detección coherente homodina y heterodina. Dentro del punto sensibilidad definiremos conceptos importantes que se ven con mucha frecuencia en comunicaciones ópticas como límite cuántico o shotnoise. Debido a que una de las grandes ventajas de la recepción coherente es la de poder hacer uso de modulaciones multinivel, se incluye un apartado en el que repasamos dichas modulaciones. También es descrita la multiplexación por polarización ya que es una tecnología de la que los receptores coherentes pueden sacar mucho provecho y será utilizada por el sistema en el que incluiremos nuestro receptor. Luego presentamos los distintos efectos que afectan a las comunicaciones ópticas coherentes y para terminar el capítulo se hace un breve repaso al estado del arte.

En el tercer capítulo se detalla el diseño del receptor digital coherente implementado. Esquematizamos el mismo y lo dividimos en distintas secciones que son analizadas individualmente. La primera sección describe el funcionamiento del recuperador de reloj diseñado. El siguiente punto analiza la compensación mediante DSP de CD y PMD que se ha implementado. El capítulo termina detallando el módulo encargado de estimar la fase de la señal para luego compensar el ruido de fase.

El capítulo cuarto se encarga de recoger las pruebas realizadas sobre el receptor. Primero se describe el sistema donde se introduce el receptor y sobre el que se realiza el estudio. En el siguiente punto se estudia cómo se comporta el receptor bajo distintos cambios en el sistema para estudiar su robustez. En el tercer y último punto de éste capítulo se estudia como mejora el receptor la transmisión haciendo siempre una comparación con el caso de detección directa bajo las mismas circunstancias.

El último capítulo recoge las conclusiones que se obtienen de este proyecto y cuál sería el camino a seguir para continuar con el estudio de este receptor coherente.

5.Conclusiones y Trabajo Futuro

En este trabajo hemos realizado un estudio sobre receptores coherentes para transmisión óptica. A lo largo del presente trabajo se ha mostrado la tecnología actual en lo que a receptores coherentes para transmisión óptica se refiere, también se han mostrado algunas técnicas de procesamiento digital de señales para la ecualización de efectos indeseables de la transmisión óptica. Después se ha diseñado y testeado un receptor digital coherente haciendo uso de la información previamente presentada. El receptor digital coherente diseñado tiene como propósitos: primero mostrar de una manera más práctica cómo este tipo de receptores son capaces de mejorar las capacidades de la transmisión por fibra óptica, al permitir, por ejemplo, modulaciones multinivel. Otro propósito del receptor diseñado era la implementación y testeo de varias técnicas de tratamiento digital de señales para compensar efectos tales como CD y PMD en el receptor, las cuales solo se pueden utilizar si como receptor se usa un receptor digital coherente.

Con receptores coherentes para fibra óptica somos capaces de recibir la fase de la señal, cosa imposible con la tecnología de detección directa utilizada hasta el momento en comunicaciones ópticas. Para poder obtener la fase de la señal transmitida utilizamos un optical coupler especial un 90º Hybrid junto con detección balanceada como arquitectura de recepción. Con esta arquitectura obtenemos la señal enviada junto con su fase en el dominio eléctrico. Una vez que tenemos la señal completa vamos a convertirla al dominio digital. En el dominio digital, gracias a que tenemos la fase de la señal y a técnicas de procesamiento digital de señales, seremos capaces de compensar los efectos indeseables clásicos de las comunicaciones ópticas: dispersión cromática, dispersión por modo de polarización y ruido de fase. Este estudio se centrado más que en nada, en esta parte del receptor, en el diseño digital del receptor coherente, obteniendo de esa forma lo que llamamos un receptor digital coherente.

El receptor digital coherente, para su fase de ecualización, necesita que la señal analógica que provee el front-end del receptor sea digitalizada. Para ellos necesitamos un conversor analógico-digital y un circuito recuperador de reloj en el receptor. Como hemos visto la recuperación de reloj juega un rol importante dentro del receptor cuando, sobre todo, se utilizan técnicas de TDS para compensar los efectos indeseables de la fibra, sobre todo si se compensan valores altos de dispersión cromática. Como ya se ha comentado, utilizando TDS la dispersión cromática que afecta a un sistema de transmisión de fibra óptica de gran longitud puede ser compensada en el dominio eléctrico. En estos sistemas, la dispersión cromática acumulada debido a la longitud de la fibra es muy importante y en cambio puede ser compensada en el receptor digital coherente sin necesidad de utilizar métodos tradicionales para compensar la dispersión a lo largo de la fibra. Sin duda, que la compensación de la dispersión se realice en el extremo receptor es una ventaja, sin embargo nos presente un problema: si evitamos la compensación de la dispersión a lo largo de la fibra (usando por ejemplo fibras compensadoras de dispersión) la señal que llega al receptor digital coherente viene muy distorsionada por la dispersión cromática lo que le causará dificultades al circuito recuperador de reloj. Si el reloj no se obtiene correctamente, el error del sistema de transmisión provendrá por lo tanto de la etapa de muestreo de la señal analógica. Para evitar esto se puede incluir una etapa de compensación de dispersión haciendo uno de un tramo de DCF antes del receptor que compense DC lo suficiente para que permita al circuito recuperador de reloj obtener la señal de reloj. Encontrar la cantidad de dispersión cromática que hay que precompensar para que el sistema funcione no es uno de los objetivos de este trabajo, algunos autores asumen en sus resultados un 2% de compensación [29] .En nuestra investigación no asumimos precompensación y por lo tanto nuestros resultados arrojan mayor número de taps en los filtros de compensación de dispersión cromática que si asumiéramos precompensación. Además de la precompensación y mucho más importante que ésta, es la tasa de muestreo. Para evitar errores en la etapa de muestreo se debe sobremuestrear la señal con una tasa $1/T = M/KTs$ donde M/K es un ratio de sobremuestreo. A lo largo de este trabajo hemos usado un sobremuestreo con $M/K = 2$ sin aparecer errores de muestreo en ningunas de las simulaciones.

El siguiente módulo del receptor digital coherente es el encargado del TDS. Este módulo es capaz de compensar dispersión cromática, dispersión por modo de polarización y ruido de fase. Antes de continuar con este módulo hay que aclarar que los resultados obtenidos de los filtros y del sistema global fueron obtenido mediante simulación. Las simulaciones fueron realizadas mandando un total de 40000 bit por el sistema de transmisión y por lo tanto y siguiendo el método de Monte Carlo podemos reportar un BER de hasta 0.001. El resto de especificaciones se encuentran descritas en el capítulo 4.

Como decíamos el modulo encargado del tratamiento digital de señales se compone de tres componentes, cada uno de estos componentes es capaz de compensar un tipo de efecto adverso de las comunicaciones ópticas. El primero se encarga de compensar dispersión cromática. Este ecualizador de DC ha sido diseñado en dos versiones una como un filtro FIR no adaptivo y la otra versión es un ecualizador adaptivo que puede usar dos algoritmos de adaptación: CMA y LMS. Con respecto a En las simulaciones se encontró que el algoritmo CMA no es válido para compensar DC. Por otro lado, el algoritmo LMS obtuvo unos Buenos resultados ecualizando DC pero en cambio no puede utilizarse cuando además existe en el sistema dispersión por modo de polarización. La otra opción para compensar DC es un filtro FIR con taps fijas. Un receptor digital coherente con un ecualizador de DC adaptivo puede usarse para cualquier fibra sin importar la cantidad de DC de la fibra, en el caso del filtro FIR con taps fijas el parámetro de dispersión de la fibra tiene que ser medido en la fibra para usar los taps adecuados a dicha fibra. Esto es porque existe una ecuación cerrada para los taps del filtro FIR ecualizador de DC, en los cuales el valor de los taps depende de dicho parámetro de dispersión D. Sin embargo esto no supone un problema ya que dicho parámetro de dispersión es normalmente un parámetro bien conocido de cada fibra. En las simulaciones el ecualizador adaptivo obtuvo ligeramente mejores resultados que el filtro FIR de taps fijas, sin embargo el filtro FIR fue escogido por la razón antes expuesta de que el algoritmo LMS impide luego la ecualización de la dispersión por modo de polarización y nuestro objetivo es tener un receptor capaz de compensar los tres efectos.

Como se ha comentado anteriormente en el filtro FIR encargado de ecualizar DC los taps dependen del parámetro de dispersión de la fibra D. Existe una ecuación cerrada para los taps del filtro que depende directamente de este parámetro. Con este filtro se puede compensar dispersión cromática acumulada en muchos kilómetros de fibra óptica. Por ejemplo se encontró que la dispersión cromática debida a 5000 km de fibra con una parámetro D=13.3286 $\frac{ps}{\mathrm{nm}.\mathrm{km}}$, esto es una dispersión total de 66643 $\frac{ps}{\mathrm{nm}}$, se compensó utilizando este filtro FIR con 100 taps. En el trabajo también se incluye una expresión matemática que aproxima el mínimo número de taps que el filtro necesita para compensar una cierta cantidad de DC. Esta expresión también es puesta a prueba en el trabajo, las simulaciones muestran que la expresión actúa como un límite ya que en ninguna simulación se encontró que se necesitaran más taps que los indicados por dicha expresión.

El receptor digital coherente diseñado también tiene un módulo encargado de la ecualización de la dispersión por modo de polarización. La PMD es un efecto que varía con el tiempo y por lo tanto el ecualizador encargado de su compensación debe ser diseñado haciendo uso de ecualizadores adaptivos. El ecualizador de PMD está por lo tanto formado por cuatro ecualizadores adaptivos en una estructura MIMO, es capaz de compensar PMD acumulada en fibras de hasta 5000 km cuando el DGD de la fibra es de $0.1\text{x}10^{-9}\frac{s}{\sqrt{Km}}$ .En nuestras simulaciones la capacidad del ecualizador de compensar PMD viene en función del ángulo entre los principales estado de polarización de la fibra (PSP) y las señales enviadas usando Pol-Mux. El ecualizador demostró que estaba capacitado para compensar señales emitidas con un ángulo PHI dentro del rango $\left[0, 0.4\frac{\pi}{2}\right[$ cuando ningún otro efecto como DC o ruido de fase estaba presente en el sistema. El número de taps que cada filtro adaptivo necesitó para poder ecualizar PMD obteniendo BER<$1\text{x}10^{-3}$ fueron entre 2 y cuatro taps, dependiendo de la longitud de la fibra.

El último módulo de receptor digital coherente es el encargado de la ecualización del ruido de fase. El ruido de fase puede venir de dos fuentes, un offset entre el laser transmisor y el oscilador local del receptor o por el ancho de banda de los lasers involucrados en el sistema de transmisión. Para éste último módulo dos tipos de ecualizadores fueron implementados. Un recuperador de frecuencia, capaz de compensar el offset de frecuencia entre transmisor y oscilador local haciendo una estimación del offset de frecuencia presente. El otro es un recuperador de portadora que es capaz de compensar el ruido de fase debido a las variaciones en la emisión de los lásers debido a su ancho de banda. El primero de ellos, el estimador de frecuencia solo es capaz de compensar el ruido de fase que proviene del offset de frecuencia y por lo tanto debe ser instalado junto con el recuperador de portadora. En cambio el recuperador de portadora es capaz de compensar ambas fuentes de ruido de fase por sí solo. Los dos métodos fueron puestos a prueba obteniendo resultados muy similares por lo que como compensador de ruido de fase fue finalmente elegido el recuperador de portadora ya que hace al receptor más simple y rápido.

Finalmente y después de habar comprobado la eficacia de los módulos involucrados en el receptor digital coherente el receptor es testeado. Cuando todos los compensadores se insertan en el módulo de TDS del receptor digital coherente y los tres efectos que éstos compensan afectan la señal, véase DC, PMD, y ruido de fase, el sistema pierde capacidades. En este escenario el número de taps necesarias para compensar la señal y obtener BER<0.001 crece y los requerimientos del sistema, como el ancho de banda de los láseres, se hacen más exigentes. Por ejemplo, anteriormente dijimos que la ecualización de PMD se puede realizar cuando el ángulo PHI se encuentra dentro del rango $\left[0, 0.4\frac{\pi}{2}\right[$, eso es cierto cuando solo PMD afecta al sistema, en este caso y con el receptor completo y viéndose el sistema también afectado por DC y ruido de fase hemos comprobado que el ángulo PHI necesario para obtener BER<0.001 debe estar comprendido en el siguiente rango $\left[0, 0.2\frac{\pi}{2}\right]$. Como vemos, las exigencias para el transmisor ahora son mayores porque necesita controlar el ángulo con el que se transmite la señal con mayor precisión. Para conseguir el BER límite de 0.001 cuando todo el sistema está ensamblado el número de taps necesarios en los filtros de DC y PMD también crece. El recuperador de portadora encargado de estimar y compensar el ruido de fase también se ve afectado cuanto los tres ecualizadores trabajan juntos en el receptor. En este caso, la estimación de la fase contiene cierto error. Este error creemos que es debido sobre todo a que los ecualizadores que le preceden (el de DC y el de PMD) modifican la fase de la señal lo que hace que el estimador de fase cometa ciertos errores en la estimación. Para que este error en la estimación de fase no haga que el BER crezca por encima de $1x10^{-3}$ el offset de frecuencia presente entre el transmisor y el oscilador local no debe superar los 100Mhz mientras que el ancho de banda de los láseres del sistema puede llegar hasta los 100Mhz.

Sin embargo aunque el número de taps y los requerimientos del sistema se vean incrementados cuando el receptor digital coherente trabaja con los tres ecualizadores el receptor se comporta bien y es capaz de recibir señales a través de 5000 km de fibra. Esto quiere decir que se podría incluso evitar la amplificación de la señal a lo largo del canal. La no amplificación interna incrementaría la velocidad de transmisión, sin embargo aún queda por ver la velocidad del receptor digital coherente una vez implementado físicamente. El diseño físico del receptor y el módulo de TDS en una placa, junto con el testeo de velocidad de estos receptores cuando están físicamente implementados debe ser el siguiente paso en el estudio de receptores digital coherentes.

Hasta aquí hemos mostrado como el receptor digital coherente trae grandes oportunidades a las comunicaciones ópticas. La detección coherente sin TDS ya de por sí trae suficientes ventajas como la mejora en la sensibilidad del receptor pero la más notable de las ventajas es la posibilidad de utilizar TDS para ecualizar los efectos adversos clásicos de la transmisión óptica. La posibilidad de compensar DC, PMD y ruido de fase en el extremo receptor es razón suficiente para pensar en los receptores digitales coherentes como una opción fuerte. Pero no solo eso, con estos receptores se pueden utilizar modulaciones multinivel y también facilitan el uso de técnicas como POL-MUX las cuales incrementan notablemente la capacidad de la fibra. Aún así todavía existen dudas sobre la capacidad de implementar el módulo de TDS de dichos receptores sobre placas. El módulo encargado de la ecualización supondría para el sistema óptico de transmisión un cuello de botella ya que el reloj de una placa DSP es más lento que la tasa de símbolos que se consigue en transmisión óptica. Una solución sería forzar la placa a operar en paralelo pero esto comprometería a los algoritmos que emplean feedback. La implementación sobre circuito integrado de la parte digital del receptor digital coherente necesita de un estudio profundo y de muchos test para llegar a conclusiones precisas. Esto podría ser una más que notable continuación del presente estudio.

El receptor digital coherente diseñado aquí es solo una versión muy simplificada de lo que serán los receptores coherentes en el futuro. Este receptor solo utiliza modulación QPSK junto con POL-MUX, sin embargo la detección coherente ya es capaz de usar modulaciones más complejas como 8-PSK y mejores. Los receptores coherentes pueden incluso ser utilizados junto con tecnología WDM lo que es estrictamente necesario, como dijimos en la introducción, para alcanzar los máximos niveles de eficiencia espectral. Los receptores coherentes son necesarios para traer a las comunicaciones ópticas la posibilidad de explotar las capacidades de la fibra óptica al máximo.

B.Presupuesto

1. **Ejecución Material**
    a. Compra de ordenador personal .... 1.400 €
    b. Material de oficina.. 80 €
    c. Software y licencias…………………………………………………1000€
    d. Total de ejecución material.. 2480 €
2. **Gastos generales**
    a. 16 % sobre Ejecución Material..396,8€
3. **Beneficio Industrial**
    a. 6% sobre Ejecución Material.. 148,8 €
4. **Honorarios Proyecto**
    a. 60 semanas/20h semanales = 640 horas a 15 € / hora...............……18000 €
5. **Material fungible**
    a. Gastos de impresión.. 60 €
    b. Encuadernación... 200 €
6. **Subtotal del presupuesto**
    a. Subtotal Presupuesto... 21285 €
7. **I.V.A. aplicable**
    a. 16% Subtotal Presupuesto .... 3405,7 €
8. **Total presupuesto**
    a. Total Presupuesto.. 24690,7 €

Madrid, Noviembre de 2009
El Ingeniero Jefe de Proyecto

Fdo.: Lázaro Hermoso Beltrán
Ingeniero Superior de Telecomunicación

C.Pliego de Condiciones

Este documento contiene las condiciones legales que guiarán la realización, en este proyecto llamado “Digital Coherent Receiver for Optical Transmission”. En lo que sigue, se supondrá que el proyecto ha sido encargado por una empresa cliente a una empresa consultora con la finalidad de realizar dicho sistema. Dicha empresa ha debido desarrollar una línea de investigación con objeto de elaborar el proyecto. Esta línea de investigación, junto con el posterior desarrollo de los programas está amparada por las condiciones particulares del siguiente pliego.

Supuesto que la utilización industrial de los métodos recogidos en el presente proyecto ha sido decidida por parte de la empresa cliente o de otras, la obra a realizar se regulará por las siguientes:

Condiciones generales

La modalidad de contratación será el concurso. La adjudicación se hará, por tanto, a la proposición más favorable sin atender exclusivamente al valor económico, dependiendo de las mayores garantías ofrecidas. La empresa que somete el proyecto a concurso se reserva el derecho a declararlo desierto.

El montaje y mecanización completa de los equipos que intervengan será realizado totalmente por la empresa licitadora.

En la oferta, se hará constar el precio total por el que se compromete a realizar la obra y el tanto por ciento de baja que supone este precio en relación con un importe límite si este se hubiera fijado.

La obra se realizará bajo la dirección técnica de un Ingeniero Superior de Telecomunicación, auxiliado por el número de Ingenieros Técnicos y Programadores que se estime preciso para el desarrollo de la misma.

Aparte del Ingeniero Director, el contratista tendrá derecho a contratar al resto del personal, pudiendo ceder esta prerrogativa a favor del Ingeniero Director, quien no estará obligado a aceptarla.

El contratista tiene derecho a sacar copias a su costa de los planos, pliego de condiciones y presupuestos. El Ingeniero autor del proyecto autorizará con su firma las copias solicitadas por el contratista después de confrontarlas.

Se abonará al contratista la obra que realmente ejecute con sujeción al proyecto que sirvió de base para la contratación, a las modificaciones autorizadas por la superioridad o a las órdenes que con arreglo a sus facultades le hayan comunicado por escrito al Ingeniero Director de obras siempre que dicha obra se haya ajustado a los preceptos de los pliegos de condiciones, con arreglo a los cuales, se harán las modificaciones y la valoración de las diversas unidades sin que el importe total pueda exceder de los presupuestos aprobados. Por consiguiente, el número de unidades que se consignan en el proyecto o en el presupuesto, no podrá servirle de fundamento para entablar reclamaciones de ninguna clase, salvo en los casos de rescisión.

Tanto en las certificaciones de obras como en la liquidación final, se abonarán los trabajos realizados por el contratista a los precios de ejecución material que figuran en el presupuesto para cada unidad de la obra.

Si excepcionalmente se hubiera ejecutado algún trabajo que no se ajustase a las condiciones de la contrata pero que sin embargo es admisible a juicio del Ingeniero Director de obras, se dará conocimiento a la Dirección, proponiendo a la vez la rebaja de precios que el Ingeniero estime justa y si la Dirección resolviera aceptar la obra, quedará el contratista obligado a conformarse con la rebaja acordada.

Cuando se juzgue necesario emplear materiales o ejecutar obras que no figuren en el presupuesto de la contrata, se evaluará su importe a los precios asignados a otras obras o materiales análogos si los hubiere y cuando no, se discutirán entre el Ingeniero Director y el contratista, sometiéndolos a la aprobación de la Dirección. Los nuevos precios convenidos por uno u otro procedimiento, se sujetarán siempre al establecido en el punto anterior.

Cuando el contratista, con autorización del Ingeniero Director de obras, emplee materiales de calidad más elevada o de mayores dimensiones de lo estipulado en el proyecto, o sustituya una clase de fabricación por otra que tenga asignado mayor precio o ejecute con mayores dimensiones cualquier otra parte de las obras, o en general, introduzca en ellas cualquier modificación que sea beneficiosa a juicio del Ingeniero Director de obras, no tendrá derecho sin embargo, sino a lo que le correspondería si hubiera realizado la obra con estricta sujeción a lo proyectado y contratado.

Las cantidades calculadas para obras accesorias, aunque figuren por partida alzada en el presupuesto final (general), no serán abonadas sino a los precios de la contrata, según las condiciones de la misma y los proyectos particulares que para ellas se formen, o en su defecto, por lo que resulte de su medición final.

El contratista queda obligado a abonar al Ingeniero autor del proyecto y director de obras así como a los Ingenieros Técnicos, el importe de sus respectivos honorarios facultativos por formación del proyecto, dirección técnica y administración en su caso, con arreglo a las tarifas y honorarios vigentes.

Concluida la ejecución de la obra, será reconocida por el Ingeniero Director que a tal efecto designe la empresa.

La garantía definitiva será del 4% del presupuesto y la provisional del 2%.

La forma de pago será por certificaciones mensuales de la obra ejecutada, de acuerdo con los precios del presupuesto, deducida la baja si la hubiera.

La fecha de comienzo de las obras será a partir de los 15 días naturales del replanteo oficial de las mismas y la definitiva, al año de haber ejecutado la provisional, procediéndose si no existe reclamación alguna, a la reclamación de la fianza.

Si el contratista al efectuar el replanteo, observase algún error en el proyecto, deberá comunicarlo en el plazo de quince días al Ingeniero Director de obras, pues transcurrido ese plazo será responsable de la exactitud del proyecto.

El contratista está obligado a designar una persona responsable que se entenderá con el Ingeniero Director de obras, o con el delegado que éste designe, para todo relacionado con ella. Al ser el Ingeniero Director de obras el que interpreta el proyecto, el contratista deberá consultarle cualquier duda que surja en su realización.

Durante la realización de la obra, se girarán visitas de inspección por personal facultativo de la empresa cliente, para hacer las comprobaciones que se crean oportunas. Es obligación del contratista, la conservación de la obra ya ejecutada hasta la recepción de la misma, por lo que el deterioro parcial o total de ella, aunque sea por agentes atmosféricos u otras causas, deberá ser reparado o reconstruido por su cuenta.

El contratista, deberá realizar la obra en el plazo mencionado a partir de la fecha del contrato, incurriendo en multa, por retraso de la ejecución siempre que éste no sea debido a causas de fuerza mayor. A la terminación de la obra, se hará una recepción provisional previo reconocimiento y examen por la dirección técnica, el depositario de efectos, el interventor y el jefe de servicio o un representante, estampando su conformidad el contratista.

Hecha la recepción provisional, se certificará al contratista el resto de la obra, reservándose la administración el importe de los gastos de conservación de la misma hasta su recepción definitiva y la fianza durante el tiempo señalado como plazo de garantía. La recepción definitiva se hará en las mismas condiciones que la provisional, extendiéndose el acta correspondiente. El Director Técnico propondrá a la Junta Económica la devolución de la fianza al contratista de acuerdo con las condiciones económicas legales establecidas.

Las tarifas para la determinación de honorarios, reguladas por orden de la Presidencia del Gobierno el 19 de Octubre de 1961, se aplicarán sobre el denominado en la actualidad “Presupuesto de Ejecución de Contrata” y anteriormente llamado ”Presupuesto de Ejecución Material” que hoy designa otro concepto.

Condiciones particulares

La empresa consultora, que ha desarrollado el presente proyecto, lo entregará a la empresa cliente bajo las condiciones generales ya formuladas, debiendo añadirse las siguientes condiciones particulares:

La propiedad intelectual de los procesos descritos y analizados en el presente trabajo, pertenece por entero a la empresa consultora representada por el Ingeniero Director del Proyecto.

La empresa consultora se reserva el derecho a la utilización total o parcial de los resultados de la investigación realizada para desarrollar el siguiente proyecto, bien para su publicación o bien para su uso en trabajos o proyectos posteriores, para la misma empresa cliente o para otra.

Cualquier tipo de reproducción aparte de las reseñadas en las condiciones generales, bien sea para uso particular de la empresa cliente, o para cualquier otra aplicación, contará con autorización expresa y por escrito del Ingeniero Director del Proyecto, que actuará en representación de la empresa consultora.

En la autorización se ha de hacer constar la aplicación a que se destinan sus reproducciones así como su cantidad.

En todas las reproducciones se indicará su procedencia, explicitando el nombre del proyecto, nombre del Ingeniero Director y de la empresa consultora.

Si el proyecto pasa la etapa de desarrollo, cualquier modificación que se realice sobre él, deberá ser notificada al Ingeniero Director del Proyecto y a criterio de éste, la empresa consultora decidirá aceptar o no la modificación propuesta.

Si la modificación se acepta, la empresa consultora se hará responsable al mismo nivel que el proyecto inicial del que resulta el añadirla. 8. Si la modificación no es aceptada, por el contrario, la empresa consultora declinará toda responsabilidad que se derive de la aplicación o influencia de la misma.

Si la empresa cliente decide desarrollar industrialmente uno o varios productos en los que resulte parcial o totalmente aplicable el estudio de este proyecto, deberá comunicarlo a la empresa consultora.

La empresa consultora no se responsabiliza de los efectos laterales que se puedan producir en el momento en que se utilice la herramienta objeto del presente proyecto para la realización de otras aplicaciones.

La empresa consultora tendrá prioridad respecto a otras en la elaboración de los proyectos auxiliares que fuese necesario desarrollar para dicha aplicación industrial, siempre que no haga explícita renuncia a este hecho. En este caso, deberá autorizar expresamente los proyectos presentados por otros.

El Ingeniero Director del presente proyecto, será el responsable de la dirección de la aplicación industrial siempre que la empresa consultora lo estime oportuno. En caso contrario, la persona designada deberá contar con la autorización del mismo, quien delegará en él las responsabilidades que ostente.

D. Acreditación de Méritos

VPIsystems™

VPIsystems GmbH · Carnotstr. 6, 10587 Berlin · Germany

To whom it may concern

Master Thesis

"Digital Coherent Receiver for Optical Transmission"

Herewith I testify that Lázaro Hermoso carried out a Master Thesis with title "Digital Coherent Receiver for Optical Transmission" under my supervision at the VPIsystems GmbH in Berlin, Germany, from May to November 2008.

Some of the results obtained in this thesis were used to define specifications for simulation models that were later included in the commercially available software VPItransmissionMaker.

Berlin, 11th of November of 2009

Dr. Hadrien Louchet, Manager Training & Services

VPIsystems GmbH
Carnotstraße 6
10587 Berlin, Germany
+49 30 398 058-0
+49 30 398 058-58 Fax
www.VPIsystems.com

Postbank Berlin
Kto 287 191 00
BLZ 100 100 10
USt.Id.Nr. DE185074787

Geschäftsführer:
Dr. André Richter,
Bhupendra Sharma
Sitz Berlin, Amtsgericht Charlottenburg
HRB 61736

Holmdel
Berlin
Minsk
Melbourne